Journal of the
OPTICAL SOCIETY
of AMERICA

VOLUME 39, NUMBER 9 SEPTEMBER, 1949

A New Series of Microscope Objectives: I. Catadioptric Newtonian Systems[*]

DAVID S. GREY
Research Laboratory, Polaroid Corporation, Cambridge, Massachusetts
AND
PAUL H. LEE[**]
Biology Department, Massachusetts Institute of Technology, Cambridge, Massachusetts

(Received June 22, 1949)

The problem of computing a microscope objective corrected for visible light and for ultraviolet light is reviewed. As it does not seem possible to achieve freedom from chromatic aberrations over this interval with purely refractive objectives of large numerical apertures, a study of catadioptric objectives limited to spherical surfaces is initiated. Catadioptric objectives containing two mirror surfaces may be described as deriving from either the Newtonian or the Schwarzschild telescope objective. Construction data are given for Newtonian objectives which have numerical aperture 1.0 and which are corrected from 220 mμ through the visible spectrum. These modified Newtonian objectives have one serious defect: a large central portion of the aperture is obscured.

INTRODUCTION

THE standard apochromatic microscope objectives which are used today are not very different from Abbe's apochromats of 1886. This is in marked contrast to the development of photographic and telescopic optics during the corresponding period. Apparently, there was little incentive to improve upon the classical microscope objectives for use in the visual region of the spectrum.

The present demand for microscope systems which function in the near ultraviolet spectrum[1] cannot be fully satisfied by objectives patterned after the standard formulas. The range of ultraviolet wave-lengths particularly interesting to biologists is the region 220 mμ to 320 mμ. It is virtually a necessity that the microscope objective be achromatized and free of spherical aberration and coma over this interval before complete freedom to investigate this region is achieved.[2] Moreover, the objective should have a common focus for ultraviolet and visible light, otherwise the difficulty of focusing for ultraviolet raises a serious barrier to the use of the instrument.

An investigation of the possibility of correcting a refractive objective for use over this spectral interval is not encouraging. Of the various isotropic optical media transparent in this region—fluorite, lithium fluoride, fused quartz, rock salt, potassium bromide, magnesium oxide and a few others—only the first three named are considered suitable for precision ultraviolet optics. The first two, fluorite and lithium fluoride, have essentially the same optical properties in the near ultraviolet, so refractive objectives may, at this date, be considered limited to elements made of fused quartz and fluorite. It is not possible to show that these materials cannot be combined to provide a refractive objective of large numerical aperture achromatized from 220 mμ to 560 mμ *if no limitation is placed on the number of lens components*. A reasonable number of lens components of these materials provides correction for chromatic aberration over a band width of only about 10 mμ at numerical aperture 0.85, as shown by Foster and Thiel.[3] As the numerical aperture of the objective becomes smaller, the wave-length band over which achromatism

---

[*] This investigation was initiated under a grant to M. I. T. from the American Cancer Society, recommended by the Committee on Growth, National Research Council. A part of the investigation was conducted jointly under the above grant, and a grant to the Polaroid Corporation from the ONR.

[**] Present address: Brookhaven National Laboratory, Upton, New York.

[1] J. R. Loofbourow, Rev. Mod. Physics **12** (1940).

[2] Land, Blout, Grey, Flower, Husek, Jones, Matz, and Merrill, A color translating Ultraviolet Microscope, Science **109**, 371–374 (1949).

[3] L. V. Foster and E. M. Thiel, J. Opt. Soc. Am. **38**, 689–692 (1948).

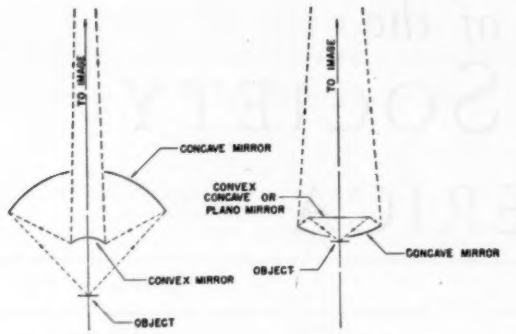

FIG. 1. Newtonian and Schwarzschild types of two-mirror objectives. In the Schwarzschild system (left) a convex mirror is optically located nearer to the long conjugate focus than is the concave mirror.

may be realized is increased rapidly; an objective of numerical aperture 0.20 achromatized from 250 mμ to 540 mμ was computed by B. K. Johnson.[4]

Preliminary investigations indicate that even if the less suitable of those optical materials listed above are utilized, the difficulties of achromatizing a refractive objective from 220 mμ to 540 mμ are not overcome. Hence, one is led to the use of reflecting objectives. Existing types of reflecting telescopes apparently provide embodiments of all the basic arrangements of mirrors from which reflecting microscopes may be developed.

Optical objectives for microscopes and for telescopes have many properties in common. Both systems are usually required to cover only a small angular field, both systems are used with one conjugate focus at a distance from the objective which is long compared with the focal length of the objective, and both are required to meet the highest standards of optical perfection. For these reasons, a type of objective which is useful in a telescope may be modified to become a microscope objective, and vice versa.

There is a fundamental difference in requirements for these two types of optical systems which implies that if the metamorphosis is to provide a generally useful system in the new role, the modification may be of major proportions. The resolving power of a telescope depends upon the *free aperture* of the objective and is independent of the ratio of free aperture to focal length. On the other hand, the resolving power of a microscope depends solely on the *ratio* of free aperture to focal length and not on the free aperture.

This fundamental difference was probably not *completely* enunciated until Abbe proved that the resolving power of a microscope objective is proportional to the numerical aperture, and Rayleigh showed that even a very large "pinhole" (say of 200-inch diameter) can resolve to practical perfection as a telescope of that free aperture, if only the telescope tube length is sufficiently great!

In the early part of the nineteenth century the constructors of microscope objectives, guided by experience and intuition, had turned away from telescope type designs and advanced towards the large numerical apertures to be prescribed later by Abbe's formula. Until that time microscope design and telescope design had been very similar. In particular, there were microscope objectives directly patterned after the various classical reflecting telescopes.

The early reflecting microscopes had many advantages over their refractive contemporaries. They did not require homogeneous optical glass, which at that time did not exist in the variety of types necessary to remove

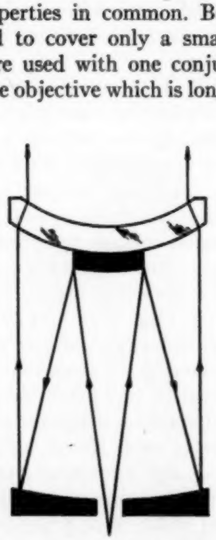

FIG. 2. Maksutov modification of the Newtonian objectives. The catadioptric Newtonian objectives described in this paper are a further development of this optical system.

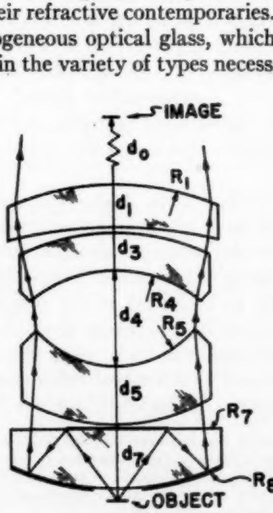

FIG. 3. Newtonian objective modified with fluorite refractive elements. This objective at Na 0.95 has maximum spherical aberration of one-quarter wave-length in the range 220 mμ to 540 mμ. Secondary spectrum slightly exceeds the quarter-wave tolerance. Coma is adequately corrected. Construction data for this objective are given in Table I.

---

[4] B. K. Johnson, An achromatic objective for use in ultraviolet microscopy, Proc. Phys. Soc. **51**, 1034–1039 (1949).

chromatic aberration throughout the visible spectrum. Two component reflecting systems which are free of spherical aberration and coma are easily computed. On the other hand, two mirrors are required to form a satisfactory reflecting microscope objective, and one of these mirrors blocks a portion of the aperture (except in off-axis types of small numerical aperture). The only reflecting combinations known at that time required aspheric surfaces to remove spherical aberration even at moderate numerical apertures. The reflectivity of the mirrors was initially low and the surfaces tarnished with age.

When the new optical glasses became available and the optical properties of fluorite were discovered, refractive objectives of high quality became possible. The freedom of reflecting systems from chromatic aberration no longer provided them with a competitive advantage which compensated for their defects. Hence, the reflecting microscope objective passed into practical oblivion until very recently.

Revival of the need for reflecting objectives presents a broad and fertile field for exploration. During the historic period when reflecting microscope objectives were first on trial, the theory of optical aberrations and simplified programs for their elimination were not yet developed, nor were our modern office type computing machines available. Our various modern methods of optical design did not come into use until after the shift to refractive optics was well established. Those trained in optical design were trained primarily in terms of lenses. A much lesser amount of attention was given to the application of mirrors, and only for very special purposes, such as astronomical objectives. In hindsight, it is amazing that the combination of curved mirrors and lenses remained almost completely neglected. It was not until 1932 that the Schmidt telescope first exhibited to the scientific world the tremendous advantages of combining mirrors and lenses into a single optical objective.

TABLE I. Construction data for the objective illustrated in Fig. 3.†,†† All dimensions are in millimeters.

	Radius		Distance	Clear aperture
		d_0	175	
R_1	5.45*	d_1	1.05	4.43
R_2	58.98*	d_2	0.026	4.27
R_3	5.108*	d_3	0.875	4.14
R_4	3.00*	d_4	2.188	3.62
R_5	2.495±0.01	d_5	1.313	3.54
R_6	4.50*	d_6	0.026	4.29
R_7	∞*	d_7	1.371	4.44
R_8	5.78±0.01			4.60

Tolerances

Surface	Radius		Distance
1	±0.04	d_1	±0.05
2	±0.6	d_2	———
3	±0.03	d_3	±0.025
4	±0.01	d_4	±0.03
5	±0.006	d_5	±0.025
6	±0.027		
7			
8	±0.02		

† Thickness of immersion liquid (cyclohexane) 0.154; Thickness of slide cover 0.182; * indicates Bausch & Lomb test glass; R_3 is concave.

†† Total distance object to image 182.2; e.f.l. = 2.28 mm; Material—fluorite.

TABLE II. Construction data for the objective illustrated in Fig. 4.† All dimensions are in millimeters.

	Radius		Distance	Clear aperture
R_1	6.00*	d_0	175.	4.37
R_2	∞*	d_1	1.050	4.22
R_3	4.70*	d_2	0.026	4.05
R_4	2.95*	d_3	0.875	3.52
R_5	2.495*	d_4	2.188	3.40
R_6	4.311*	d_5	0.875	3.95
R_7	∞	d_6	0.210	4.13
R_8	5.483	d_7	1.269	4.27

† Total distance object to image = 181.85 mm; Immersion liquid (cyclohexane) 0.173 mm; Slide Cover 0.182 mm; * Indicates Bausch & Lomb test glass.

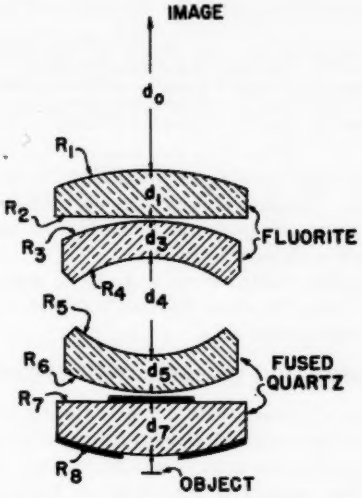

FIG. 4. Newtonian objective modified with refractive elements of fused quartz and fluorite. This objective has NA 1.0. The spherical aberration and secondary spectrum for wave-lengths 220 mμ to 540 mμ are well under one-quarter wave-length. Construction data for this objective are given in Table II.

At the time of Schmidt's invention one might have contended that the virtue of the Schmidt telescope derived not from combination of reflection and refraction, but from the use of an aspheric surface. However, subsequent investigations have produced catadioptric objectives (combining lenses and mirrors) using only spherical surfaces which rival or even better the performance of the Schmidt telescope.

The objectives described in this series of papers are a continuation of the development of catadioptric systems. The "rules" adopted at the outset and maintained throughout the investigation are:

1. Only spherical surfaces are to be used, so that the designs are adapted to quantity production.

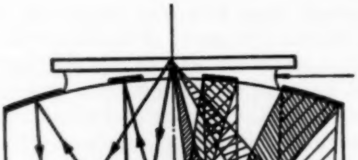

FIG. 5. Detail of concentric annular reflecting areas on the secondary mirror. The great defect of a catadioptric Newtonian objective for use at large NA is that about 50 percent of the objective aperture is obscured by the secondary mirror. A portion of the obscured aperture may be recovered as indicated in this figure.

2. Only fused quartz and fluorite are to be used for lens media. (Lithium fluoride was not definitely ruled out, but no justification was found for the use of this slightly less suitable material.)

3. Only fully coated mirrors are to be used; that is, an element of surface may not function both as a mirror and as a transparent area.[5]

CLASSIFICATION OF REFLECTING OBJECTIVES

It seems apparent that, if the conjugate foci of an objective of large numerical aperture are to be accessible and separated, there must be at least two mirrors in the system. For reasons of simplicity of treatment and construction, and to avoid unnecessary light loss, objectives containing only two mirrors are considered.

Co-axial objectives containing two mirrors may be separated into two basic classifications. If the mirror optically nearest to the long conjugate focus of the system is a concave mirror, the objective may be said to be a modification of the Newtonian type of reflecting system. The secondary mirror may be plane (Newtonian proper), convex (Cassegrainian) or concave (Gregorian).

If the mirror optically nearest to the long conjugate focus is convex, the objective is of the Schwarzschild type.[6] The second mirror is then necessarily concave. Two subclasses of the Schwarzschild objective are distinguished by whether rays from the concave mirror to the short conjugate focus pass outside the diameter of the convex mirror, or through a hole in the center of the convex mirror. The latter case is not an attractive approach to a microscope objective because the comatic aberration of the two spherical mirrors adds, and the net comatic term from the mirrors seems too large for correction by other means. In the former case the coma of the two mirrors is mutually compensating, at least in part. The spherical aberration of the concave and convex mirrors are partially compensating for either case.

The Newtonian and Schwarzschild systems are shown in Fig. 1.

MODIFICATION OF THE NEWTONIAN SYSTEM

It was decided first to investigate modification of the Newtonian system. One motive for this choice was that optical designs of this sort are available in the literature as a good starting point.[5, 7–9] Maksutov[7] shows how he used a thick meniscus lens as a substitute for the aspheric member of the Schmidt telescope. (Fig. 2.) As Maksutov states, his system can be readily adapted for use as a microscope of low or moderate numerical aperture. Several modifications were found necessary to develop this system for use at numerical apertures about equal to unity.

The concave mirror must be converted to the solid or "in glass" type of mirror shown in Figs. 3 and 4. (Construction data for these objectives are given in Tables I and II.) Otherwise the extreme obliquity of the marginal ray in passing from the concave mirror to the object would preclude the possibility of inserting a secondary mirror, and the object point would not be conveniently accessible.

The thick meniscus element must be compounded to reduce zonal aberrations. Then, spherical aberration and coma can be corrected within the Rayleigh quarter-wave tolerance for numerical apertures up to 1.0, over the wave-length interval 220 mμ to 540 mμ. This correction can be obtained using lens elements of only one refractive medium, either fluorite or fused quartz.

It was not found possible to remove secondary spectrum without introducing refractive elements of both fused quartz and fluorite.

The final results of the investigation of Newtonian systems are shown in Figs. 3 and 4. Detailed computation methods for the Newtonian system are omitted because of their length and because the Schwarzschild system has proved to be generally superior for microscope objectives. The "all fluorite" design of Fig. 3 has NA 0.95. Spherical aberration is just within the Rayleigh tolerance. Coma, astigmatism and Petzval sum are completely negligible for the purpose of a microscope objective. The secondary spectrum between 220 mμ and 540 mμ slightly exceeds the Rayleigh tolerance. The quartz-fluorite objective of Fig. 4 represents a considerable improvement over the all-fluorite design, for secondary spectrum and spherochromatic aberration are well under the Rayleigh tolerance at NA 1.0.

---

[5] An ingenious series of objectives which contain partially reflecting surfaces has been computed: B. K. Johnson, An achromatic reflection microscope for use with visible or ultraviolet light. Proc. Phys. Soc. **53**, 714–719 (1941). B. K. Johnson, A compound reflecting microscope of high aperture for use in ultraviolet light. J. Sci. Inst. **26** (1949).

[6] K. Schwarzschild, *Theorie der Spiegeteleskop* (Göttingen Observatory, 1905).

[7] D. D. Maksutov, New catadioptric meniscus systems, J. Opt. Soc. Am. **34**, 270–284 (1944).

[8] E. H. Linfoot, An application of the Schmidt principle to microscopy, J. Scient. Inst. **15**, 405–406 (1938).

[9] A. Bouwers, *Achievements in Optics* (Elsevier Publishing Company, New York, 1946), p. 16–45.

The most serious defect of this objective type is the very large obscuring ratio. As is evident from the figures, the diameter of the secondary mirror is much more than half the diameter of the primary mirror. For smaller numerical apertures the obscuring ratio may be decreased by use of a convex secondary mirror. Some of the obscured part of the aperture may be recaptured if the secondary mirror is deposited as a series of concentric annuli. The otherwise unused central portion of the secondary mirror is thereby permitted to function as an inner objective of small aperture. (See Fig. 5.) Even when concentric annuli are used on the secondary mirror, the total area obscured is greater than forty percent of the aperture at numerical aperture 1.0. A particular mechanical difficulty of these objectives is that the aluminized surface of the concave mirror is adjacent to the immersion liquid.

The objectives shown in Figs. 3 and 4 were constructed by the Bausch and Lomb Optical Company. The reflecting surfaces were formed of evaporated aluminum. The performance was as should be expected from the large fraction of obscured aperture. Paper II of this series will present the derivation of a tolerance for obscuring ratio. This tolerance is not satisfied by the objectives described above, but may be satisfied by catadioptric Schwarzschild objectives.

ACKNOWLEDGMENT

The authors wish to thank Mr. Samuel A. Stone of the Polaroid Corporation[10] for his valuable assistance in computing the objectives described in this paper.

The authors also wish to thank Mr. Leon V. Foster and the Bausch and Lomb Optical Company for constructing the objectives described and for designing and constructing the objective mountings.

---

[10] Mr. Stone is at present with the Bradford-Durfee Technical Institute, Fall River, Massachusetts.

JOURNAL OF THE OPTICAL SOCIETY OF AMERICA VOLUME 39, NUMBER 9 SEPTEMBER, 1949

A New Series of Microscope Objectives: II. Preliminary Investigation of Catadioptric Schwarzschild Systems*

David S. Grey
Research Laboratory, Polaroid Corporation, Cambridge, Massachusetts

(Received June 22, 1949)

This paper presents a preliminary study of combining the Schwarzschild pair of mirrors with lenses of fused quartz and fluorite to obtain an ultraviolet microscope objective. It is found that the catadioptric Schwarzschild objective is superior to the catadioptric Newtonian objectives described in Paper I.

An objective using spherical surfaces and corrected from 220 mμ into the near infra-red is described. The obscuring ratio of this objective is 7 percent in area at NA 1.1.

INTRODUCTION

Paper I of this series has presented the problem of combining spherical lenses of fused quartz and fluorite with spherical mirrors to provide a microscope objective achromatized for ultraviolet and visible light. Catadioptric objectives are classified according to whether the lens elements are combined with the Newtonian pair of mirrors or with the Schwarzschild pair of mirrors. Two catadioptric Newtonian objectives are shown in Paper I. An evaluation of these objectives leads to the conclusion that although their aberrations may be well corrected over a large wave-length range at NA 1.0, the portion of the aperture which is obscured by the secondary mirror is excessive (as will be explained subsequently) at this numerical aperture.

This paper will present a preliminary evaluation of catadioptric Schwarzschild objectives.

The usual catadioptric objective is handled as an elaboration of the Schmidt principle whereby the refracting components are treated as a means of correcting the aberrations of the mirrors. Lens elements which function as aberration correcting devices do, it is true, permit the design of a well corrected catadioptric Schwarzschild objective. However, an evaluation of the knowledge gained by computing this objective indicated that the lens elements could be used not merely as "correcting elements," but also as dominant light converging elements. Objectives computed on the basis of this broader concept of catadioptrics will be presented in future papers of this series.

DESCRIPTION OF THE OBJECTIVE

The first catadioptric modification of the Schwarzschild mirrors is illustrated in Fig. 1. (Construction data for this objective are given in Table I.) It has excellent computed performance, but it is large and awkward to construct. Although this objective was never made, the computation served a valuable purpose: it showed that the catadioptric Schwarzschild objective is superior to the catadioptric Newtonian objective in both obscuring ratio and numerical aperture. At NA 1.1, spherical

---

* This investigation was supported by the ONR.

TABLE I. Construction data for the objective shown in Fig. 1.†

	Radius	Tolerance	Clear aperture (diameter)		Distance
R_1	4.626* mm		3.70	d_1	1.500 mm
R_2	10.70*		3.70	d_2	4.400
R_3	−3.10	±0.010	2.62	d_3	1.000
R_4	56.85*		2.84	d_4	6.100
R_5	5.85*	±0.005	4.67	d_5	37.400
R_6	44.20*	±0.005	76.5	d_6	38.950
R_7	28.80*	±0.010	18.32	d_7	2.000
R_8	27.95	±0.010	15.91	d_8	0.025
R_9	7.75	±0.005	12.15	d_9	8.086
R_{10}	∞				

† Immersion liquid (cyclohexane) 0.175 mm; Cover slip (fused quartz) 0.175 mm; All lenses of fluorite; * Indicates Bausch and Lomb test glass.

aberration, coma, and shift of focal point with wavelength are corrected over the spectral interval 220 mμ into the near infra-red, and to less than the Rayleigh tolerance. Only 7 percent (in area) of the objective aperture is obscured by the convex mirror.

EVOLUTION OF THE DESIGN

This design evolved from the following considerations. The Schwarzschild mirrors used in spherical form and without lenses may be corrected for third-order (primary) spherical aberration, coma, and astigmatism.[1] If third-order aberrations are balanced against those of higher order, the zonal aberrations permit a numerical aperture of about 0.5.[2] In this form, the obscuring ratio is about 20 percent in area. Sacrifice of numerical aperture improves the obscuring ratio slightly. Use of wavelengths longer or shorter than visible light alters these figures in directions favorable or unfavorable, respectively. In addition, an appreciable portion of the aperture is obscured by supports for the convex mirror.

If the mirrors are rearranged to provide a very small obscurring ratio, the objective is no longer corrected for spherical aberration and coma. Burch[3] uses aspheric mirrors to make his system aplanatic with large numerical apertures and small obscuring ratios. The refractive elements in the objective of Fig. 1 are a substitute for the aspheric surfaces used by Burch, and provide a transparent supporting member for the convex mirror. Conceptually, these were the *only* functions of the refractive components throughout the computation of this objective. In retrospect it is evident that this limitation of the role assigned the refractive elements caused the objective to become much larger than necessary for a given focal length. Subsequent papers in this series will demonstrate how the design becomes more elegant (for both the manufacturer and the user) when the refractive elements provide a large fraction of the light converging power.

Prior to obtaining experience and familiarity with this type of objective, use of lenses primarily as aberration correcting elements seemed logical. The Schwarzschild spherical mirrors present in themselves an optical system which is nearly adequate. If this system is to be aided by refractive elements, one reasonable approach is to require that the refractive elements perform a minimum function. This approach seemed good because the less "work" the refractive elements perform, the less difficulty one might expect to have with chromatic aberrations. It was found that when the net third-order spherical aberration of the two mirrors is changed, the higher orders of spherical aberration change in the opposite algebraic sense. The higher order spherical aberration produced by the mirrors was always an overcorrection. If the third-order contribution of the mirrors is an undercorrection, the lens elements must contribute overcorrected third-order and undercorrected higher order spherical aberration. As the undercorrection from the mirrors becomes larger, the third-order overcorrection and the higher order undercorrection required of the lens elements become greater. It appears to follow that if minimum requirements are to be placed upon the refractive elements, the net third-order spherical aberration of the mirrors should not be an undercorrection. Also, it was found that when the net third-order contribution of the lenses is changed in the direction of over correction, the volume of the objective increases (for a given obscuring ratio). In accordance with the facts and reasoning outlined above, the third-order spherical aberration coefficients of the two reflecting surfaces were made to compensate each other. The misdirection of this reasoning was not discovered until, in the computation of an objective of smaller numerical aperture, the author had the temerity to abandon the "logical" approach in order to achieve a compact objective. Subsequent papers will present an alternative and far more successful division of optical function between the lenses and mirrors. The mathematical relationships on which this re-evaluation was made became separately apparent during computation of this objective, but were not immediately correlated to full advantage.

When it was decided that the spherical aberration of the mirrors should be very nearly compensating, there remained only one degree of freedom to apply to the mirrors—their separation. Third-order aberrations and Gaussian optics were computed for light traveling in the reverse direction, from long conjugate focus to short conjugate focus. Under this convention, the Gaussian image distance at the convex mirror was made a fixed parameter. (Obviously one variable of an optical system may be fixed with no loss of generality.) The curvature of the convex mirror was therefore determined by the object distance at that mirror. This in turn was dependent on the refractive components (if any) between the convex mirror and the long conjugate focus. For any given separation of the mirrors, the curvature of the concave mirror was prescribed by the condition set above for net contribution of the mirrors to spherical aberration. As the mirror separation increased, the obscuring ratio decreased, and, of course, the necessary clear aperture of the concave mirror became greater. This process was pursued until the obscuring ratio was reduced to about seven percent in area. The algebraic sign of the coma residual to the mirrors was the same as for a paraboloidal mirror, and the magnitude of coma increased as the mirror separation increased.

---

[1] K. Schwarzschild, *Theorie der Spiegelteleskop* (Gesellschaft der Wissenschaften zü Göttingen Math-Phys Classe N.F. iv, 2, 1905).

[2] This is the type of objective used by Brumberg and apparently computed by Gershgorin after suggestions by Maksutov; E. M. Brumberg, Nature (London) **152**, 357 (1943), D. D. Maksutov, U.S.S.R. Pat. No. 40859 (1932).

The Gershgorin-Maksutov objective does not appear to be truly a catadioptric *modification*. A weak lens is inserted between the convex mirror and the long conjugate focus. The function of this lens is to correct chromatic aberration caused by the cover slip rather than to provide an essential modification of the Schwarzschild mirrors. No detailed account of this design has been found.

[3] C. R. Burch, Proc. Phys. Soc. (London) **59**, 41–49 (1947).

Thus at the very outset it was established that (for this method of attack) the refractive components should perform as follows:

Net third-order (primary) spherical aberration—about zero.
Higher order spherical aberration—undercorrected.
Third-order coma—inward for light considered traveling from the long conjugate to the short conjugate focus.

There are three distinctly different choices of location for refractive elements (see Fig. 2).

A. They may be in the optical path between the short conjugate focus and the concave mirror, but not in the optical path between the concave mirror and the convex mirror.

B. They may be in the optical path between the convex mirror and the long conjugate focus, but not in the optical path between the mirrors.

C. They may be in the optical path between the mirrors.

It is very desirable that at least one refractive element be located in position A. A refractive surface should be closely adjacent to the convex mirror so that this mirror can be cemented to the lens surface and opaque mounting members can be eliminated. Also, if numerical apertures greater than unity are to be achieved, there must be a lens element in optical contact with the cover slip.

The logic under which this objective was computed made it virtually a necessity that there be at least one lens in position B. It was not found possible to compensate the coma and spherical aberration residual in the mirrors by means of any reasonable configuration of lenses in position A alone, whereas lenses in position B could give a large comatic term with comparatively little spherical aberration.

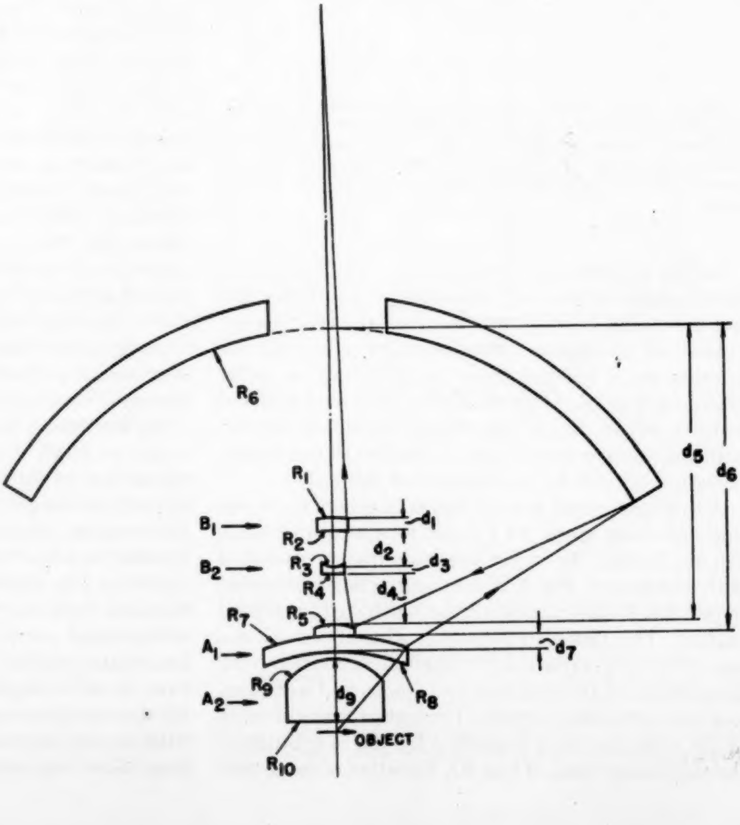

FIG. 1. Schwarzschild mirrors combined with fluorite lenses to form a microscope objective corrected from 220 $m\mu$ into the near infra-red region. The NA is 1.1 and the obscuring ratio is 7 percent in area. The knowledge acquired in computing this objective led to the series of microscope objectives which will be described in subsequent papers of this series. Construction data for this objective are given in Table I.

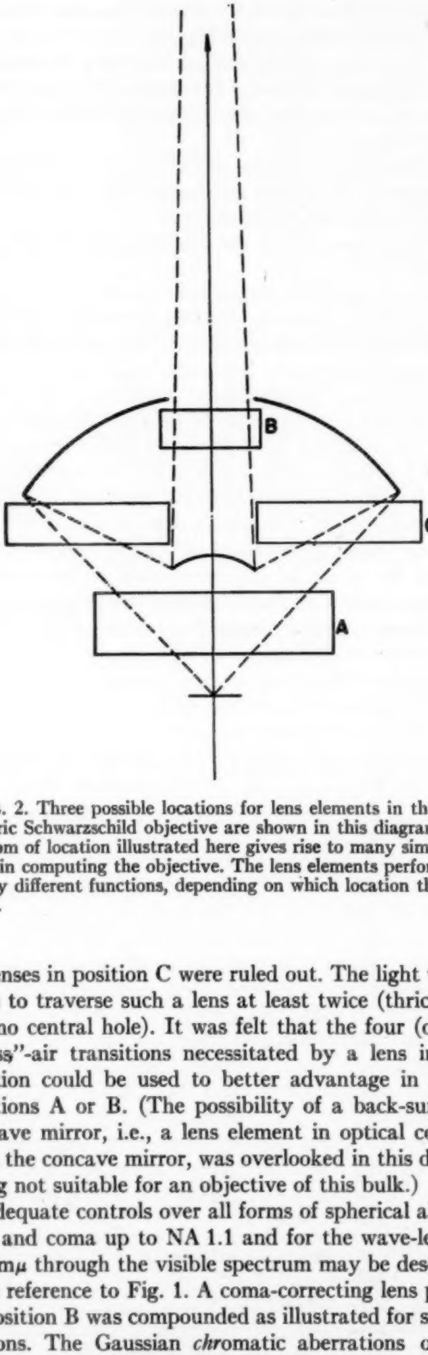

FIG. 2. Three possible locations for lens elements in the catadioptric Schwarzschild objective are shown in this diagram. The freedom of location illustrated here gives rise to many simplifications in computing the objective. The lens elements perform distinctly different functions, depending on which location they are given.

Lenses in position C were ruled out. The light would have to traverse such a lens at least twice (thrice if it has no central hole). It was felt that the four (or six) "glass"-air transitions necessitated by a lens in this position could be used to better advantage in either positions A or B. (The possibility of a back-surfaced concave mirror, i.e., a lens element in optical contact with the concave mirror, was overlooked in this design, being not suitable for an objective of this bulk.)

Adequate controls over all forms of spherical aberration and coma up to NA 1.1 and for the wave-lengths 220 mμ through the visible spectrum may be described with reference to Fig. 1. A coma-correcting lens placed in position B was compounded as illustrated for several reasons. The Gaussian *chr*omatic aberrations of this lens affect the variation of spherical aberration with wave-length of the objective as a whole, and were used as a control for this purpose. The higher orders of coma of the objective were controlled by the magnitude of the third-order coma of lens *B2*. Variation of coma with wave-length was controlled by the power of lens *B1* and the spacing between *B1* and *B2*.

Spherical aberration was compensated by lens *A1*. The thickness and bending of this component, considered together, provided a control for both third- and higher-order spherical aberration.

Lens element *A2* is a hemisphere with center approximately at the short conjugate focus. Small variations from this form provided a control of longitudinal chromatic aberration.

Secondary spectrum of anomalous sign necessarily arises because the refractive surfaces enumerated above are separated. During the early stages of computation, this was compensated by compounding lens element *A2* into a positive fluorite element and a negative fused quartz element. The secondary spectrum of the refractive components could be made so small that this compounding was not necessary; the secondary spectrum contributed by the quartz cover slide and the immersion liquid provided an adequate compensation.

In the manner outlined above, spherical aberration and coma were completely controlled for the third- and fifth-order at one wave-length. Variation of spherical aberration and coma with wave-length were controlled in the third-order, and secondary spectrum could be eliminated. Proper balancing of the controlled aberrations against residual aberrations gave more than adequate control of spherical aberration and coma at numerical aperture 1.1 from the wave-lengths 220 mμ into the near infra-red region.

The prospect of using a larger numerical aperture with this design is poor because there is a variation of spherical aberration with angle, apparently caused by lens element *B2*. At numerical aperture 1.1 this aberration barely permits obtaining an object field 80μ in diameter. [This is a reasonable field size when one considers that NA 1.1 in the ultraviolet gives resolving power about equivalent to NA 2.2 in visible light.] Even a small increase of numerical aperture would drastically reduce the field size.

Astigmatism (from lens element *B2*) requires the use of a special projection eyepiece. The complete optical system is illustrated in Fig. 3.

An interesting feature of these computations is the extent to which third-order theory proved useful. The summation of third-order aberrations *per se* indicated virtually nothing as to the performance of the objective, but with the tracing of a very few rays it was found possible to relate the aberration controls enumerated above to the third-order aberration coefficients and Gaussian optics at the individual surfaces. Once these relationships were discovered they gave very nearly linear interpolation and extrapolation over large intervals. As an example, the higher order offense against the sine condition was reduced from about 0.01 to about 0.001 in one step, while control of other higher order aberrations was maintained, both via inferences from third-order computations. This general simplicity of control is largely attributable to the lack of constraint in positioning the lens surfaces.

EFFECT OF OBSCURING RATIO

Obscuring ratio has a direct bearing on the ultimate usefulness of an objective. A quantitative evaluation of the effect of obscuring a portion of the objective aperture is a necessary guide in computing these objectives and in comparing different reflecting systems.

If an aberrationless lens system of unobscured circular aperture is used to form an image of a monochromatic light source which is too small to be resolved, diffraction causes the image to appear as a bright central disk surrounded by a series of concentric rings. Roughly 85 percent of the light passed by the optical system falls within the central disk, the remainder falls in the rings. If a small amount of aberration is introduced or if interior portions of the aperture are obscured, the effects on the diffraction pattern are very similar; the percent of energy falling within the central disk is decreased and the size of the central disk becomes verys lightly smaller. The effect on resolving power depends greatly on the specific use of the instrument. If the target observed has high contrast, resolving power may actually be improved very slightly. If the target has low contrast, the scattering of energy into the outer rings may greatly reduce the resolving power. Whether the target is of high or low contrast, loss of light from the central disc makes it difficult to evaluate absorption in fine structure of a specimen.

Because aberrations and obscuration of aperture have much the same effect on the image, it is reasonable to specify a combined tolerance. Rayleigh's generally accepted specification for practical perfection in optical instruments implies that aberrations may cause a loss of not more than 22 percent in the fraction of energy falling within the central disc of the diffraction pattern. The obvious extension of this tolerance to reflecting systems is: The aberrations and the obscuring ratio together shall not cause a loss greater than 22 percent in the fraction of energy within the central disk. Acceptance of this argument eliminates Newtonian objectives of large numerical aperture (see Part I).

If the obscuring ratio is small, it causes a reduction in the percent of energy falling within the central disk equal to the percent of aperture obscured. Consequently, if the combined tolerance is accepted, the obscuration in a reflecting system must be less than 22 percent of the free aperture. There must also be some tolerance allowed for lens design and execution. An obscuring ratio of 10 percent in area was taken as a practical tolerance, to be bettered if convenient. Only a small portion of the aberration tolerance which is permissible for an unobscured aperture is consumed if the obscured area is less than 10 percent, because the effect of small aberrations is proportional to powers of the aberrations higher than the first power.

Computations of the effect of obscuring a portion of the area were carried out by application of methods described by R. Clark Jones[4] and are summarized in Fig. 4. In these graphs the intensity distribution in the neighborhood of the image of a "point" object is plotted against radial distance from the center of the diffraction pattern. The abscissa is radial distance R from the center of the image, the ordinate is the integrated intensity within the ring R to $R+\Delta R$. It should be noted that the curves of Fig. 4 apply only to an aberration-free objective.[5]

ON APOCHROMATISM

The objective described above satisfies at least the intent of the classification "apochromatic." An apochromatic objective is often understood to be an objective which has a common focus for three wave-lengths and which is corrected for spherical aberration and

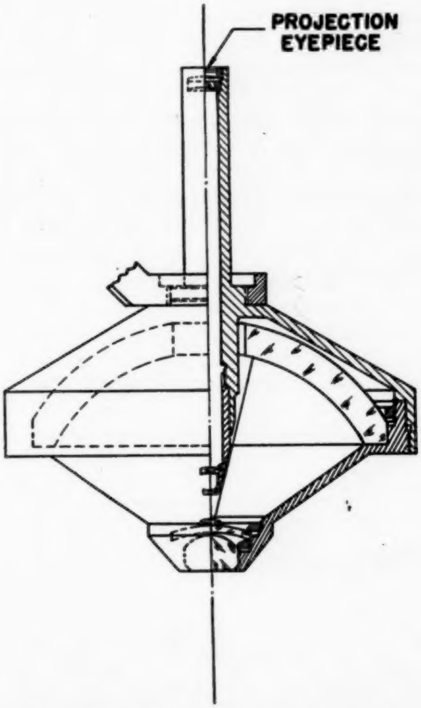

FIG. 3. The objective of Fig. 1 is shown here combined with its projection "eyepiece." The eyepiece corrects astigmatism residual in the objective.

---

[4] R. Clark Jones, J. Acous. Soc. Am. 16, 1947–171 (1945).

[5] Experimental evaluation of the effect of obscuration has been reported by T. Dunham, Jr., Special Report No. 2, American Cancer Society Grant No. PH-1B (Massachusetts Institute of Technology) (1948). The general conclusions of Dr. Dunham's report are in harmony with the theoretical treatment presented in this paper.

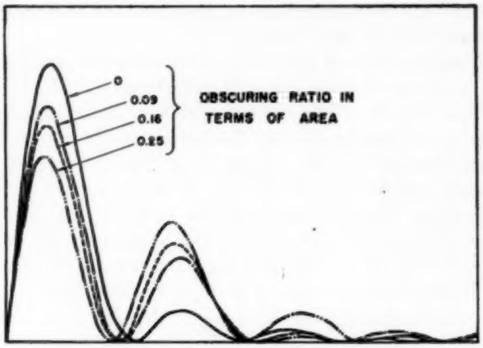

FIG. 4. The effect on diffraction of obscuring a central portion of the aperture is shown here. The abscissa is radial distance R from the center of the diffraction pattern. The ordinate is integrated intensity within the ring R to $R+\Delta R$.

coma at two wave-lengths. A less frequently used definition is: An apochromatic objective is one which is free of secondary spectrum and which is corrected for spherical aberration and coma at two wave-lengths. In many respects the latter definition is more suitable, for it places a certain positive limitation on the magnitude of chromatic aberration. The former definition merely requires that tertiary spectrum be so large that it obscures secondary spectrum. A catadioptric objective may have a residual shift of focus with wave-length which is of secondary, tertiary, or even higher order. This objective may not necessarily bring three wave-lengths of light to an exact common focus, but it may be better corrected than the usual apochromat.

It is suggested that an objective for which spherical aberration, coma, and shift of focal point with wavelength are corrected to within the Rayleigh tolerance over a large spectral interval be called *apochromatic over that spectral interval*. If the objective is a reflecting objective, the corrections for aberrations should be better than the classical Rayleigh tolerance in accordance with the principles enunciated above on obscuring ratio. This use of the term *apochromatic over a stated interval* introduces no ambiguity, for the term *apochromatic* (with no qualification) retains its classical implication.

CONCLUSIONS

The Schwarzschild reflecting objective may be combined with lens elements of fluorite, or fluorite and fused quartz, to provide an objective which is apochromatic over the wave-lengths 220 mμ into the near infra-red, without resort to aspheric surfaces. Numerical apertures at least as large as 1.1 may be realized.

The objective described in this paper is not considered to be a practical design. It serves to illustrate the adaptability of the Schwarzschild system and to provide a basis for the design of the new series of microscope objectives which will be described in subsequent papers of this series.

ACKNOWLEDGMENT

The author wishes to thank Mr. Samuel A. Stone of the Polaroid Corporation[6] for his valuable assistance in computing the objective described in this paper.

---

[6] Mr. Stone is at present with the Bradford-Durfee Technical Institute, Fall River, Massachusetts.

JOURNAL OF THE OPTICAL SOCIETY OF AMERICA VOLUME 39, NUMBER 9 SEPTEMBER, 1949

The Rise in Brightness of Infra-Red Sensitive Phosphors*

ROBERT C. HERMAN AND CHARLES F. MEYER
Applied Physics Laboratory, The Johns Hopkins University, Silver Spring, Maryland

(Received May 6, 1949)

A phenomenological theory of infra-red sensitive phosphors is given which assumes the existence of two types of luminescent centers in order to account for the so-called "inertia" effects in the rise of brightness. The equations describing the electron transfer processes have been integrated and show under certain conditions a very rapid initial rise in brightness followed by a relatively slow attainment of the maximum. The effect of varying the intensity of the stimulating infra-red radiation is discussed.

IN a recent paper, Scott, Thompson and Ellickson[1] have reported measurements of the time required for infra-red sensitive phosphors to reach maximum brightness when stimulated with infra-red radiation. These experiments were performed with phosphors of the strontium sulphide or selenide type activated with rare earths. The brightness of strontium sulphide phosphors activated with cerium and samarium (Standard VII) has a rise time of less than 10^{-4} sec. The brightness of strontium selenide phosphors activated with europium and samarium ($B-1$), on the other hand, rises to its maximum relatively slowly and some samples (Standard VI) show a very rapid initial rise of brightness which is followed by a slow rise to the maximum. These investigators conclude that this indicates the existence of two simultaneous processes.

The phenomenological approach in the study of the behavior of infra-red phosphors consists in setting up a set of rate equations which describe the transfer of electrons between trapping states, conduction band and luminescent centers. Equations of this type, first proposed by de Groot,[2] have been developed by the authors and applied to the problems of thermoluminescence, conductivity, and electron retrapping in phosphors.[3,4] These studies involve one type of luminescent center. The recent studies on the so-called "inertia" effects[1] led us to a reformulation of the basic rate equations for the case of two types of luminescent centers and consequently two simultaneous emission processes.

A qualitative examination of the problem indicates that in order to describe a slow and a fast component of the brightness variation with time it is necessary to postulate the existence of two types of luminescent centers, one having normal atomic emission transition probabilities from an excited state to the ground state and the other a long lived metastable state. The latter case might arise either from a normally forbidden transition between a perturbed excited state and the ground state or from an unperturbed excited state which is emptied thermally by the excitation of electrons to some other state of the same luminescent center which combines with the ground state.

The above physical situation can be described in the following manner. In Fig. 1 is shown the usual energy band scheme used to represent the states involved in the transfer processes. Consider a phosphor which has been previously activated so that the N trapping states per cm^3, all assumed at the same energy below the conduction band, are completely filled. Upon illumination with infra-red radiation of frequency ν and intensity I_0, electrons will be ejected into the conduction band from which they can either make transitions into the ground states of either type of luminescent center via excited states, or be retrapped. Let n_1 and n be the number of electrons per cm^3 in trapping and conduction states, respectively, at any time t. Let n' and n'' be the concentrations of electrons in the excited states of the luminescent centers and n_0' and n_0'' the concentrations of vacant ground states in the corresponding centers. The lifetime of electrons in states n'' (the centers yielding the fast rise time) is sufficiently short so that we shall consider transitions from the conduction band to ground states directly. Under these assumptions one obtains the

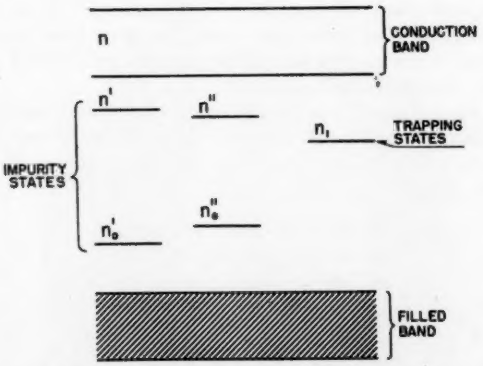

FIG. 1. Energy states of electron in infra-red phosphor containing two types of luminescent centers. The quantities n, n_1, n', and n'' designate the concentrations of electrons in the conduction band, trapping states and upper states of the luminescent centers, while n_0' and n_0'' are the concentrations of vacant ground states in the luminescent centers.

---

* The work described in this paper was supported by the Bureau of Ordnance, U. S. Navy under Contract NOrd-7386.

[1] Scott, Thompson, and Ellickson, J. Opt. Soc. Am. 39, 64 (1949).

[2] W. de Groot, Physica 6, 275 (1939).

[3] R. C. Herman and C. F. Meyer, J. App. Phys. 17, 743 (1946); J. App. Phys. 18, 258 (1947).

[4] Herman, Meyer, and Hopfield, J. Opt. Soc. Am. 38, 999 (1948).

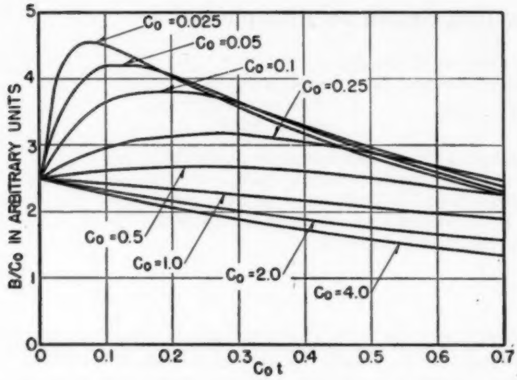

FIG. 2. Solutions of the rate equations describing an infra-red phosphor with two types of luminescent centers (see Eqs. 2), for the case $\epsilon=0.2$. Plot of B/C_0 (where B is the brightness in arbitrary units) *versus* C_0t for various values of C_0, which is proportional to the intensity of the stimulating infra-red light.

following set of differential equations:

$$\begin{aligned} dn_1/dt&=-C_0n_1+K(N-n_1)n,\\ dn/dt&=C_0n_1-K(N-n_1)n-Ann_0''-An(n_0'-n'),\\ dn_0''/dt&=-Ann_0'',\\ dn'/dt&=An(n_0'-n')-Pn',\\ dn_0'/dt&=-Pn', \end{aligned} \tag{1}$$

and

$$n_0'+n_0''=n+n_1+n',$$

where $C_0=\sigma_I I_0/h\nu$, $A=\sigma_L v$, and $K=\sigma_T v$. The quantities σ_L and σ_T are the capture cross sections of luminescent centers and traps for conduction electrons of velocity v, while σ_I is the cross section of a trapped electron for a photon of energy $h\nu$. It should be noted that it has been assumed that the probability of capture of conduction electrons into the ground state of one type of luminescent center is equal to the capture probability into the excited state of the other. The quantity P is the probability of transitions from the long lived upper state to the ground state in the centers which yield the slow brightness component.

Equations (1) can be written in convenient form by letting $\xi=n/N=\gamma\phi$, $\zeta=n_1/N$, $\eta''=n_0''/N$, $\eta'=n_0'/N$, $\omega=n'/N$, $\tau=C_0t$, $\tau'=ANt$, $\gamma=C_0/AN$, and $\epsilon=K/A$. We obtain,

$$\begin{aligned} d\xi/d\tau'&=\gamma\zeta-\epsilon\xi-(1-\epsilon)\xi\zeta-\xi^2,\\ d\zeta/d\tau'&=-\gamma\zeta+\epsilon\xi-\epsilon\xi\zeta,\\ d\eta''/d\tau&=-\phi\eta,\\ d\omega/d\tau&=\phi(\eta'-\omega)-(P/C_0)\omega, \end{aligned} \tag{2}$$

and

$$d\eta'/d\tau=-(P/C_0)\omega.$$

This set of non-linear differential equations has been integrated with the aid of a Reeves Electronic Analogue Computer. All the solutions were obtained for $AN=10^8$ sec.$^{-1}$, $P=1$ sec.$^{-1}$ and were subject to the condition that there are equal concentrations of the two types of luminescent centers. Several solutions were run for various values of C_0 between 0.025 and 4.0. When C_0 has the value unity the intensity of the stimulating infra-red radiation at 1μ is of the order of 670 millilamberts (10^{-3} watt/cm^2). The values of ϵ were selected on the basis of previous work[4, 5] to lie between 0 and 1.

Since the results of the integrations for various values of ϵ are qualitatively similar, those for $\epsilon=0.2$ only are shown in Fig. 2. We have plotted B/C_0 *versus* C_0t where B, the brightness, is given by $B\propto d(\eta'+\eta'')/d\tau$. The experimental data given in reference 1 can be replotted in this fashion and agrees qualitatively with the results shown here over the range of times and light intensities involved in the former. The experimental data were not obtained for times as long nor over as large a range of infra-red intensities as those used in the calculations. Furthermore it should be remembered that we have assumed equal concentrations of the two types of luminescent centers. This boundary condition, of course, can be varied in any desired manner and will change the relative values of the maximum brightness and the brightness corresponding to the initial rapid rise. The results shown in Fig. 2 for the case $\epsilon=0.2$ have been replotted in Fig. 3 in the form B *versus* t. It is in this representation that qualitative agreement with the experimental results of Scott, Thompson, and Ellickson[1] is evident for the smaller values of C_0. It is to be noted that for values of C_0 equal to or less than about 0.5 the rapid rise followed by the slow rise in brightness is

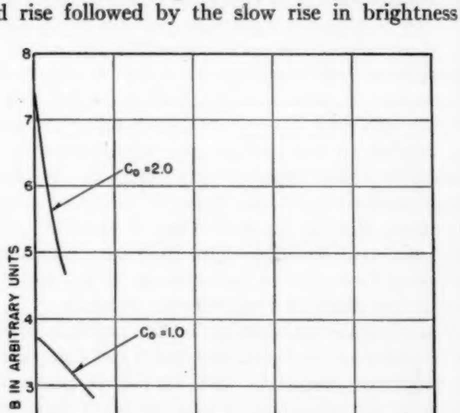

FIG. 3. Plot of the brightness, B (in arbitrary units), *versus* t in seconds for the case $\epsilon=0.2$. (Note that when $C_0=1$, the intensity of the stimulating infra-red radiation at 1μ is of the order of 7×10^2 millilamberts.)

---

[5] W. L. Parker and J. J. Dropkin, Phys. Rev. **74**, 1242 (1948).

clearly seen. The rapid initial rise occurs in a time of the order of $AN\ \ln(AN/2C_0)$, which is about 10^{-7} second.[4] For $C_0 \geqq \sim 1$ there is no indication of this phenomenon. This is apparently a result of the fact that very high light intensities quickly empty the traps so that the brightness maximum for both types of luminescent centers is reached quite early. It should prove interesting to extend experimental studies to higher infra-red intensities if possible, as well as to investigate these processes at various temperatures.

We wish to thank Dr. J. W. Follin, Jr. for profitable discussions and Dr. R. B. Kershner and Mr. J. D. Jordan for their interest and cooperation in the use of the Reeves Electronic Analogue Computer.

JOURNAL OF THE OPTICAL SOCIETY OF AMERICA VOLUME 39, NUMBER 9 SEPTEMBER, 1949

Artificial Fluorite

DONALD C. STOCKBARGER
George Eastman Research Laboratory of Physics, Massachusetts Institute of Technology, Cambridge, Massachusetts

(Received March 21, 1949)

This paper presents a condensed history of the research on artificial optical fluorite growth which was begun in the middle 1920's and reduced to practice under N.D.R.C. Contract OEMsr-45 with the Massachusetts Institute of Technology during 1940–45.

Fluorite castings were produced eventually by freezing purified molten CaF_2, contained in chemically clean graphite crucibles, in a vacuum-type contrivance patterned after the atmospheric furnace which had been developed earlier for growing lithium fluoride crystals.

The melt was prepared by heating selected fragments of colorless fluorspar mixed with about 2 percent PbF_2 which acted as a scavenger to eliminate certain more or less unavoidable impurities, notably products of hydrolysis, and which escaped before the crystallization. In a few instances it was made from a specially synthesized material although this procedure was not wholly desirable.

The crucibles were made by boring, reaming and turning graphite rods which possessed exceptional strength, homogeneity, and chemical purity. Their wall thickness was approximately 0.03 inch when feasible.

Crystallization occurred preferably in a thermal field characterized by a high, nonlinear temperature gradient which remained nearly constant with time.

Specimens chosen from about 1500 crystals, ranging up to 6 inches in diameter, were comparable with good natural fluorite in all essential properties and equal or superior to the best in soundness and dimensions.

INTRODUCTION

THE development of methods and apparatus for the growth of calcium fluoride crystals was begun many years ago with the hope of supplying material suitable for making optical parts needed in a spectroscopic research program.[1] Although visible accomplishments had not been striking, they had been sufficiently encouraging to warrant a continuation of the work on a small scale[*] during the lithium fluoride crystallization studies,[2] which suggested new methods of attack, until 1940 when practically colorless, transparent single crystals one-quarter inch or more in diameter were being grown almost at will.

Toward the end of that year the National Defense Research Committee requested the Massachusetts Institute of Technology to extend and improve the development with a view to producing artificial fluorite of useful quality and dimensions.[3] (See Fig. 1.) The request was vindicated, of course, by the growing need for optical fluorite (a) for the fabrication of lens systems having practically no chromatic aberration and (b) for making prisms, lenses and windows useful in the Schumann ultraviolet and near infra-red regions of the spectrum. It was further justified by the fact that the

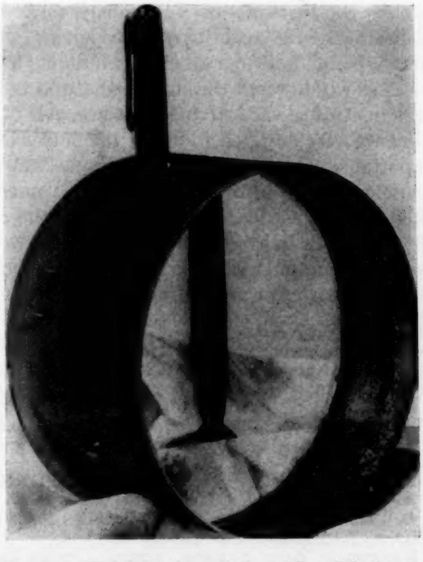

FIG. 1. Artificial fluorite cylinder with polished ends (3¾-in. diameter×2 in.).

---

[1] D. C. Stockbarger, J. Opt. Soc. Am. 14, 488 (1927); Am. Mineral. 12, 26 (1927).

[*] Much of the equipment used in this early work was purchased with funds granted by the Rumford Committee of the American Academy of Arts and Sciences.

[2] D. C. Stockbarger, Rev. Sci. Inst. 7, 133 (1936); see also D. C. Stockbarger, U. S. Pat. Number 2,149,076.

[3] N.D.R.C. Contract OEMsr-45.

known supply of natural material, always inadequate, was dwindling rapidly.

Under the pressure of the war emergency, foresighted optical scientists and technicians began to visualize applications of fluorite which would have been considered fantastic theretofore, e.g., in aerial camera and telescope systems. They were quick, therefore, to take advantage of the possibilities as soon as the first real signs of successful production were seen and so, not only during the war but increasingly ever since, they have created a demand which exceeds the now unprecedented supply. This fact suggests the need for a summary of the research and a condensed description of the methods and apparatus[4] which were selected for growing approximately 1500 artificial fluorite crystals, ranging up to six inches in diameter, during the contract period.†

HISTORICAL

The literature contains relatively few accounts of attempts to prepare alkaline-earth halide crystals although it seems safe to assume that studies have been undertaken in many laboratories.

Most of the workers have relied largely or wholly on (a) metathesis in complex melts without adequate control of the atmosphere or (b) precipitation from aqueous solution.[5–7] In some instances they obtained small, recognizable crystals but they did not develop successful methods of producing optically useful material. One worker crystallized five alkaline-earth chlorides and bromides from simple melts in room air[8] by the Kyropoulos method[9] but obtained no water-clear products even in the most successful experiments.

In the earliest work on calcium fluoride at the Massachusetts Institute of Technology most of the crystallizations were made by the Bridgman method[10] in which a pointed bottom crucible containing a simple melt was slowly lowered through the natural temperature gradient of a vertical tube furnace. All of those experiments were destined to fail at the outset because the importance of atmosphere composition, CaF_2 purity and temperature control was not fully appreciated. Although some consideration was given to the atmosphere, with a view to lengthening the lives of the carbon and molybdenum heaters, it was wholly inadequate in the essential matter of preventing deleterious chemical reactions with the already too impure melts. Commercial C. P. precipitated CaF_2 was fused and solidified in impure graphite crucibles. Temperatures were controlled as well as possible with the means at hand but even so they wandered widely. In retrospect, it seems remarkable that any moderately promising results were had.

Taking advantage of the lithium fluoride crystallization experience, later experiments were performed under more favorable conditions with greatly improved apparatus. Relatively superior CaF_2 was crystallized by the Stockbarger modification[2] of the Bridgman method[11] in pure platinum crucibles within a platinum-rhodium wire-wound furnace whose temperature was precisely controlled by a special regulator.[12] Unfortunately, however, the work was done in room air at atmospheric pressure. The single crystal castings, 1.5 inches in diameter, were translucent at best. It is noteworthy that some crystal samples, which had been set aside for possible future study, were found to have disintegrated into gray powder several months later!

The 1940 experiments, which first gave promise of practical success, were performed in small, evacuated molybdenum wire-wound furnaces. Fluorspar of near-optical quality was melted and frozen in crucibles made from rods of purified graphite intended for spectroscopic work. The method was that of Stöber[13] in which a stationary crucible filled with melt was slowly cooled in a vertical temperature gradient. The natural gradients were enhanced by supporting the crucibles on well-conducting pedestals mounted on the cooled furnace bases. Temperatures were controlled manually through regulation of power inputs even during the slow cooling. This circumstance was not favorable but evidently it was comparatively unimportant since fair, although small, crystals were produced.

GENERAL METHOD

During the development period of the Artificial Fluorite project,[3] calcium fluoride crystals were grown on a small scale from aqueous solution, from the vapor phase, and from the simple melt. The selected general method was growth from the melt by slow cooling in an appropriate temperature gradient. Furnace experiments were conducted within atmospheres of different compositions including practically pure nitrogen, hydrogen, and argon at pressures ranging from nearly zero to 76 cm. The preferred atmosphere was purified, dry nitrogen, at a pressure between 10 and 100 microns, maintained fresh by continuous streaming.

CaF_2 STOCK

The preferred material for conversion into fluorite was the best fluorspar obtainable. It approached optical fluorite in matrix quality and departed from it mainly in internal defects ranging from cracks to particulate inclusions of associated minerals such as galena, pyrite, sphalerite, quartz, calcite, and barite.[14]

---

[4] O.S.R.D. Report Number 4690.

† An extensive stockpile of the crystals was transferred by the O.S.R.D. to the National Bureau of Standards to make them available for use by government laboratories and, under certain circumstances, for non-commercial studies elsewhere.

[5] J. W. Mellor, *Comprehensive Treatise on Inorganic and Theoretical Chemistry*, III (Longmans, Green and Company, New York, 1923).

[6] J. N. Friend, *Text-Book of Inorganic Chemistry*, III (Charles Griffin and Company, Limited, London, 1925).

[7] E. V. Tsekhnovitser, J. Phys. Chem. (U.S.S.R.) **10**, 88 (1937).

[8] G. Heyse, Zeits. f. Physik **63**, 138 (1930).

[9] S. Kyropoulos, Zeits. f. anorg. allgem. Chemie **154**, 308 (1926).

[10] P. W. Bridgman, Proc. Am. Acad. **60**, 305 (1925).

[11] P. W. Bridgman, U. S. Patent Number 1,793,672.

[12] D. C. Stockbarger, Rev. Sci. Inst. **10**, 205 (1939).

[13] F. Stöber, Zeits. f. Krist. **61**, 299 (1925).

During the early months of the N.D.R.C. research the spar was purchased from a mining company operating in a region near Alamogordo, New Mexico.** Following the restriction of that area for U. S. Army bombing practice, it was obtained from deposits in the Kentucky-Illinois mining district through the cooperation of a special N.D.R.C. fluospar field survey[15] which had been established by request.

The latter fluorspar was hand-selected by an agent at the mines, shipped to the laboratory and there dissected to permit removal of unwanted inclusions and separated into graded fractions by a specially trained staff of spar pickers. After repeated inspections, the useful portions were washed with a solvent such as alcohol, dried quickly in a filtered air stream and finally stored in closed containers.

Three fractions, selected largely on the basis of color, clarity, etc., were retained. Grade A was so nearly perfect that usually it could be crystallized successfully, after addition of PbF_2 (see section on scavenging), with a single furnace treatment. Grade B generally required one or more recrystallizations each of which was preceded by crushing and addition of PbF_2. Grade C was useful mainly in the leaching of impurities from new crucibles but sometimes it had to be utilized in testing new furnace designs or, through repeated recrystallizations, in the growth of optical fluorite.

The quantity ratios of A to B and B to C grades were small. Furthermore, the total useful fraction of the fluorspar shipped to the laboratory was often so low that tons of ore were handled in preparing tens of pounds of desirable material. The reason was that the harmful included minerals were sometimes so badly disseminated or intergrown that even fine dissection was ineffectual.

The preparation of CaF_2 stock from fluorspar presented a psychological problem since only alert, intelligent pickers could do the work well. Naturally such workers found the task tedious at best and consequently, in the interests of morale and efficiency, they had to be relieved from tension by alternations of assignments, recesses and the like. Clearly there was need for high-precision automatic ore dressing means. Flotation and all other known methods were evidently unsuitable.

SCAVENGING

When progress in the production of fluorite crystals had reached the stage in which gross defects, such as opacity and color, were of rare occurrence, a new crystal defect was discovered. This was directional light scattering caused by tiny thin pockets—often clearly seen to be hexagonal in outline under the microscope—which lay well oriented in the 111 crystallographic planes. The defect was usually of minor magnitude if class A fluorspar had been used and sometimes was not noticed until after the crystal had been annealed. It was nearly always troublesome, however, and in extraordinary cases it was practically as bad as opacity.

It would be beyond the scope of this paper to include a full account of the many experiments and reasoning steps which led to a solution of the light-scattering problem. Briefly, the pockets were believed to be repositories of impurities which had been precipitated from solid solution, and the hexagonal ones were evidently well-formed negative crystals. The impurities were not all identified but were traced directly or indirectly (a) to associated minerals which had not been rejected completely during the dissection of the fluorspar and (b) to hydrolytic reactions.

The sensitivity of hot CaF_2 to water vapor, previously noted by Fremy,[16] was demonstrated clearly through a series of critical experiments in which hydrolysis was found to be appreciable at 100°C and to increase rapidly with rising temperature.[4]

Since the natural internal impurities, including water, were usually present in small quantities and water was always adsorbed on fluorspar surfaces, the simplest approach to a solution appeared to be the introduction of a scavenger.[17] Therefore a careful search was made for an addition agent which would react with and remove sulfides and oxides, these having been believed at the time to be largely responsible for the scattering. A further requirement was the complete disappearance of the scavenger in order that there should be no new contamination of the crystal as may have occurred to some extent in the scavenging of LiF.[18] The search led to the adoption of PbF_2.[19]

PbF_2, as a specific scavenger for use with fluorspar, was soon seen to be helpful in the control of light scattering when added in the ratio 1:50, but it was no panacea. Although it often permitted direct crystallization of grade A fluorspar, it was only partially effective with lower grades (see section on CaF_2 stock). It brought little or no relief from the vigilance required of the stock pickers.

The relatively low boiling point of PbF_2 limited its efficiency and necessitated the establishment of rather critical heating and melting schedules to insure maximum reaction, but it satisfied the escape requirement. The concentration of lead in twelve specimens was found spectroscopically to be less than one part per million in nine cases; one part per million in one case;

---

[14] W. Lindgren, *Mineral Deposits* (McGraw-Hill Book Company, Inc., New York, 1933), p. 635.

** This had been chosen because of its exceptional suitability.

[15] N.D.R.C. Contract OEMsr-563 with Princeton University.

[16] E. Fremy, Ann. Chim. Phys. 47, 5 (1856).

[17] D. C. Stockbarger, Faraday Soc. Discussion 5, 299 (1949).

[18] N. Wright, Rev. Sci. Inst. 15, 22 (1944).

[19] D. C. Stockbarger and A. A. Blanchard, U. S. Patent applied for.

TABLE I. Spectrochemical analyses (parts per million).

Material	Ba	Cu	Ga*	Fe	Mg	Na	Pb	Si	Yt
Butler Cave fluorspar	$^\mu$2.0	0.3	$^\mu$0.3	1.5	$^\mu$0.5	5.0	$^\mu$1	$^\mu$0.5	
III-362 Interface	$^\mu$2.0	1.0	$^\mu$0.3	1.0	1.0	3.0	10	$^\mu$0.5	
Natural optical fluorite	$^\mu$2.0	2.0	$^\mu$0.3	1.5	1.5	1.0	1	$^\mu$0.5	minor
III-372 Center	$^\mu$2.0	$^\mu$0.1	$^\mu$0.3	$^\mu$0.3	0.5	1.0	$^\mu$1	$^\mu$0.5	
III-372 Interface	$^\mu$2.0	0.2	$^\mu$0.3	0.3	1.0	2.0	$^\mu$1	1.0	
Synthetic CaF_2	$^\mu$2.0	0.5	$^\mu$0.3	0.5	1.0	0.5	$^\mu$1	1.0	
VI-79 Interface	$^\mu$2.0	0.5	$^\mu$0.3	0.5	1.0	0.5	$^\mu$1	0.5	
Selected Illinois fluorspar	$^\mu$2.0	0.5	0.5	0.8	0.5	0.8	$^\mu$1	0.6	
VI-79 Center	$^\mu$2.0	0.5	0.3	0.3	1.0	4.0	$^\mu$1	0.8	
Natural optical fluorite	$^\mu$2.0	0.3	$^\mu$0.3	0.3	0.5	5.0	$^\mu$1	1.0	minor
Selected Butler Cave fluorspar	$^\mu$2.0	0.5	$^\mu$0.3	0.3	0.5	10.0	$^\mu$1	1.5	
III-362 Center	$^\mu$2.0	0.3	$^\mu$0.3	$^\mu$0.3	0.5	2.0	10	1.0	

* Ga showed only occasionally.
$^\mu$ less than.

TABLE II.

Spar origin	Scavenger	N_D for 15°C	Laboratory
Arizona	No	1.43389	Eastman Kodak Company, Rochester, New York
New Mexico	Yes	1.433898	National Bureau of Standards, Washington, D. C.
Kentucky	Yes	1.433888	

TABLE III. Ultraviolet transmission limits.

Sample from	Thickness (mm)	Cut-off (Å)
2-inch cylinders grown in elevator furnace	5	1310
	3.5	1310
	4	1310
	5.5	1290
VI-86, a 4-inch cylinder grown in elevator furnace	9.5	1310
	2.5	1390
VI-96, a 4-inch cylinder grown in elevator furnace	10	1290
	2	1160

and ten parts per million in two cases. It was generally too low to have much if any ill effects on spectral transmissions and refractive indices (see Tables I–III).

SYNTHESIS

When the first principal source of desirable fluorspar had been cut off by military operations, a subproject was established in the Department of Chemistry, at the Massachusetts Institute of Technology, to study the synthesis of CaF_2. Although this project made notable contributions to the knowledge and art of preparing pure material, it failed to produce anything which gave even remote promise of being useful for crystal growing purposes. Treatment with anhydrous HF at temperatures above 600°C to counteract hydrolysis was ineffectual as was the addition of PbF_2. It was tentatively concluded, therefore, that synthetic CaF_2 was an unsuitable substitute for fluorspar and the project was largely disbanded.

Somewhat later Emeritus Professor A. A. Blanchard, the research chemist who had conducted the search for specific scavengers, worked out a simple coprecipitation procedure for producing a material which presumably was a complex fluoride of calcium and lead.[4] This salt usually could be crystallized successfully after one or more trials, with intermediate crushing and addition of PbF_2, as in the case of grade B fluorspar. Sometimes it could be crystallized directly. It possessed, however, the fluffiness characteristic of most synthetic CaF_2 preparations so that its use required either preliminary compression, or else sintering or fusion, followed by crushing and addition of scavenger, when it was desired to fill the crucible with melt.

FURNACES

The preferred means for fusion and crystallization of the CaF_2 was the "elevator" furnace, of the type developed during the lithium fluoride research,[2] in which the crucible was slowly lowered through an annular baffle[20] introduced to provide a short freezing region characterized by a nearly constant, high, non-linear vertical temperature gradient[12, 17] (see Fig. 2).

A second means was the "pot" furnace[12] in which the crucible was stationary and cooling was brought about by slow reduction in power input. Its tall freezing region was characterized by a changing, relatively low vertical temperature gradient. Except for omission of the annular gradient baffle and means for lowering the crucible during the crystallization, the pot furnace construction was similar to that of the elevator furnace.

The second type of furnace was studied to determine whether or not it could be used to grow relatively thin, large diameter lens blanks directly. It did produce many castings up to six inches in diameter and gave promise of making much larger ones. As predicted at the outset, however, its low vertical temperature gradient was unfavorable to controlled crystallization. Even small random changes in power input resulting from line voltage fluctuations often caused disastrous shifts in freezing level.

The furnaces consisted of graphite heating elements, thermally shielded by molybdenum and stainless steel radiation baffles, enclosed within water-cooled steel or

---

[20] D. C. Stockbarger, U. S. Patent Number 2,214,976.

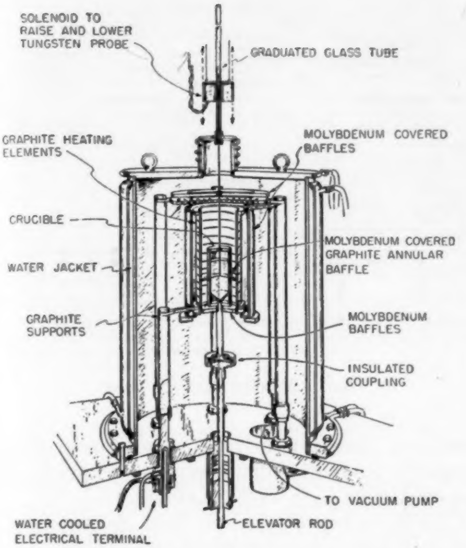
SOLENOID TO RAISE AND LOWER TUNGSTEN PROBE
GRADUATED GLASS TUBE
GRAPHITE HEATING ELEMENTS
MOLYBDENUM COVERED BAFFLES
CRUCIBLE
MOLYBDENUM COVERED GRAPHITE ANNULAR BAFFLE
WATER JACKET
GRAPHITE SUPPORTS
MOLYBDENUM BAFFLES
INSULATED COUPLING
TO VACUUM PUMP
WATER COOLED ELECTRICAL TERMINAL
ELEVATOR ROD

FIG. 2. Cut-away view of typical elevator furnace designed for growing fluorite crystals.

brass bell jars which rested on water-cooled steel baseplates. The housings were sealed to the bases by means of rubber or soft alloy gaskets and were rendered sufficiently tight so that they could be evacuated easily to pressures less than 0.1 micron and were maintained tight in all work regardless of the working pressure.

The bell jar water-cooling was provided in the form of welded outer jackets and/or tubing wrapped snugly around and soldered or welded in place to insure efficient heat transfer. The baseplates had loops of copper tubing soldered to their undersides.

Power for the heaters was conducted through internally water-cooled copper electrodes projecting up through the baseplates from which they were electrically insulated by mica washers and sleeves. Gas leaks were eliminated by applying red G. E. Glyptal lacquer on the undersides of the plates and baking overnight.

Means for raising and lowering the crucibles through the heated region comprised a polished steel shaft passing up through a water-cooled stuffing box centrally located beneath the baseplate. The upper end of the shaft had an electrically insulated graphite rod extension terminated by a seat (see Fig. 3); the lower end had provision for coupling to a motor-driven gear train whose output speed could be adjusted by means of a simple transmission mechanism. The stuffing box relied for tightness on compression of oil-lubricated Neoprene washers.

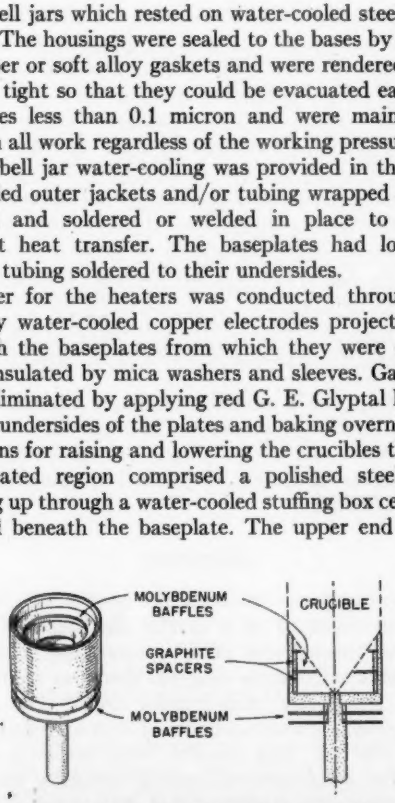
MOLYBDENUM BAFFLES
CRUCIBLE
GRAPHITE SPACERS
MOLYBDENUM BAFFLES

FIG. 3. Elevator seat for supporting crucible during crystallization.

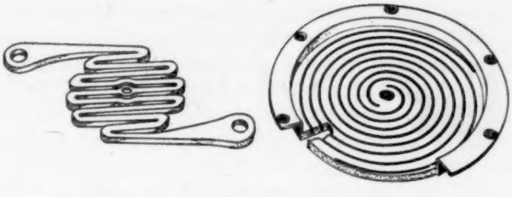

FIG. 4. Experimental top heaters machined from single graphite plates.

Each furnace was connected, through the baseplate, to an evacuation system consisting of two or more mercury vapor condensation pumps backed by a mechanical pump. A demountable vapor trap, kept cold with liquid nitrogen for safety, was placed between the vapor pumps and the mechanical pump. In its preferred modification the furnace had two tubing lines, passing through the baseplate, one of which led to a source of dry oxygen-free nitrogen; the other, to a pressure gauge.

Two graphite heating elements were used. One was cylindrical in shape and was mounted with its axis vertical; the other, flat and held symmetrically above the former with its plane horizontal. In order to increase the electrical resistance without reducing the thickness too much, as well as to facilitate the design and construction, they were cut in the forms of helices, spirals or grids (see Fig. 4). Electrical and mechanical connections to the water-cooled electrodes were made through graphite straps and rods by means of shrink fits and graphite screws and pins. Thermal conduction losses from the elements were controlled through choice of path lengths and cross sections, advantage being taken of I^2R heating at important points.

Heater power was individually supplied and regulated between zero and 14 kw by combinations of transformers and 7-kva G. R. Variacs. Depending on the design and usage, 20–40 volts per heater sufficed.

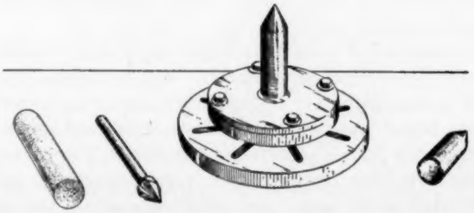

FIG. 5. Crucible tools and workpiece before and after machining.

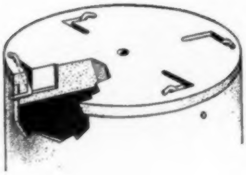

FIG. 6. View of crucible lid with retaining pins.

Automatic, variable-speed motor drives were provided for controlling the Variacs when necessary.

The nitrogen, whose role was to reduce the entrance of mercury vapor and to lower the evaporation losses of CaF_2, was passed over hot copper to remove oxygen and was tested by passing it over additional freshly reduced hot copper and sometimes by conducting it through a molybdenum filament incandescent lamp. Water vapor and carbon dioxide were removed by liquid nitrogen refrigeration. The furnace nitrogen pressure was regulated by a needle-type leak valve operated either manually or preferably automatically by means of a reversible motor controlled by the electronically amplified signal from an a.c. Pirani gauge bridge.

CRUCIBLES

Thin-walled, conical-bottom graphite crucibles, ranging up to six inches in diameter, held the melt and served as molds for the crystal castings. These articles were turned on the lathe from material selected with particular regard to purity, density and homogeneity.

An oversized rod, somewhat longer than the desired crucible, was drilled, bored, and finally reamed by a special tool to fit easily over an accurately centered mandrel of complementary shape. The mandrel material was preferably cast iron but often was seasoned wood (see Fig. 5). The crucible blank was slipped in place and anchored at the open end by means of a bit of adhesive tape or twine. It was then turned to shape and size on the outside, with the cutting tool traveling toward the open end, leaving a ring to hold the anchor until the final step which was the removal of the ring.

The wall thickness was approximately 0.03 inch under favorable circumstances. This dimension should have been smaller since thermal shielding and consequent interference with temperature gradient control depended on it. Often it was somewhat larger because its lower limit was set by leakage through the natural pores and tiny defects which were characteristic of the graphite stock.

It was found to be practically impossible to make a perfect crucible of any desirable wall thickness. Therefore it was customary to grade each one on an empirical scale based roughly on the estimated leakage after filling with liquids of different viscosities. For example, some crucibles dripped and were discarded; others exhibited moist spots and were retained if the total moist areas did not exceed certain amounts. It was sometimes necessary to make several trial turnings, especially when the diameter was relatively great, because hidden flaws were uncovered.

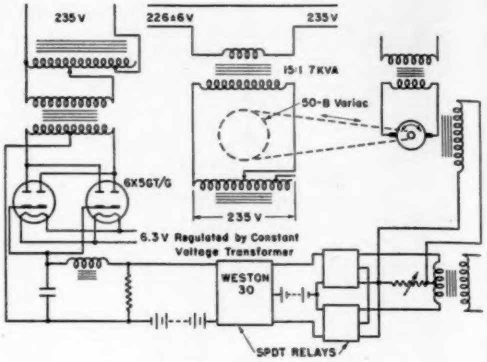

FIG. 7. Voltage regulator circuit.

Crucible covers of relatively thick graphite, e.g., 0.2 inch, were held in place by molybdenum pins to prevent accidental dislodgment by gas bursts which were common during the heating and melting of the CaF_2 and which were especially noticeable when synthetic stock was being used. Each cover had a centrally located vertical hole about 0.1 inch in diameter to facilitate the escape of gas and, in some instances, to serve as an entrance for a depth probe (see Fig. 6).

Before normal use, the crucibles were treated by melting grade C fluorspar in them and maintaining them well above the spar melting point for eight hours or longer (see section on CaF_2 stock). The leaching was usually necessary and sufficient to remove the small amounts of harmful impurities present within the graphite. Following the preliminary treatment, the crucibles were touched only with well-scrubbed hands or clean gloves and were thoroughly washed with alcohol before reloading as a further precaution against surface soil.

Crucibles could generally be reused several times if handled carefully because the castings did not adhere to the walls and always shrank enough in cooling to permit removal. Rarely, they failed by cracking during the first heating.

SOUNDING

Apparatus for determining the position of the freezing level consisted of a slender tungsten rod which could be lowered and raised magnetically through a series of small axially aligned apertures in the top baffles, top heater, and crucible cover. The driving armature was a small cylinder of iron attached to the top of the rod. This traveled freely within a sealed, graduated glass tube, extending vertically from the furnace top, with the translation of an external coaxial electromagnet. Levels were read off the tube gradua-

TABLE IV.

Wave-length (angstroms)	Indices of refraction* 15°C	35°C	55°C
†7678.58	1.430984	1.430768	1.430546
7065.188	1.431763	1.431553	1.431331
6678.149	1.432356	1.432142	1.431922
6562.793	1.432545	1.432335	1.432114
†5892.62	1.433893	1.433683	1.433465
5460.740	1.435023	1.434813	1.434593
4861.327	1.437106	1.436894	1.436680
4358.342	1.439555	1.439354	1.439143
4046.563	1.441573	1.441378	1.441168

* Averaged values of measurements taken on two prisms of artificial fluorite submitted to the National Bureau of Standards, United States Department of Commerce on September 29, 1944.
† Intensity-weighed mean of doublet.

tions with the aid of an index carried by the rod (see Fig. 2).

The described sounding method and means were useful but evidently they were not wholly essential since most of the 1500 castings were grown empirically without their benefit. Experience provided a basis for establishing provisional crystallization schedules and often made it possible to recommend schedule changes through inspection of preliminary results.

TEMPERATURE REGULATION

Furnace temperatures were regulated conventionally when necessary by raising and lowering electrical inputs. Usually the crystallization furnaces were sufficiently stable, electrically and thermally, to permit adjustments to be made empirically through Variac settings without the use of pyrometers. For the same reason there was no apparent need for thermostatic controls when the line voltage was kept from wandering more than a small fraction of one percent.[21]

Annealing furnace temperatures were measured (with a thermocouple) because the relationship between them and the Variac settings was not as well defined as it was in the crystallization furnaces. They were not stabilized by any kind of thermostatic equipment.

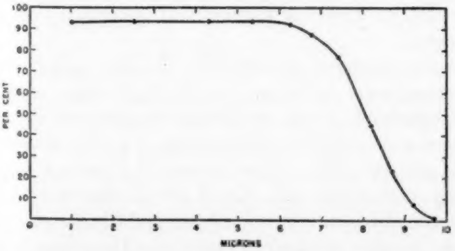

FIG. 8. Spectral transmission curve for randomly selected artificial fluorite crystal (thickness 33 mm).

During the crystallizations in the pot furnaces nonlinear input-time schedules were followed by driving the Variacs through specially designed cams and gear trains. This was necessary in order to insure nearly constant rates of growth. In all other processes, during which temperatures were slowly raised or lowered, linear input-time schedules were employed. During the crystallizations in the elevator furnaces, the Variac settings were fixed partly because complete data for establishing change schedules had not been accumulated, but more largely because the need for immediate introduction of such schedules was less evident than in the case of the pot furnaces.

LINE VOLTAGE CONTROL

Fluctuations in the line voltage and their effects were greatly reduced by connecting the secondary winding of an automatically controlled 7-kva 15:1 step-down booster transformer in one side of the line leading from the single phase 90-kva transformer which supplied power to the project at 226±6 volts, 60 cycles. The laboratory line voltage was raised to an average value of 235 volts.

The input to the booster transformer was provided by a motor-driven 7-kva Variac. The drive motor was directionally operated by relays activated by a potentiometer circuit in which the potential drop of rectified current, flowing from the primary source of power through a fixed resistor, was balanced against the e.m.f. of a battery of dry cells (see Fig. 7).

The regulator held the average line voltage constant within a small fraction of one percent over periods of hours and moreover controlled it even when practically the entire output of the 90-kva transformer was used. Without it, the six-inch crystals could not have been produced successfully since they were grown in a pot furnace which was very sensitive to temperature variations.

A similar voltage regulator was developed elsewhere[22] for the purpose of meeting the needs of an entire laboratory.

CHEMICAL PURITY

Spectrochemical analyses, a few of which are reported in Table I, showed plainly that the (cation) composition

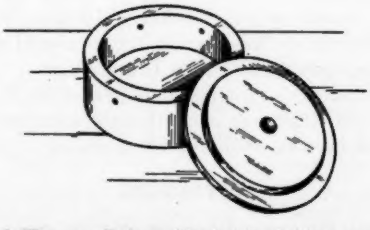

FIG. 9. Heavy-walled graphite box for holding crystals during final heat treatment.

---

[1] D. C. Stockbarger, Faraday Soc. Discussion 5, 294 (1949).

[22] R. H. Wallace, Plant Physiol. 20, 295 (1945).

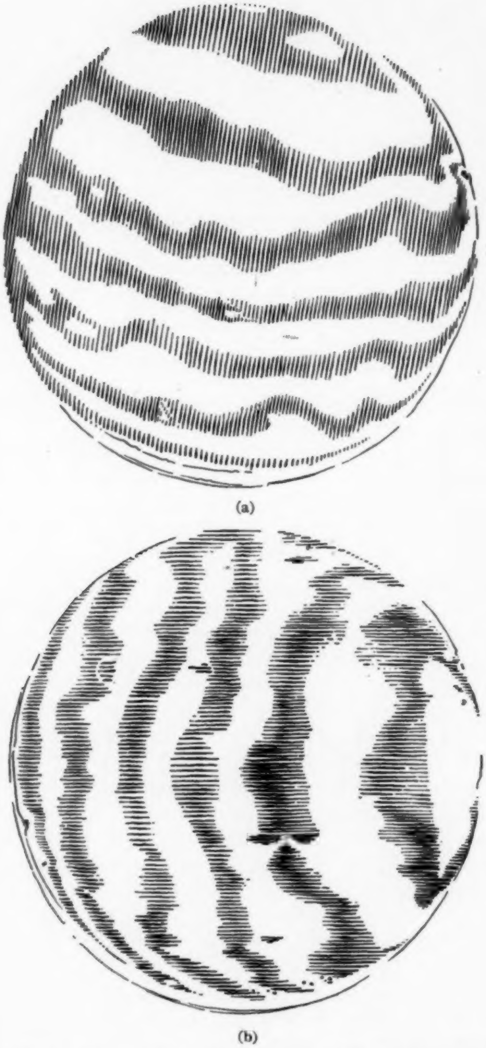

FIG. 10. Interference patterns exhibited by 3.9-inch artificial fluorite specimen in unpolarized light through 1.9 inches. Fringe curvature was caused by surface errors. (Drawn from photographs.)

of the artificial crystals was substantially the same as that of natural optical fluorite. Still better evidence of practical identity was seen in the measured refractive indices reproduced in Tables II and IV.

It is of particular interest to note that the Pb content was almost negligible even though large amounts of PbF_2 had been introduced for scavenging.

STRUCTURE

Natural fluorspar differs greatly in gross physical structure. It has been classed conveniently as (a) cleavable or crystallized, (b) fibrous to columnar, (c) coarse to fine granular and (d) earthy.[23] It may be said, therefore, that it ranges in crystallographic structure from near-perfect to near-disordered.

The artificial fluorite definitely fell in the first classification. Some of the factors which had contributed to the introduction of strain had evidently been unfavorable to perfection in fine structure, however, for cleavage surfaces were often inferior and oscillating-crystal x-ray line spectra were not sharply resolved. Such departures were of greater academic than practical interest.

CLARITY

Internal light scattering was observed, as in much of the natural fluorspar, when extreme care in preparation was not exercised. It usually arose from particulate impurities, either solid or gaseous, (a) generally disseminated, (b) confined in veils, or (c) crystallographically orientated in the 111 planes. In the last circumstance it was highly directional so that something like specular reflection occurred at certain incidence angles.

Light scattering resulted mainly from the use of improperly selected fluorspar, faulty growing conditions, and hydrolysis of the CaF_2. Its control in the last instance depended largely on efficient utilization of the scavenger or the temperature gradient during crystallization or, usually, of both.

Light scattering was not seen in the best crystals.

LIGHT TRANSMISSION

Table III presents reported ultraviolet transmission limits of several colorless crystal samples which were chosen at random.*** The figures compare favorably with those published for natural fluorite[24–26] and, in one case, indicate unverified exceptional performance.

Color is a common defect in fluorspar. It ranges from blue through red to brown,[23,27] and it is often beautiful enough to attract gem hunters. It is associated in the mind with ultraviolet absorption[24] although there appears to be little evidence of direct relationship. Further, its cause is various and generally somewhat obscure.

Color appeared in artificial fluorite under certain circumstances. Although its physical origin remained undetermined, it was recognized empirically as a consequence of errors in preparation, e.g., (a) use of impure graphite, (b) failure to seal the furnace housing nearly completely, (c) fusion of the fluorspar in the presence of too much evolved gas and (d) use of colored stock. It also resulted occasionally from exposure of the final product to sunlight or arc radiation. In some instances it could be altered or nearly eliminated through heat treatment, as has been possible sometimes with natural crystals.[24]

---

[23] E. S. Dana, *A Textbook of Mineralogy* (John Wiley and Sons, Inc., New York, 1932), p. 463.

*** Measurements made in Physical Measurements Laboratory, M.I.T.

[24] T. Lyman, Astrophys. J. **25**, 45 (1907).

[25] E. C. Schneider, Phys. Rev. **45**, 152 (1934).

[26] W. M. Powell, Jr., Phys. Rev. **45**, 154 (1934).

[27] A. N. Winchell, *Elements of Optical Mineralogy* (John Wiley and Sons, Inc., New York, 1932), p. 31.

Color was not visually detectable, even through a thickness of six inches, if the crystal casting had been made properly and therefore it was seldom found during the latter part of the contract period. It was not seen in the best crystals under any circumstances.

Infra-red transmission characteristics were determined**** for only one randomly selected casting (see Fig. 8). The long wave-length limit is in agreement with the accepted value for natural fluorite.

STRAINS

Internal strain in natural calcium fluoride crystals had been found to such an extent that the consequent birefringence was listed among the properties of fluorite.[23,27] As is well known today, it has been a defect rather than a characteristic.

Strain was present in freshly grown fluorite much as it had been from the beginning in many other artificial crystals. It was attributed to unfavorable historical circumstances of which faulty distribution of heat flow during growth was evidently paramount. It commonly varied considerably in magnitude with apparent close dependence on furnace design and operation, e.g., freezing level control.

Strain, at its minimum, caused little inconvenience. When great, however, it prevented successful shaping in the optical shop and so would have rendered the crystals useless for most optical purposes had they not been susceptible to heat treatment.

Strains were reduced somewhat by reheating the castings nearly to the melting point and then slowly cooling them in the upper heated region of an elevator-type crystallizing furnace where the temperature gradient was relatively low. They were more nearly completely removed by tempering in a special furnace which was intended to be practically free from temperature gradients.

Several annealing furnaces were built. The best one, which was far from satisfactory, consisted of an evacuated vertical stainless steel cylinder heated to approximately 800°C by a brick-insulated coil of Nichrome wire. It is to be noted that the temperature was far below the melting point of pure CaF_2. It contained massive, covered cylindrical graphite boxes into which the crystals were placed (see Fig. 9). The furnace failed principally through inability of the steel shell to withstand atmospheric pressure at the elevated temperature.

A somewhat representative empirical heat-treatment schedule for four-inch crystals consisted in raising the temperature over a period of three hours, holding it at 800°C for nine hours and then lowering it to 75°C during the following thirty-five hours. The boxes were not opened until they had reached room temperature.

Crystals treated in the annealing furnace contained so little residual strain that they could be cut with safety. Moreover they were suitable for incorporation in precision optical systems. They did often exhibit a little birefringence, however, and so were not always suitable for use in polarized light.

New designs of both crystallizing and annealing furnaces were expected to lead to further reduction of strain but had not been tested at the termination of the contract.

HOMOGENEITY

All of the crystals were homogeneous mechanically and chemically. They were devoid of cracks and fissures of all kinds and, except for minute amounts of other substances, they were pure CaF_2 throughout (see Table I).

All of the acceptable castings were completely devoid of color, body cloudiness, and directional scattering. A few had occasional thin hazy veils which were shown by tests to be optically harmless.

Probably few, if any, of the specimens possessed uniform ultraviolet transmission characteristics because the freezing level and other factors, to which the transparency was extremely sensitive, were only beginning to be controlled properly during the final months of the work. Table III, which includes all of the accumulated data, clearly indicates some variation in crystal VI-86.

Optical homogeneity, in the usual sense, was judged to be good by the facts that (a) precise index of refraction measurements could be made and (b) all tested telescope and camera lenses performed satisfactorily according to available reports. In substantiation, the maximum variation in path length was found interferometrically to be 0.3–0.7 wave-length per inch in five 4-inch diameter specimens;†† 0.1 wave-length per

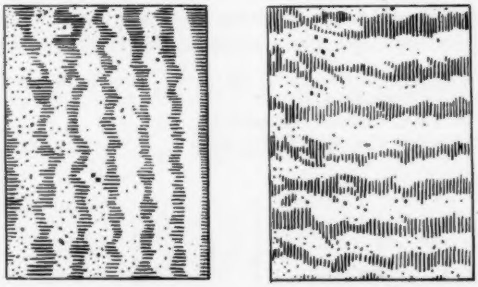

FIG. 11. Interference patterns exhibited by natural fluorite prism. Variation in fringe appearance was caused by changing path length. (Drawn from photographs.)

**** Courtesy, Perkin-Elmer Corporation, Glenbrook, Connecticut.

†† Measurements made at the U. S. National Bureau of Standards and reported by L. J. Briggs, Director.

TABLE V. Comparison between natural and artificial optical fluorite in 1945.*

Property	Natural	Artificial
Index, N_D (15°C)	1.43388†	1.43389
Ultraviolet limit (μ)	0.12†††	0.12††
Infra-red limit (μ)	9	9
Color	None	None
Light scattering	None	None
Size	Small	Large
Availability	Poor	Good
Internal cracks	Likely	None
Strain	Likely	Present (minor)
Optical inhomogeneity	Likely	Present (minor)

* Data refer to different selected crystals.
† Mean value, courtesy U. S. National Bureau of Standards.
†† 2-mm sample from 100-mm crystal.
††† Harrison, Lord, and Loofbourow, *Practical Spectroscopy* (Prentice-Hall, Inc., New York, 1948) p. 477.

inch in one 2-inch specimen.††† Two patterns for the worst case are sketched in Fig. 10. Two patterns for a natural crystal 60° prism (with better surfaces), considered suitable for fairly exacting work, are drawn for comparison in Fig. 11. Assuming chemical uniformity, it is concluded that departure from optical homogeneity was attributable to strain.

Only a small fraction of the many castings approached homogeneity in gross crystallographic structure. Most of the larger ones consisted of two or more tightly adhering components which differed appreciably in orientation. This was of no essential concern because the material is optically isotropic but it did introduce some difficulty in polishing because fluorite, like several other optical crystals, is noticeably anisotropic mechanically.

It is pertinent to add that with individual exceptions homogeneity, in general, was seen to be a far rarer property of natural fluorspar than it was of the artificial crystals.

OPTICAL-SHOP PROCESSING

The combined experiences of the Harvard Observatory Optical Shop,[28] the Perkin-Elmer Corporation,[29] the Massachusetts Institute of Technology Crystal Laboratory,[3] and others indicated clearly the necessity of avoiding both mechanical and thermal shock in working large pieces of artificial fluorite. This necessity was imposed by inherent physical properties of crystalline CaF_2 and not, insofar as is known, by defects in the crystals. Presumably it had not been generally recognized because usually theretofore optical fluorite had been available only in small pieces. At any rate, it was painfully demonstrated in several instances by breakage of good specimens and so, to avoid repetition of such expensive disasters, a few precautions are suggested:

(1) Impacts should be minimized. This is to be carried from the gross to the minute magnitude, e.g., shaping and grinding should be done with grains no coarser than Number 120 Carborundum. A smooth bevel must be maintained throughout grinding.

(2) Experience has demonstrated that, regardless of the degree of annealing, large artificial fluorite crystals are quickly cracked when chilled. Similar experience has been had with large pieces of natural fluorspar. The material should be sawed, ground, and polished at practically constant temperature. Use of water as little as 5°C cooler than the fluorite is likely to cause fracture.

(3) Low-temperature or air-drying cements should be used and the crystal element should be heated slowly and uniformly, if at all necessary, before application.

(4) Special care must be exercised in lens edging to avoid both mechanical and thermal shock.

SUMMARY

Fifteen hundred artificial fluorite crystal castings were produced by controlled freezing of purified molten CaF_2 in harmless surroundings. These ranged in diameter up to six inches and, in many instances, were comparable in optical quality with the relatively rare acceptable natural material (see Table V).

PERSONNEL

The following were awarded Certificates of Merit by the N.D.R.C. in recognition of continuous employment for six months or more during the four-year contract period: Isadore Åmdur, Hilda Benson, Arthur A. Blanchard, Marie Early, Walter Hargreaves, Arthur W. Knudsen, Raymond H. McFee, Louis O. Mitchell, Gerald M. Reed, Jr., Samuel Solar, Roy C. Stacy, Thomas Sullivan, Barbara Tate, Orville F. Tuttle.

Many others contributed to the work (a) officially as M.I.T. employees or students prior to the contract, (b) officially for less than six months during the contract, or (c) unofficially before the contract termination.

Thanks are extended to all who helped in any way.

---

††† Measurements made at Mt. Wilson Observatory and reported by T. Dunham, Jr.

[28] N.D.R.C. Contract OEMsr-474.

[29] N.D.R.C. Contract OEMsr-1177.

JOURNAL OF THE OPTICAL SOCIETY OF AMERICA VOLUME 39, NUMBER 9 SEPTEMBER, 1949

X-Ray Optics: The Production of Converging Beams by Total Reflection

W. Ehrenberg
Birkbeck College Research Laboratory, University of London, London, England

(Received March 22, 1949)

The total reflection of x-rays is applied to focusing the rays issuing from a fine slit. A method of computing the geometrical optics of surfaces of bent beams is given; it is shown that under certain conditions lateral aberrations for practical apertures are of the order of one micron or less. These results are confirmed by experiment.

INTRODUCTION

It has only recently[1] been pointed out that the inner surface of a right elliptic cylinder may form the ideal basis of an optical element which can be used in the optics of x-rays, as it retains its perfect focusing properties even if the angle χ between the rays and the surface approaches zero. X-rays are reflected only if χ is smaller than the critical angle of total reflection χ_c; $\chi_c \sim 9\times 10^{-3}$ for Cu$K\alpha$-radiation falling on an Au surface, and $\chi_c \sim 4\times 10^{-3}$ for the same radiation falling on a glass surface. For an ellipse with a and b as major and minor semi-axes, χ has a minimum $\chi_0 \sim b/a$ for the ray reflected at a curve element near the center of the ellipse where its radius of curvature is given by $r=a^2/b=a/\chi$. Hence, only elliptic cylinders with $b/a<\chi_c$ or with central radii of curvature $r>a/\chi_c$ can be used for refocusing x-rays. For practical reasons, one would desire the separation of object and image to be somewhere in the neighborhood of 10 cm. In the tests subsequently described, a value of $a=17.5$ cm was adopted, for which the minimum radii of curvature come to 20 and 44 meters, respectively.

Any part of an elliptic cylinder would reunite the rays coming from a correctly placed fine slit perfectly, but it is obviously difficult to produce such a surface. On account of the large radii of curvature involved, the central portion of a suitable elliptic cylinder can be approximated by the concave surface of a bent rectangular beam, but then the focus can no longer be perfect. Even for an ellipse the focus is perfect only if the object slit is infinitely fine and absolutely in the correct position. Hence, it is of interest to investigate the optical properties of surfaces of bent beams by computing the rays issuing from a line object and reflected from such surfaces. It should be pointed out that the problem of refocusing is different from that of imaging, as the latter requires that different elements of the reflector give the same magnification, a condition not required in the first case and not satisfied by the method here described. In spite of this, for sake of simplicity, the terms "image" etc. will be used.

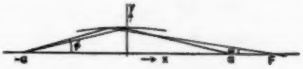

Fig. 1. Reflection of x-rays by a bent optical flat.

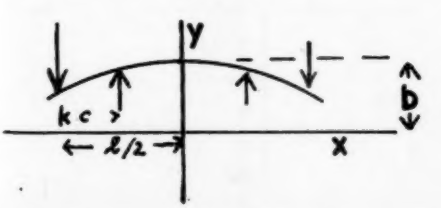

Fig. 2. Bending an optical flat by a symmetric pair of couples.

THE GEOMETRICAL OPTICS OF BENT BEAMS

Let rays coming from a point $-a$, 0 (Fig. 1) be reflected at a line $y=y(x)$, $y(x)$ an even function. Then the ray which is reflected at $x=0$ will cross the x axis at $+a$. A ray reflected at x will cross the x axis at $F=a+\Delta$; Δ is the longitudinal spherical aberration. The corresponding lateral aberration S is then $\omega\Delta$ where ω is the angle between the reflected ray and the x axis. The following relations are readily verified.

$$\psi=y' \quad (1) \qquad \omega=\phi-2\psi \quad (4)$$

$$\phi=y/(a+x) \quad (2) \qquad F=y/\omega+x=a+\Delta \quad (5)$$

$$\chi=\phi-\psi \quad (3) \qquad S=\omega\Delta \quad (6)$$

$$\Phi=\phi(x_-)-\phi(x_+). \quad (7)$$

ϕ is the angle between the x axis and the incident ray, χ is the angle between the surface tangent and the ray. An element of the surface will reflect the x-rays if $\chi<\chi_c$. In addition, it must be required that S remain smaller than a given value for such a range of x between x_- and x_+ that the aperture Φ of the bundle used is satisfactorily large. Rigorously, in (1), (2), (5), the

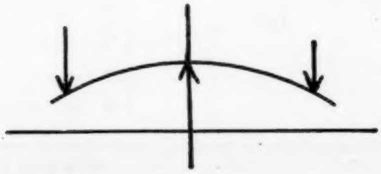

Fig. 3. Simplest method of bending an optical flat.

---

[1] (a) W. Ehrenberg, Nature **160**, 330 (1947); (b) P. Kirkpatrick and A. V. Baez, J. Opt. Soc. Am. **38**, 766 (1948).

angles should be replaced by their tangents, but one easily satisfies oneself that for the range of values here considered, i.e., $y\sim 0.1$ cm or smaller, $\omega<0.01$, $\phi<0.01$, $\psi<0.001$, no appreciable error arises through the use of radians instead. Equations (1)–(6) permit computing χ and S for any value of x, if $y(x)$ is a known function.

It is in general possible and it is here convenient to place a curve of any shape so that it approximates at $x=0$ to an ellipse with its center at the origin and its major semi-axis of length a coinciding with the x axis. Then, at $x=0$,

$$y'=0,\quad y=b=-a^2y'',\quad y''=-b/a^2=-1/r. \tag{8}$$

Any curve so placed reunites at $x=+a$ rays issuing from $x=-a$ and reflected in the immediate neighborhood of $x=0$.

A detailed discussion of the shapes of bent beams has been given by J. W. Landon.[2] Landon uses a co-ordinate frame so that the ends of the beam lie on the x axis, one end at $x=0$, and he approximates the radius of curvature r at any point by $1/r=d^2y/dx^2$. If the expressions given are specialized so as to cover the case of a symmetric pair of couples (Fig. 2), it appears that in the region between the inner supports the radius of curvature r is constant so that in this region $y(x)$ becomes rigorously a circle given, in the preferred co-ordinates, by

$$y=b-(\tfrac{1}{2}r)x^2-(\tfrac{1}{8}r^3)x^4+\cdots. \tag{9}$$

On inserting such values of b, r, x as were suggested at the beginning, one sees that the third term is smaller than the second one by a factor of the order 10^{-6}. Hence, it can safely be neglected and the surface of a bent optical flat can between the inner supports be taken as a parabola described by

$$y=b-(\tfrac{1}{2}r)x^2=b-(b/2a^2)x^2. \tag{10}$$

FIG. 4.

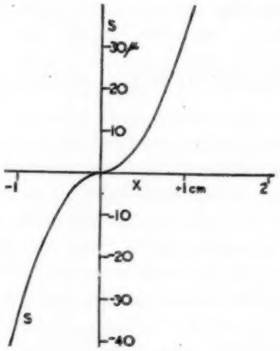

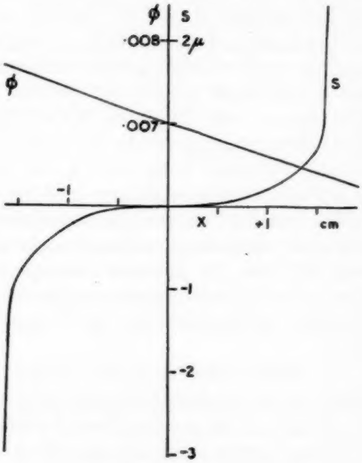

FIG. 6.

FIG. 5.

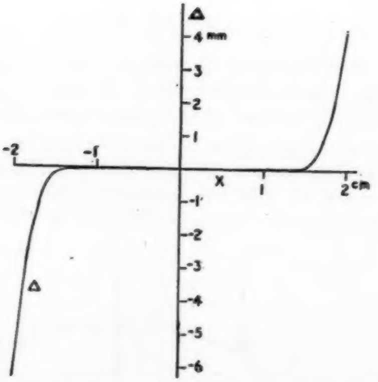

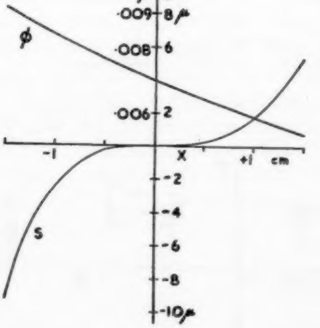

FIG. 7.

FIGS. 4–7. Lateral (S) and longitudinal (Δ) aberrations and the corresponding angles ϕ between the x axis and the outgoing rays, arising on focusing x-rays by differently bent optical flats.

---

[2] Sir R. Glazebrook, *A Dictionary of Applied Physics* (MacMillan Company, Ltd., London, England, 1922), Vol. 1, p. 810.

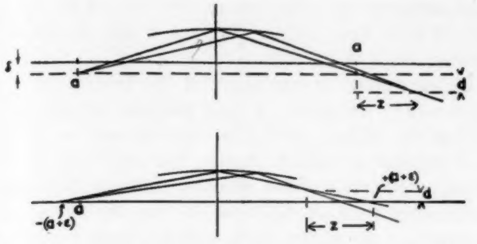

FIGS. 8 and 9. Displacement of object from correct position.

It will be shown presently that this inner region is of exclusive interest.

Neglecting the third term in (9) is equivalent to approximating $1/r=d^2y/dx^2$ so that the approximation introduced by Landon will not here introduce an appreciable error. This is of interest because, in order to establish the optical properties over the whole extent of the reflector, and also in order to find the forces arising on bending the optical flat, it is necessary to use the integrated expression given by Landon. When this is specialized to the case given by Fig. 2, and transformed to the co-ordinate frame described, Eq. (10) is reproduced for the inner region. The outer portions are given by

$$y=b-(b/l\gamma a^2)[-|x|^3+3lx^2/2 \\ +3l^2|x|(\tfrac{1}{2}-\gamma)^2+l^3(\tfrac{1}{2}-\gamma)^3], \quad (11)$$

where γ is the ratio of the arm of each couple to the total length l of the beam. For the special case $\gamma=\frac{1}{2}$ (Fig. 3), the inner region vanishes altogether and the entire curve is described by

$$y=b-(b/2a^2)x^2+(b/3la^2)|x|^3. \quad (12)$$

The expressions (10) to (12) should be compared with the equation for the ellipse

$$y=b-(b/2a^2)x^2-(b/8a^4)x^4+\cdots. \quad (13)$$

It is seen that the inner region of a surface of a bent beam (Eq. (10)) differs from the ellipse (Eq. (13)) by a fourth-order term in x. For the outer portions of a bent beam (Eq. (11)), and the case Eq. (12) a third-order term arises. The significance of these deviations can be found by inserting these equations into the relations (1)–(7) and computing the aberrations S etc., for given values of a and b of the ellipse to be approximated and for given values of l and γ. In general, one sees that y in (10) is independent of l and γ, so that in this case l and γ determine only the range over which (10) holds, but not the aberrations arising from the part of the surface between the inner supports.

TABLE I.

δ	$x=+1.5$ cm	$x=-1.5$ cm
+0.01	−1.6	−3.5
−0.01	+2.6	+1.4
+0.005	−0.35	−2.1
−0.005	+1.7	+0.31

TABLE II.

ϵ	$x=+1.5$ cm	$x=-1.5$ cm
+0.5 cm	+1.8	+0.86
−0.5 cm	−1.1	−2.5

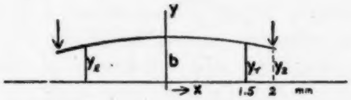

FIG. 10. Varying the thrusts indicated by arrows while the diameters of the supporting pins Y_l and Y_r are fixed.

In (10), (11), and (12) y is proportional to b. As according to (1)–(6) χ, ω, and S are proportional to y, one set of computations provides information for all values of b. Results of computations are shown in Figs. 4–7.

Figure 4 shows the aberrations S arising when rays are reflected by the surface of a beam bent according to (12), with $a=17.5$ cm, $b=0.1225$ cm, and $l=4$ cm. For the range of the diagram χ varies only between 0.0069 and 0.0071, so that χ remains with a safe margin below the critical angle of Cu$K\alpha$-radiation falling on a Au surface. The aberrations are very large.

In Figs. 5 and 6 the longitudinal and transverse aberrations arising in the case covered by (10) and (11) are shown for the same values of a, b, and l with $\gamma=\frac{1}{8}$. Here χ varies practically between the same limits as above, but it is seen that between $x=-1.5$ cm and $x=+1.5$ cm, that is, between the inner supports, S varies only from -0.8 micron to $+0.6$ micron. Between $x=-1$ cm to $x=+1$ cm, S changes from -0.25 micron to $+0.2$ micron. The aberrations rise rapidly only outside the inner supports. From the curve $\phi(x)$ also given in Fig. 7 it is seen that the aperture permissible for $S<1\mu$ comes to $\Phi=0.0012$. Figure 7 gives the aberrations for a smaller value of a with b chosen so that χ remains very near to 0.007. Here, for $a=5.8$ cm, $b=0.041$ cm, Φ goes up to 0.0035. The diagrams suggest that a definition of 1 micron and better should easily be obtained.

This conclusion is based on the assumption that the slit, the center of curvature of the reflector, and its

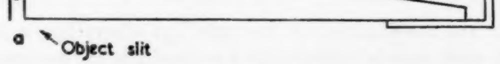

FIG. 11. Diagram of camera. The surface *bb* is flat and serves as a reference. Rays issuing from the object slit are defined by the selector slit and after reflection reunited in the plane of the photographic plate.

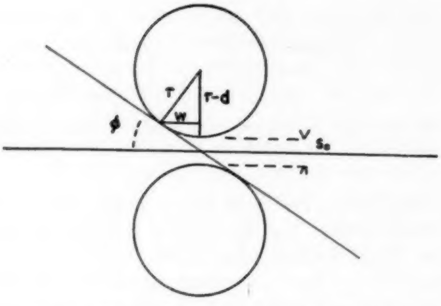

FIG. 12. Slit consisting of two parallel cylinders.

radius can actually be set with absolute accuracy. This, of course, will not be possible. Hence, it remains to see what aberrations will be introduced by the errors inadvertently incurred in setting up a focusing reflector, the interest now being restricted to a surface of the shape (10). Errors can arise in the first instance through a normal or lateral displacement of the object slit, Figs. 8 and 9. If the object is displaced normally to the "axis" of the system by δ (Fig. 8), an elementary if slightly tedious calculation following substantially the lines indicated by Eqs. (1) to (6) shows that for rays reflected near $x=0$, the image point is displaced from the symmetric point $x=a$, $y=-\delta$ to a point $x=z+a$ and $y=-d-\delta$, where z and d are given by

$$z=2a\delta/(b+\delta)\quad d=2\delta(b+\delta)/(b-\delta). \tag{14}$$

For example, for $a=17.5$ cm, $b=0.1225$ cm, a displacement $\delta=0.01$ cm of the object results in a displacement of the image $z=3.1$ cm, $d=0.023$ cm. These displacements are not small, so that the aberration arising must be calculated for the neighborhood of the new image point; experimentally, one may search for the focal plane by a set of trial exposures. The calculation of aberrations proceeds along the lines of Eqs. (1) to (6). It is only necessary to replace in (2) y by $y+\delta$ and to replace Eq. (5) by

$$F=(y+d+\delta)/\omega+x=a+z+\Delta.$$

Aberrations have been computed for $\delta=\pm0.01$ cm and $\delta=\pm0.005$ cm. The values of S in microns for the limiting cases $x=\pm1.5$ cm are given in Table I. Again, if the object is displaced by a small amount ϵ along the "axis" away from the center (Fig. 9), the "paraxial" image is displaced from the symmetric position by amounts z and d given by

$$\begin{aligned} z&=-4\epsilon+10\epsilon^2/a\\ d&=-4b\epsilon/a+14b\epsilon^2/a^2. \end{aligned} \tag{15}$$

For the computation of the spherical aberration, a in (2) must now be replaced by $a+\epsilon$, and Eq. (5) becomes

$$F=(\gamma+d)/\omega+x=a+z+\Delta.$$

A displacement of the object by $\epsilon=0.5$ cm results in displacements of the image by $z=-1.9$ cm and $d=-0.0125$ cm. Table II gives a set of values of aberrations S in microns.

As the radius of curvature of the reflector is given by $r=a^2/b$, an error of two percent permissible in setting the object ($\epsilon=0.02a$) corresponds to an error of 4 percent in radius. Again, one may ask to what accuracy the ends of the reflector must be depressed if $Y_l=Y_r$ are fixed as indicated in Fig. 10. As the force increases, a decreases from infinity, and b increases. Now from (11) with $\gamma=\frac{1}{8}$, $l=4$ cm, at $x=2$ cm, $Y=Y_2=b(1-47/24a^2)$, while at the fixed points at $x=\pm1.5$ cm, $Y=Y_r=b(1-1.25/a^2)$. Hence b can be eliminated, and a change in Y_2 is related to a change in a by

$$dY_2\sim(1.75Y_r/a^3)da. \tag{16}$$

Here Y_r can be replaced by b, when with $a=17.5$ cm and $b=0.1225$ cm, $dy_2=0.0004$ da. If (Table II) an error in a of 0.5 cm is permissible, the error in y_2 should not exceed 0.2 micron. Good uniformity and equality is required of the supports marked by Y_l and Y_r in Fig. 10, for the difference between Y_l and Y_r can be considered transferred to the object where it is ten times magnified, hence the difference Y_l-Y_r should be less than one-tenth of the permissible δ. The effect of a small asymmetry in the length of the outer portions of the beam has not been calculated, but tested experimentally, and no difficulties were found to arise from that cause.

The discussion shows that the accuracy required for about 1-micron definition is high but not beyond reasonably good design and workmanship.

EXPERIMENTAL RESULTS

The experimental arrangement used is shown diagrammatically in Fig. 11. The actual dimensions are: distance between object slit and center of reflector, 17.5 cm, between center of reflector and plate, 17.5±1.5 cm. The optical flat is 4 cm long, 1.5 cm wide, and about 4.5 mm thick; the inner supports are placed 5 mm from each end, the supporting pins have a diameter of 1.18 mm. Copper radiation was used throughout. Only the slit system and the reflector assembly warrant some further explanation.

The object slit aa' consists of two round steel rods separated by spacers and pressed together by set

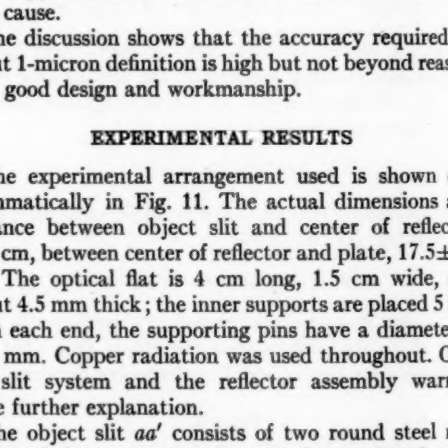

FIG. 13. Mechanism for bending optical flat.

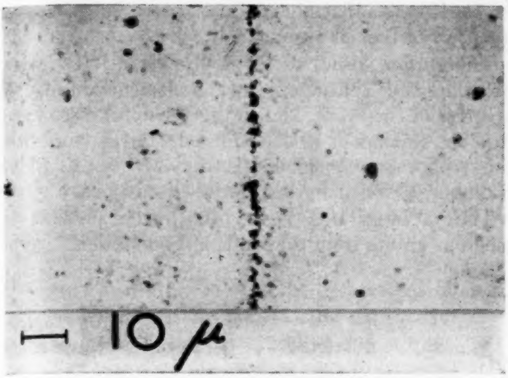

FIG. 14. Microphotograph of image of slit obtained by reflection of x-rays on a bent optical flat.

screws. The rod *a* is set with reference to the flat surface *bb* by means of a feeler gauge. The following relations hold for such a slit system (Fig. 12): (a) Rods touching; rays normal. ($\phi=0$, $s_0=0$). Let the effective width $2d$ of the slit be defined so that at its boundaries the intensity is reduced to 0.1; then $2\omega\mu\sim 3$, where μ is the absorption coefficient, e.g., 2×10^3 cm^{-1} for copper radiation in iron. Then $\omega^2=2rd=5\times 10^{-7}$ and for $r=0.2$ cm, $2d=2\times 10^{-6}$ cm; as the interest of this paper is confined to slits which are at least ten times wider, the slit material may be considered as impenetrable. (b) Rods not touching. If s_0 is the slit width for normal rays, the effective slit width s for rays making an angle ϕ with the normal rays is given by $s_0-s=r\phi^2$. The largest value of ϕ arising here is 10^{-2}, the angle of total reflection of copper radiation on gold; with $r=0.2$ cm, $s_0-s=0.2\times 10^{-4}$ cm so that the change in effective slit width with angle may be neglected.

The reflector is pressed against the reference flat *bb* via the steel pins *cc* (Fig. 13) which are reduced in the middle to allow the x-rays to pass. Commercial ground silver steel rods are satisfactorily accurate. The movement of the micrometer screw *d* is transferred to the ends of the reflector via the steel spring *a*, so chosen that a transverse of the screw of 1 mm corresponds to a movement of 0.01 mm of the edges, *e*—*e*. In this way the curvature of the reflector can be controlled with very good accuracy. A similar idea was used by Michelson and Benoit, 1895, for setting a bearing pin of an interferometer mirror. As the diameter of the supporting pins *cc* is given, the angle χ_0 between the central ray and the mirror is controlled by the position of the object slit *aa′* (Fig. 11).

It was believed at first that it would be necessary to adjust the reflector by visible light, and provisions were made to test both its radius and center of curvature. While these tests were useful in confirming calculations which indicated that the bending of the reflector would not lead to a rupture of the glass, and in drawing attention to a non-uniformity of the original support pins, etc., it was found later on far easier to make all adjustments by means of x-rays. So long as the object slit was not extremely fine, say still several microns wide, the reflected beam could easily be seen on a fluorescent screen. Then, after narrowing down the slit if required, a short series of trial exposures led at once to both the correct curvature of the mirror and the correct plate distance. As an example of the focal lines obtained Fig. 14 shows a micro photograph of an image produced by a glass reflector (copper anticathode, $a=17.5$ cm, nuclear particle emulsion). The background is fog only and not due to x-rays. Without the reflector the beam at the position of the plate would be about 0.15 mm wide.

A line width of 1 to 2 microns was readily obtained, but it appeared not easy to get finer lines. One would probably require special thin emulsion in order to observe them. For, the photoelectrons responsible for making the photographic grains developable must be expected to have a range of a micron or two in the photographic emulsion. And further, as the x-rays penetrate the emulsion, a line finer than 1 micron would not be clearly visible in an ordinary emulsion with a microscope objective of sufficient aperture and hence low depths of focus.

The concentration of intensity provided by the focusing reflector may be estimated as follows: For a bent reflector, the intensity (x-ray density) of the image should for a sufficiently large anticathode be proportional to the angular width Φ of the beam and inverse to the separation $2l$ of object slit and image, as the magnification of the slit is about unity:

$$I=\Phi/2l. \tag{17}$$

The denominator accounts for the direction of the line focus, the numerator for the direction normal to it. The intensity does not depend on the width of the image.

For a system of slits, on the other hand, consisting of two equal slits spaced as indicated in Fig. 15, the

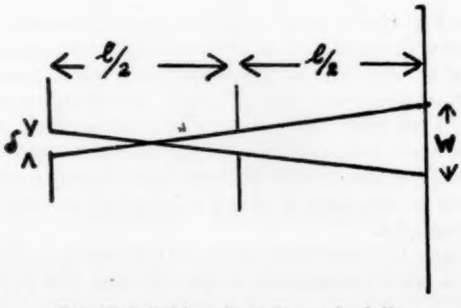

FIG. 15. Definition of rays by a pair of slits.

width of the image $W=3\delta$ and hence its intensity is approximately given by

$$I=\frac{1}{l}\frac{1}{3}\frac{2\delta}{l}=2\delta/3l^2=2W/9l^2. \qquad (18)$$

In either case, a clear path of length about $l/2$ is available in front of the image. To give a numerical example, let $l/2=3$ cm and $W=10^{-4}$ cm. Then in the first case $I=12\times10^{-5}$ for $\phi=0.0014$, and in the second $I=6\times10^{-7}$, so that the reflector gives 200 times the intensity of the slit system.

The author wishes to thank Professor J. D. Bernal (London) for continuous encouragement during the progress of this work, and for very helpful discussions. Also Dr. R. Herz of Kodak Limited, Harrow, for advice about photographic materials, and Mr. R. E. Siday, (Edinburgh) for many instructive discussions.

The investigations have been made possible by generous grants from the Nuffield Foundation.

JOURNAL OF THE OPTICAL SOCIETY OF AMERICA VOLUME 39, NUMBER 9 SEPTEMBER, 1949

X-Ray Optics: Imperfections of Optical Flats and Their Effect on the Reflection of X-Rays

W. Ehrenberg
Birkbeck College Research Laboratory, University of London, London, England

(Received March 22, 1949)

It has been observed that some stray light (x-rays) is thrown into the neighborhood of the focus obtained if x-rays are focused by a bent optical flat. Most of this extra light is due to imperfections of the optical flats, while halation, Fresnel diffraction at the slits and air scattering make only minor contributions. An analysis of the distribution of this extra light, a study of the effect of controlled irregularities and pin hole images of surfaces taken with x-rays lead to definite conclusions about the structure of such surfaces.

INTRODUCTION

THE possibility of producing fine focal lines of x-rays at a large distance from the optical system suggests that the total reflection of x-rays can throw new light on the structure of optical surfaces. This structure must reveal itself through radiation thrown into the neighborhood of the focus. Even if the optical surface used were perfect, one would expect the focal line to widen somewhat for prolonged exposures, due to the shape of the wave-optical focus and due to halation (scattering of x-rays in the photographic emulsion). Also Kiessig[1] has observed some stray light when reflecting x-rays from tarnished mirrors. In fact, however, the stray light observed in the neighborhood of the focus is due almost exclusively to a permanent surface structure.

HALATION AND FRESNEL DIFFRACTION

In Fig. 1(a–e), a series of photographs is reproduced, taken with the camera described in the preceding paper using an object slit of 10μ, which show the increase in width of the image with increased time of exposure. A G.E. CA6 diffraction tube with Cu anti-cathode provided the x-rays, as it did for all experiments described below. The reproduction does not show the very gradual fading at the edges observed on some of the original photographs.

Figure 1f demonstrates that halation makes, at most, only a small contribution to the widening. The photograph is a repeat of 1d with a length of Pt wire of 0.01-mm diameter placed a few mm in front of the plate, almost parallel to the focal line. The shadow of the wire is still clearly visible which shows that the rays blackening the plate come from the direction of the source and not from the image in the plate. (Separate tests have shown that the extent of halation depends on the presence of matter of low atomic number in the neighborhood of the emulsion. X-ray film shows halation strongest owing to its thick carrier, stripped, i.e., unbacked, emulsion shows it least.)

Fresnel diffraction at the defining aperture of the beam produces, as will now be shown, a very noticeable widening, but does not account for the effect observed. The defining aperture is either the "selector" shown in Fig. 11 of the preceding paper, which prevents x-rays from falling onto the outer parts of the reflector, or the edges of the reflector itself.

When photographs are taken with object slit (a few μ wide), selector (1–3 mil wide), and plate in their normal positions, but without the reflector, a rather wide but well-defined line is recorded, of slightly more than double the width of the selector. On prolonged exposure this line widens, too, and develops wings, in a manner similar to that shown by the focused line. Striking evidence that this effect is in fact due to diffraction is afforded by the following experiments.

The beam issuing from the anti-cathode is restricted by three slits, *viz.* the two slits just described, and in addition by a slit (about 4-mil wide) perpendicular to the other two, immediately in front of the photographic material, in this case an x-ray film showing comparatively strong halation. Thus in the absence of diffraction a squarish blob is formed on the film (Fig. 2a). On prolonged exposure this blob grows with diffuse boundaries due to halation; the size of the halo is a measure of the x-ray dose received by the film (Fig. 2b and c). In addition, however, there are streaks where the slit in front of the film allows radiation coming from the selector to fall onto it. These streaks cannot be caused by halation.

---

[1] H. Kiessig, Ann. d. Physik **10**, 715 (1931).

Now it is known that diffraction effects arising from apertures depend on the rate of decrease of intensity at their edges. In particular, if in the aperture plane the intensity of light decreases gradually, the intensity in the image plane in the shadow region decreases more rapidly than for a sharp edged boundary of the aperture. If the light passed through a slit has the distribution of a gauss error curve, the intensity in the image plane decreases exponentially. In order to approximate these conditions, the sharp edged selector slit was replaced by a slit produced by pressing a fine (0.15-mm diameter) tungsten wire into a thin lead sheet. When the tungsten wire was removed a narrow gap about 0.01 mm appeared in the lead sheet, defined by feather edges of slowly increasing thickness. As the lead was too thin to absorb the x-rays completely, the slit so produced was backed by a much wider slit of thicker material. For short exposures, then, the blob on the film widens somewhat, Fig. 2d showing the results of an exposure about equivalent to that of 2a. An exposure equivalent to that of 2c is shown in e. The side streaks are now almost suppressed. This shows that the streaks of 2b and c are in fact due to Fresnel diffraction and not to other causes one might suspect, such as air scattering.

The detailed theory of the diffraction shown in b and c is rather involved. One might think that either edge of the selector acts independently, as its width is large compared with λ and the problem is simply that of diffraction by an edge, of light originating at the object slit. The solution of this problem is known in terms of Cornu's spiral and an approximation valid far in the shadow region is in fact readily derived. The intensity calculated is, however, well below that observed by comparing the density of a (Fig. 2d) with that in the wings of c. The failure is due probably to the fact that no coherent wave front exists in the region of the selector. The actual source of light, the anti-cathode, is so far away from the object slit and this is so wide in terms of λ that it selects beams from points of the anti-cathode which, according to the position of these points either pass freely through the selector or foul one edge or the other. The beams which foul it may effectively be limited by a very narrow slit, one cheek of which is one side of the object slit and the other the opposite cheek of the selector, and the width of this composite slit goes to zero as the origin on the anti-cathode shifts; very intense contributions far out in the shadow regions may well be expected. A study of diffraction by two non-coplanar obstacles has recently been published by C. F. Ellis[2] but the theory has not been carried sufficiently far to allow calculating the intensities in the shadow region.

If now the test of replacing the sharp edge selector by a gradually fading one is repeated with the focusing mirror in position, no noticeable difference between the wings in the two cases is observed. Hence it must be concluded that the widening shown in Fig. 1 is mainly due to the action of the reflector. It should be added that air scattering plays no important role. This was confirmed by comparing the development of wings with the whole camera in air and in vacuum.

THE STRUCTURE OF THE REFLECTING SURFACES

One must, by exclusion, conclude that the wings are caused by the reflecting surfaces; no decisive improvement was found, however, by varying the material of the reflector and its condition. A bare glass surface gave somewhat less wings than a surface coated with gold. Gold surfaces seemed to deteriorate with time, but not glass surfaces. There was no certain difference between an optically finished glass surface and an optically finished quartz surface. Trebling the time of polishing a glass surface had no noticeable affect. A

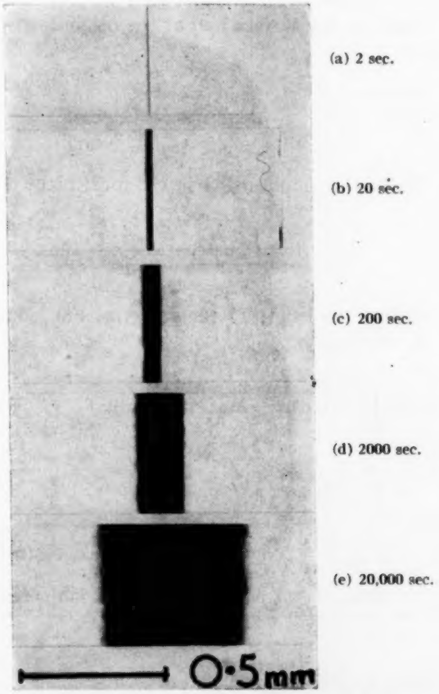

FIG. 1(a–e). Change of appearance of the x-ray optical image of a slit with time of exposure.

---

[2] C. F. Ellis, Am. J. Phys. **16**, 8 (1948).

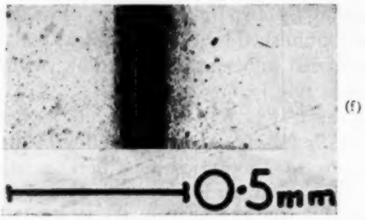

FIG. 1f. Shadow of wire in heavily darkened region of image.

number of experiments which will now be described led to the view that the process of polishing leaves a surface in a state of imperfect flatness, similar to the state of a beach from which the sea has receded. The separation of the valleys and hills may be of the order of 0.1 cm but the height of the hills is only of the order of angström units.

The appearance of light at any particular distance from the geometric focus due to the reflector can be interpreted as due to a particular Fourier component of the irregularity of the surface. Let a particular Fourier component be a modulation in height of the average surface level so that (Fig. 3),

$$h=h_0\sin\omega x=h_0\sin 2\pi x/d.$$

The phase difference between light reflected at any point on the surface and at the origin is given by

$$\cos(x\mu+h\mu'),$$

where

$$\begin{aligned}\mu&=(2\pi/\lambda)(\cos\theta-\cos\theta')\\ \mu'&=(2\pi/\lambda)(\sin\theta+\sin\theta').\end{aligned}\qquad(1)$$

Hence the amplitude A in the focal plane comes to

$$A=\int_0^l dx\cos(\mu x+h_0\mu'\sin\omega x),\qquad(2)$$

l being the length of the reflector. For small values of h_0 or of $h_0\mu'$

$$\begin{aligned}A&=\int_0^l dx(\cos\mu x-h_0\mu'\sin\omega x\sin\mu x)\\ &=\int_0^l dx(\cos\mu x-(h_0\mu'/2)\cos(\omega-\mu)x\\ &\qquad\qquad+(h_0\mu'/2)\cos(\omega+\mu)x)\\ &=\frac{\sin l\mu}{\mu}-\frac{1}{2}\frac{h_0\mu'\sin(\omega-\mu)l}{\omega-\mu}+\frac{1}{2}\frac{h_0\mu'\sin(\omega+\mu)l}{\omega+\mu}.\end{aligned}\qquad(3)$$

Only in the neighborhood of

$$\begin{aligned}\mu&=0\\ \omega-\mu&=0\\ \omega+\mu&=0,\end{aligned}$$

the amplitude has an appreciable value; $\mu=0$ denotes the reflected beam and $\mu=\pm\omega$ the $\pm$ first order of interference, no other orders arising. With $\phi=\theta'-\theta$

$$\mu\approx 2\pi\phi\sin\theta/\lambda\qquad(4)$$

so that for the reflected beam $\phi=0$, and for the diffracted beams

$$\phi=\pm\lambda/d\sin\theta\approx\pm\lambda/d\theta.\qquad(5)$$

The intensity in the neighborhood of any region is given by

$$I=\int A^2d\phi,$$

and hence the intensity of the reflected beam

$$I_0\approx\int_{-\infty}^{+\infty}d\phi\frac{\sin^2[(2\pi/\lambda)l\phi\sin\theta]}{[(2\pi/\lambda)\phi\sin\theta]^2}=\frac{l\lambda}{2\sin\theta}\qquad(6)$$

and similarly by integrating over the neighborhood of

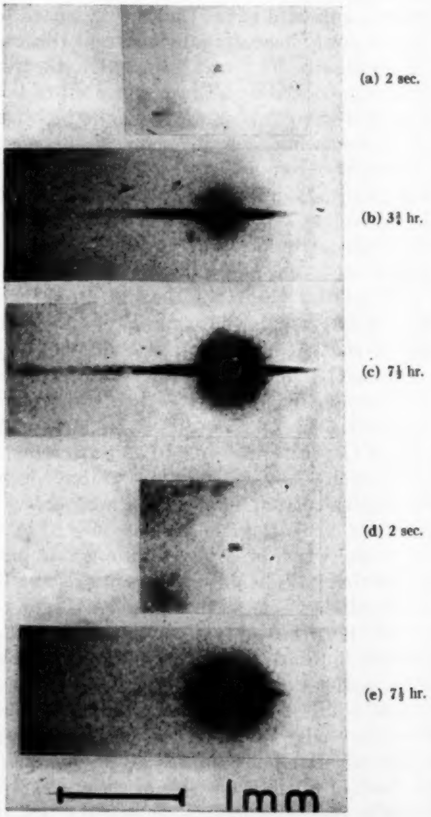

FIG. 2. The blobs caused by halation are clearly distinguished from the streaks due to Fresnel diffraction (b, c). The streaks can be suppressed by shaping the diffracting slit (e).

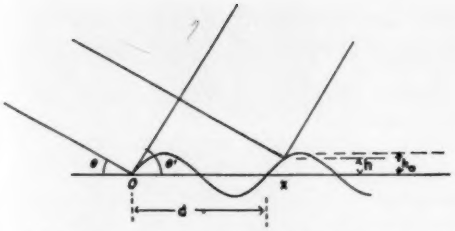

FIG. 3. Reflection of x-rays by a "flat" with super-imposed sinusoidal variation in height.

the diffracted beam

$$I_{\pm} \approx (h_0\mu'/2)^2 \cdot l\lambda/2 \sin\theta, \tag{7}$$

and hence the ratio of the intensities of the diffracted beam to the reflected beam

$$I_{\pm}/I_0 = (h_0\mu'/2)^2. \tag{8}$$

This expression holds obviously only at a distance from the center large compared with the slit width. Now from (Fig. 1f), and similar records not here reproduced, one may estimate the distance D from the center at which the intensity had dropped to that of the shortest exposure. Hence, with $a=17.5$ cm as the image-reflector distance, and $\theta=0.0031$, values for ϕ, μ' and d are obtained, and with the exposure time ratio as the intensity ratio $I_{\pm}/I_0$, also the corresponding amplitude of the Fourier component. Table I summarizes such computations.

Jentzsch[3] has suggested that an optical reflector for x-rays may have irregularities in height not exceeding $\lambda/8\theta$, so that here irregularities up to 60A should be permissible. The calculation given shows, however, that far smaller irregularities give rise to an appreciable background.

TABLE I.

$I_{\pm}/I_0$	0.1	0.01	0.001	0.0001	0.00006
D(cm)	0.0005	0.0025	0.01	0.03	0.043
ϕ	0.00003	0.00014	0.0006	0.0017	0.0025
$10^{-6}\mu'(\text{cm}^{-1})$	0.025	0.025	0.027	0.031	0.035
d(cm)	0.17	0.035	0.008	0.003	0.002
h_0(A)	25	8	2.3	0.65	0.45

In order to confirm these ideas by direct evidence, an irregularity of the type described was artificially produced on an optically flat surface such as was used for the focusing experiments: an optical flat was placed behind a set of parallel wires of 0.35-mm diameter spaced 0.7 mm apart and through this wire grid gold was evaporated onto it; the grating so obtained was just visible, which, according to some data given in the literature[4] leads to an estimate of 5-A thickness in agreement with the thickness calculated from the amount of gold evaporated and the distance of the glass plate from the evaporator. Also in view of the geometric arrangement of the evaporator and the small amount deposited, this grating of 0.7-mm period may be considered as sinusoidal. The reflector thus prepared was put into the camera, bent to focusing curvature and exposures were taken with Cu radiation as before. For very short exposures single sharp lines were obtained as before, but for only slightly longer exposures—a few minutes—interference fringes appeared on either side of the geometric focus. These are shown in Fig. 4 for different values of χ_0. Prolonged exposure led to no new effects. The spacing of the fringes was found to be in agreement with the simple theory of gratings. The occurrence of only one set of fringes shows that the grating is nearly sinusoidal. The intensity of the fringes of ± first order to that of the center line could be estimated from exposures of different duration, and from these experimental values for $I_{\pm}/I_0$ the height of the grating computed from Eq. (8) came to 10A, in reasonable

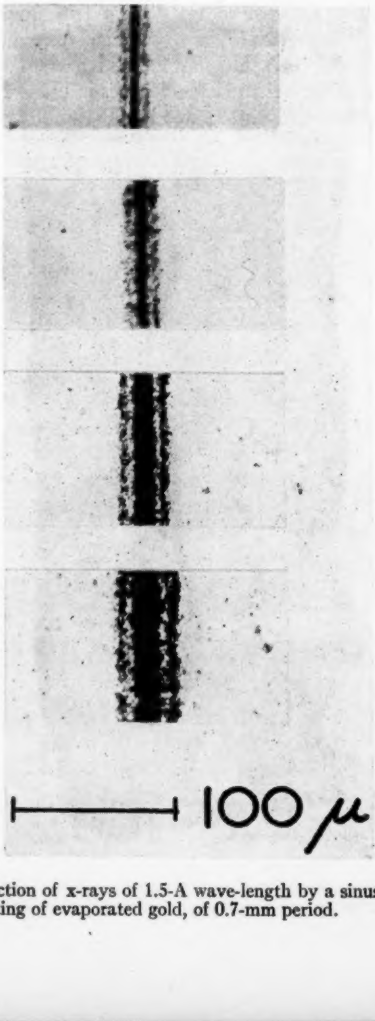

(a) $\chi_0=0.0053$

(b) $\chi_0=0.0038$

(c) $\chi_0=0.0031$

(d) $\chi_0=0.0022$

FIG. 4. Diffraction of x-rays of 1.5-A wave-length by a sinusoidal grating of evaporated gold, of 0.7-mm period.

---

[3] F. Jentzsch, Physik. Zeits. 30, 268 (1929).

[4] F. Coeterier and M. C. Teves, Physika 3, 968 (1937).

agreement with the previous estimate. It is remarkable how clearly these fringes show up. This shows that the corresponding Fourier components of the irregularities of the optical glass are far smaller than the value of 10A.

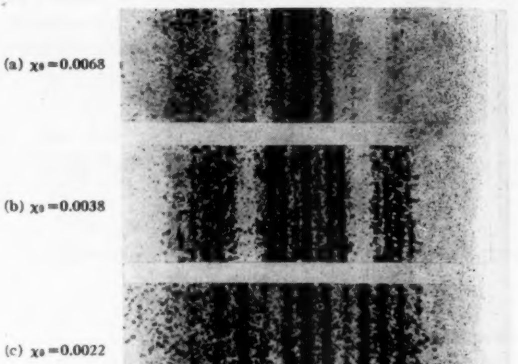

FIG. 6. Diffraction of x-rays of 1.5-A wave-length by a "thick" grating of 0.7-mm period.

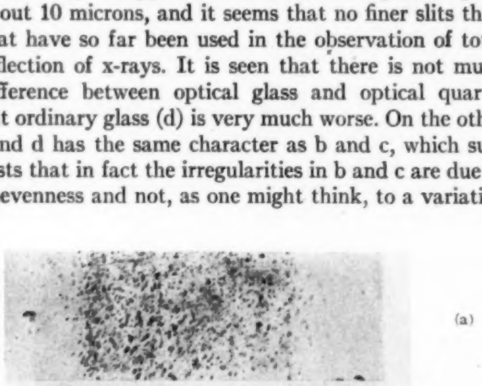

FIG. 5. Rays issuing uniformly from a fine slit (a) are modulated on reflection by optical surfaces, disclosing their uneveness (b–d).

These ideas were confirmed by another experiment. When, in preparation for refocusing the very fine object slit, the reflector is inserted but left plane, a kind of one-dimensional pin-hole image of the reflecting surface is produced on the photographic plate. Such photographs are shown in Fig. 5 b–d. That the striations are not, as was suspected first, due to the irregularities of the anti-cathode, is shown by a, taken without reflector. This image is quite uniform, and that the uniformity of a as compared with b (glass optical flat), and c (quartz optical flat) is not due to a different spectral distribution was checked by repeating a over a wide range of voltages. The striations in b and c are observed only with a very fine object slit, probably less than 1-micron wide. They disappear when the slit is opened up to about 10 microns, and it seems that no finer slits than that have so far been used in the observation of total reflection of x-rays. It is seen that there is not much difference between optical glass and optical quartz, but ordinary glass (d) is very much worse. On the other hand d has the same character as b and c, which suggests that in fact the irregularities in b and c are due to unevenness and not, as one might think, to a variation of the reflection coefficient. c and d are produced by the whole length (40 mm) of the reflector whereas the stop (selector) was in position for a and b. One can count about 25 streaks in c, one for each mirror element of about 1.5-mm width. Now under the conditions of experiment a curvature of about 50 meters would produce complete focus: as the focusing is far from complete let us assume that the elements have a curvature of 200 meters. This means that each element forms a valley of about 10-A depth, in reasonable agreement with the estimate of the Fourier components.

Now, the reflector should on the average be isotropic. Hence the conclusion that the surfaces themselves consist of irregular hills and valleys of about 10-A height and 1-mm wide so shaped that the Fourier components come as indicated above. These conclusions are compatible with the results of an examination of optical flats by means of multiple beam interferences obtained by Tolansky and Wilcock.[5] A more detailed theoretical and experimental study on the lines indicated may lead to a more precise insight into the structure of surfaces.

Photographs similar to those in Fig. 4, but with more gold evaporated, to about 300-A thickness, are shown in Fig. 6. The grating is no longer sinusoidal so that a great number of orders appear. Again the separation of the fringes is that predicted by the elementary theory, but the intensities are complicated.

---

[5] Tolansky and Wilcock, Proc. Roy. Soc. **A191**, 182 (1947).

For (a), χ_0 is well outside the angle of total reflection of glass, so that only the gold covered portions should contribute. It is interesting to see that the ± first orders are stronger than the zero order. Qualitatively the intensities are explained by the facts that the width of the reflecting portion about equals that of the nonreflecting portion, and that the reflecting portion is of varying height. A quantitative discussion would be somewhat complicated and barely worth while. For b and c, χ_0 is within the angle of total reflection of glass and only the distribution in height should be responsible for the intensities. That this is not quite true is shown by d, which is a repeat of c after a thick layer of gold has been coated over the whole surface. d is a pure variation-in-height grating. The intensities in d are different from those in c, which shows that c cannot be such a grating.

Now, it is known that if a glass surface is metallized, the reflecting properties change only gradually nonmonotonically to those of the metal[6–8] though quantitative data for gold on glass are missing. Further, it appears that a thick gold coat at small values of χ such as in c and d may have a reflection coefficient a few percent below that of glass. Such effects would qualitatively explain the difference between c and d, although it is doubtful that they can do so quantitatively. On the other hand, reflection on gold and on glass may take place with a difference in phase which could have a very great effect on the intensities.

CONCLUSION

The study of surfaces by x-ray reflection is of interest by itself, but it may not be easy to improve optical surfaces to such an extent as to reduce appreciably the stray light near an x-ray optical focus. In some applications of the optical element described, this stray light will do no harm. For others, it will be the limiting factor. If, for instance, the optical element is used as a collimator in an x-ray diffraction camera, the stray light will prevent the observation of weak interferences in the neighborhood of the direct beam, unless it is cut off by an additional stop. This stop must seriously decrease the efficiency of such a collimator, but preliminary calculations and tests have indicated the existence of a well defined range of usefulness in this field.

The author wishes to thank Professor J. D. Bernal (London) for continued encouragement and for helpful discussions. Also Professor O. Pryce (Oxford) for drawing his attention to the method of suppression of high order diffraction effects and for a discussion of interference phenomena on evaporated gratings, and Professor S. Tolansky (London) for a discussion on the results of multiple beam interference tests of optical flats.

---

[6] H. Kiessig, Ann. d. Physik **10**, 715 (1931).

[7] E. Nähring, Physik. Zeits. **32**, 730 (1931).

[8] A. I. Alichanow and L. A. Arzimovic, Zeits. f. Physik. **82**, 489 (1933).

JOURNAL OF THE OPTICAL SOCIETY OF AMERICA VOLUME 39, NUMBER 9 SEPTEMBER, 1949

On the Corrector Plates of Schmidt Cameras

E. H. Linfoot and E. Wolf
The Observatory, Cambridge, England

(Received May 2, 1949)

The paper discusses the problem of designing the aspheric surface of a Schmidt camera so as to obtain optimum performance, in an agreed sense, over the field taken as a whole. A solution is obtained in a form which allows the optimum plate-profile to be quickly determined for a Schmidt camera of given aperture-ratio and field-size, working over a given spectral range. It is shown that at apertures near $f/3$ the optimum plate can be obtained by slightly decreasing the strength of an ordinary "color-minimised" Schmidt plate, while in wide-field systems working at apertures near $f/1$, it is better to use a plate with neutral zone at the edge of the aperture.

1. INTRODUCTION

As a rule the corrector plates of Schmidt cameras are designed without paying much attention to the off-axis images. The aspheric profile is calculated so that the system gives an error-free axial image in light of one particular wave-length, and at the same time the paraxial convexity of the plate is chosen so as to make the axial color-error as small as possible.

This simple procedure gives satisfactory results in medium-sized cameras of not too short focal ratio. However, it is evident from the theoretical point of view that some improvement could be obtained by a more careful choice of plate-profile. For the sizes and shapes of the off-axis images depend on the monochromatic off-axis aberrations of the system as well as on its chromatism, and the correct choice of plate-profile would take account of these two aberrations simultaneously, combining them with axial undercorrection to the best advantage over the field taken as a whole.

The present paper shows how a choice of plate-profile can be made which, in a certain sense, optimises the optical performance of the camera over a given field. In Section 2 the aberration theory of the Schmidt camera is summarised in a form suitable for the later discussion. In Section 3 a definition of effective image-radius is set up, and in Section 4 this image-radius is evaluated, for a Schmidt of given aperture-ratio and field, in terms of two parameters a and p which describe the plate-profile. Lastly, in Section 5, the results obtained are used to design optimum plate-profiles in two numerical cases and to draw one or two general conclusions. In particular, it appears that in wide-field systems of apertures approaching $f/1$ the optimal plate-profile is one which is nearly flat at the edge; while at apertures near $f/3$ an optimised plate can be obtained, with neutral zone at or near 0.866 of the full radius, simply by shortening the wave-length at which the plate is designed to give axial stigmatism.

2. THE ABERRATIONS OF THE SCHMIDT CAMERA

We wish to see what choice of plate-profile will give optimum imaging (in some agreed sense) over the whole of a given field.

Let R denote the radius of curvature of the mirror, H the radius of the effective plate-aperture, and set

$$\mu = H/R. \tag{1}$$

Since the focal length f of the system is nearly equal to $\frac{1}{2}R$, it follows that 2μ is very nearly equal to the numerical aperture of the system, so that in an $f/2$-camera $\mu=\frac{1}{8}$, approximately.

It can be shown that, to the order of approximation adopted in treating μ^2 as negligible in comparison with unity, there is no loss of generality in supposing that the corrector plate has its aspheric surface towards the mirror.*

If we use ordinary Cartesian coordinates in the plane of the aperture-stop, with origin on the axis of the system, the edge of the aperture stop is the circle $x^2+y^2=H^2$. It is more convenient to introduce new coordinates u, v, connected with x, y by the scale-relation,

$$x = Hu, \quad y = Hv; \tag{2}$$

then the edge of the aperture stop is the circle $u^2+v^2=1$ (see Fig. 1).

To simplify the formulas, we now choose R as the unit of length, setting $R=1$. Then $H=\mu$, and Eqs. (2) become

$$x = \mu u, \quad y = \mu v. \tag{3}$$

The plate-profile which gives axial stigmatism in light for which the plate has refractive index N is then given by the equation

$$(N-1)s = \tfrac{1}{4}\mu^4(r^2-r_0^2)^2(1+(5/2)r_0^2\mu^2) + \tfrac{3}{8}\mu^6(r^2-r_0^2)^3 + \text{constant} + O(\mu^8), \tag{4}$$

where s denotes the 'figuring depth,'** $r^2=u^2+v^2$ and r_0 is the radius of the neutral zone of the plate. The actual focal length of the system is then

$$f = \tfrac{1}{2}(1-\mu^2 r_0^2)^{-\frac{1}{2}} \tag{5}$$

---

* See Linfoot (2) for a proof of this statement and also of Eqs. (4), (9), and (11) below.

** i.e., the depth of glass which, laid on to a plane surface, would produce the desired profile. It is convenient to allow s to take both positive and negative values and to suppose that $s=0$ at the center of the aspheric surface.

and its numerical aperture

$$2\lambda = 2\mu(1-\mu^2 r_0^2)^{\frac{1}{2}}. \tag{6}$$

If terms of order μ^6 may be neglected, (4) can be written in the simpler form

$$(N-1)s = \tfrac{1}{4}\mu^4(r^4 - ar^2) + O(\mu^6), \tag{7}$$

where $a = 2r_0^2$, or in the equivalent form

$$(N-1)s = \tfrac{1}{4}\lambda^4(r^4 - ar^2) + O(\lambda^6), \tag{8}$$

in virtue of (6). Whether or not terms of order μ^6 are small enough to be negligible in the equation of the plate-surface, the off-axis aberrations δX, δY of the system, measured in seconds of arc, are given at the point of angular off-axis displacement $\varphi = O(\mu)$ in the u-direction on the spherical field surface by the equation†

$$\delta X + i\delta Y = \tfrac{1}{4}K\mu^3\varphi^2\left[\frac{N+1}{2N}\frac{\partial}{\partial u} + \tfrac{1}{2}u\frac{\partial^2}{\partial u^2} + \frac{i}{2N}\frac{\partial}{\partial v} + \tfrac{1}{2}iu\frac{\partial^2}{\partial u \partial v}\right](r^4 - ar^2) + O(K\mu^7), \tag{9}$$

where $K = 648{,}000/\pi$. Since $\mu = \lambda[1 + O(\lambda^2)]$, this equation remains valid if μ is replaced by λ. In an $f/2$ system, λ^2 and μ^2 are approximately 1/64 and (9) gives δX and δY accurately to within a few percent of their biggest values.

In light of a different wave-length, for which the refractive index of the plate is n, the rays of the axial parallel pencil are no longer brought to a sharp focus. If

$$n - N = O(\mu^2), \tag{10}$$

the aberrations are now given by the equation

$$\delta X + i\delta Y = \tfrac{1}{4}K\mu^3\varphi^2\frac{n-1}{N-1}\left[\frac{n+1}{2n}\frac{\partial}{\partial u} + \tfrac{1}{2}u\frac{\partial^2}{\partial u^2} + \frac{i}{2n}\frac{\partial}{\partial v} + \tfrac{1}{2}iu\frac{\partial^2}{\partial u \partial v}\right](r^4 - ar^2) + \tfrac{1}{4}K\mu^3\frac{n-N}{N-1}\left(\frac{\partial}{\partial u} + i\frac{\partial}{\partial v}\right) \times (r^4 - ar^2) + O(K\mu^7). \tag{11}$$

Let n_0 be the value of the refractive index of the plate at some selected point of the spectrum and suppose, what is true in a practical case, that $n - n_0$ and $N - n_0$ are both $O(\mu^2)$. Then if we use, in place of δX, δY, the quantities δX^*, δY^* defined by the equation

$$\delta X^* + i\delta Y^* = \tfrac{1}{4}K\mu^3\varphi^2\left[\frac{n_0+1}{2n_0}\frac{\partial}{\partial u} + \tfrac{1}{2}u\frac{\partial^2}{\partial u^2} + \frac{i}{2n_0}\frac{\partial}{\partial v} + \tfrac{1}{2}iu\frac{\partial^2}{\partial u \partial v}\right](r^4 - ar^2) + \tfrac{1}{4}K\mu^3\frac{n-N}{n_0-1}\left(\frac{\partial}{\partial u} + i\frac{\partial}{\partial v}\right)(r^4 - ar^2), \tag{12}$$

the error committed is only $O(K\mu^7)$ in each case.

From (12) it follows that the aberrations δX, δY of the system depend, to within an accuracy $O(K\mu^7)$, only on $n - N$, a, μ and φ; to this accuracy, they are effectively independent of the choice of n_0 because the value chosen for n_0 can only be varied by $O(\mu^2)$.

The two fifth-order aberrations of the Schmidt camera are lateral spherical aberration and a species of higher astigmatism. We can balance the lateral spherical aberration by undercorrecting the system on axis, and can compensate the higher astigmatism to some extent by increasing the 'central bulge' of the plate, i.e., by increasing a. However, too big a departure from the value which minimizes the greatest slope of the plate-profile (namely $a = \frac{3}{2}$) will give excessive chromatism and so spoil the performance of the system.

Axial undercorrection in n-light can be obtained by choosing a plate-profile (4) with $N = n$. The quantity N here takes on the role of a parameter which, together with a, specifies the coefficients of r^2 and r^4 in the geometrical plate-profile. (N and a still possess physical interpretations, of course; N is the refractive index at which the plate would give a stigmatic axial image, while a is $2r_0^2$—twice the squared radius of the neutral zone in our present units.) Changes in N and a will, in accordance with (4), alter the sixth-power term in the plate-profile, as well as the squared and fourth-power terms, but only the changes in the squared and fourth-power terms affect the form of the expressions (11) and (12) for the aberrations of the system.

Since n and N enter (12) only through their difference $n - N$, the optimal choice of N depends strongly on the

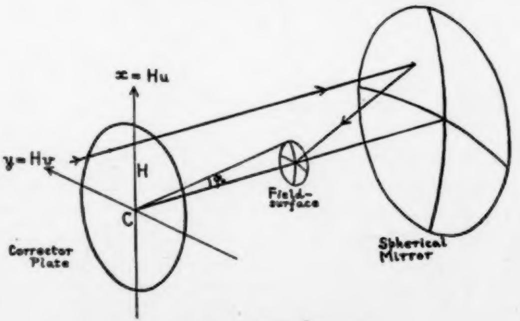

FIG. 1. The Schmidt camera.

---

† In a system of central obstruction-ratio $\leqq\frac{1}{2}$, we have $\sin\varphi_0 \leqq \mu$, so that the condition $\varphi = O(\mu)$ is always satisfied.

spectral characteristics of the light to be transmitted by the system.

In wide-field systems, $(n-N/n_0-1)\ll\varphi_0^2$ and it appears from (12) that chromatism is not very important. But in large astronomical Schmidt cameras, working over a 5- or 6-degree field at a focal ratio of $f/2.5$ or longer, considerations of chromatism play an essential part in determining the optimum plate-profile.

3.

The notion of optimising the performance of the system over a given field $\varphi\leqq\varphi_0$ can be interpreted in various ways. The most primitive interpretation, and for some purposes the best, is to take the greatest image-diameter for all object points in the given field and for all wave-lengths in the adopted spectral range, and to say that the performance is optimised when this diameter is made as small as possible. But even if diffraction effects are disregarded, this procedure does not correspond very well to the requirements of the physical situation when, for example, the effective intensity of the light rises to a peak at a certain point in its spectrum and tails off to very small values at either end.

Moreover, in cases where the size of the image is comparable with the resolving power of the photographic film, the performance is affected by photographic image-spread and there is no very close correspondence, even in monochromatic light, between image-diameter as defined above and the diameter of the star-images actually formed on a photographic plate.

In such cases it seems more appropriate physically, as well as more convenient analytically, to define the effective radius of a single monochromatic image as the square root of the expression

$$\frac{1}{\pi H^2}\iint\limits_{x^2+y^2\leqq H^2}[(\delta X)^2+(\delta Y)^2]dxdy \tag{13}$$

and the effective monochromatic image-radius for the system working over the field $\varphi\leqq\varphi_0$ as the square root of

$$E=\frac{2}{\pi H^2\varphi_0{}^2}\int_0^{\varphi_0}\varphi d\varphi\iint\limits_{x^2+y^2\leqq H^2}[(\delta X)^2+(\delta Y)^2]dxdy$$

$$=\frac{2}{\pi\varphi_0{}^2}\int_0^{\varphi_0}\varphi d\varphi\iint\limits_{u^2+v^2\leqq 1}[(\delta X)^2+(\delta Y)^2]dudv. \tag{14}$$

This definition will therefore be adopted in the present discussion. It is equivalent, if we imagine the ray-density distribution in each stellar image to be replaced by a mass-distribution, to defining the effective radius of the image as its radius of gyration about its center $(\delta X,\ \delta Y)=(0,0)$ and the effective monochromatic image-radius over the whole field as the mean-square average of these effective radii over the field-circle $\varphi\leqq\varphi_0$.

The value of $E=E(\varphi_0;a,N-n)$ is different for different wave-lengths, and in assessing the performance of the system it is necessary to take account of the fact that the images are not monochromatic.

4. EVALUATION OF E

The Eq. (12) can be written in the form

$$\left.\begin{aligned}\delta X&=K\mu^3[Pu(r^2-\tfrac{1}{2}a)+\varphi^2u^3]+O(K\mu^7)\\ \delta Y&=K\mu^3[Qv(r^2-\tfrac{1}{2}a)+\varphi^2u^2v]+O(K\mu^7)\end{aligned}\right\}, \tag{15}$$

where $\varphi=O(\mu)$ and the quantities

$$P=\frac{2n_0+1}{2n_0}\varphi^2+\frac{n-N}{n_0-1},\quad Q=P-\varphi^2 \tag{16}$$

are each $O(\mu^2)$.

By (11), (12) and (14) we can write

$$E=E^*[1+O(\mu^2)], \tag{17}$$

where

$$E^*=\frac{2}{\pi\varphi_0{}^2}\int_0^{\varphi_0}\varphi d\varphi\iint\limits_{u^2+v^2\leqq 1}[(\delta X^*)^2+(\delta Y^*)^2]dudv \tag{18}$$

$$\left.\begin{aligned}\delta X^*&=K\mu^3[Pu(r^2-\tfrac{1}{2}a)+\varphi^2u^3]\\ \delta Y^*&=K\mu^3[Qv(r^2-\tfrac{1}{2}a)+\varphi^2u^2v]\end{aligned}\right\}. \tag{19}$$

From (19)

$$\begin{aligned}(\delta X^*)^2+(\delta Y^*)^2=K^2\mu^6[&(P^2u^2+Q^2v^2)(r^2-\tfrac{1}{2}a)^2\\ &+2\varphi^2u^2(Pu^2+Qv^2)(r^2-\tfrac{1}{2}a)+\varphi^4u^4r^2].\end{aligned} \tag{20}$$

Now

$$\iint\limits_{u^2+v^2\leqq 1}(P^2u^2+Q^2v^2)(r^2-\tfrac{1}{2}a)^2dudv$$

$$=\tfrac{1}{2}(P^2+Q^2)\iint\limits_{u^2+v^2\leqq 1}r^2(r^2-\tfrac{1}{2}a)^2dudv$$

$$=\frac{\pi}{16}(P^2+Q^2)(a^2-\tfrac{8}{3}a+2); \tag{21}$$

$$\iint\limits_{u^2+v^2\leqq 1}(Pu^2+Qv^2)u^2(r^2-\tfrac{1}{2}a)dudv$$

$$=\frac{\pi}{16}(3P+Q)(\tfrac{1}{2}-\tfrac{1}{3}a); \tag{22}$$

$$\iint\limits_{u^2+v^2\leqq 1}u^4r^2dudv=\int_0^{2\pi}\cos^4\theta d\theta\int_0^1 r^7dr=\frac{3\pi}{32}. \tag{23}$$

Hence,

$$\iint\limits_{u^2+v^2\leqq 1}[(\delta X^*)^2+(\delta Y^*)^2]dudv$$

$$=\frac{\pi}{16}K^2\mu^6[(P^2+Q^2)(a^2-\tfrac{8}{3}a+2)$$

$$+2(3P+Q)(\tfrac{1}{2}-\tfrac{1}{3}a)\varphi^2+\tfrac{3}{2}\varphi^4]. \quad (24)$$

Set

$$\alpha=\frac{1}{2n_0},\quad p=\frac{n-N}{n_0-1}\frac{1}{\varphi_0{}^2}; \quad (25)$$

then, by (16),

$$P=(1+\alpha)\varphi^2+p\varphi_0{}^2,\quad Q=\alpha\varphi^2+p\varphi_0{}^2;$$

$$\int_0^{\varphi_0}\varphi d\varphi(P^2+Q^2)=\varphi_0{}^6[\tfrac{1}{6}(1+2\alpha+2\alpha^2)+\tfrac{1}{2}p(1+2\alpha)+p^2],$$

$$\int_0^{\varphi_0}\varphi d\varphi\cdot\varphi^2(3P+Q)=\varphi_0{}^6[\tfrac{1}{6}(3+4\alpha)+p],$$

$$\int_0^{\varphi_0}\varphi d\varphi\cdot\varphi^4=\tfrac{1}{6}\varphi_0{}^6.$$

Substituting from (24) into (18) and using the last three equations, we finally obtain

$$\begin{aligned}E^*=\tfrac{1}{8}K^2\mu^6\varphi_0{}^4\{&(a^2-8a/3+2)[\tfrac{1}{6}(1+2\alpha+2\alpha^2)\\&+\tfrac{1}{2}p(1+2\alpha)+p^2]\\&+2(\tfrac{1}{2}-\tfrac{1}{3}a)[\tfrac{1}{6}(3+4\alpha)+p]+\tfrac{1}{4}\},\end{aligned} \quad (26)$$

and the effective image-radius in n-light is

$$E^{\frac{1}{2}}=(E^*)^{\frac{1}{2}}\{1+O(\mu^2)\}.$$

If we define

$$\begin{aligned}e^*=(a^2-8a/3+2)[&\tfrac{1}{6}(1+2\alpha+2\alpha^2)\\&+\tfrac{1}{2}p(1+2\alpha)+p^2]\\&+2(\tfrac{1}{2}-\tfrac{1}{3}a)[\tfrac{1}{6}(3+4\alpha)+p]+\tfrac{1}{4},\end{aligned} \quad (27)$$

where α, p are given as before by (25), then the effective image-radius in n-light is $\frac{1}{2}(e^*/2)^{\frac{1}{2}}K\mu^3\varphi_0{}^2$.

Figure 2 shows $(e^*)^{\frac{1}{2}}$ as a function of a and p. $(e^*)^{\frac{1}{2}}$ is effectively independent of the choice of n_0 since, as already remarked, this is true of $\delta X^*+i\delta Y^*$. In the actual computation of Fig. 2, n_0 was taken as 1.55.

5.

Conclusions of some practical interest can be drawn from Fig. 2 about the optimum choice of plate-profile in Schmidt cameras of given focal ratio and field-size, working in light of known wave-length range.

As an example, suppose that the camera works at $f/3.5$ over a field of 8° diameter, i.e., with obstruction ratio $\frac{1}{7}$. Then $\varphi_0=1/14$ and if $n_0=1.55$ we obtain from (25)

$$\alpha=\frac{1}{3.10}=0.32,\quad p=\frac{n-N}{0.55}\cdot(14)^2=356(n-N). \quad (28)$$

Suppose that at the two ends of the adopted wave-length-range n has the values 1.53123 and 1.54011. This would be the case with a plate of Chance glass HC525588

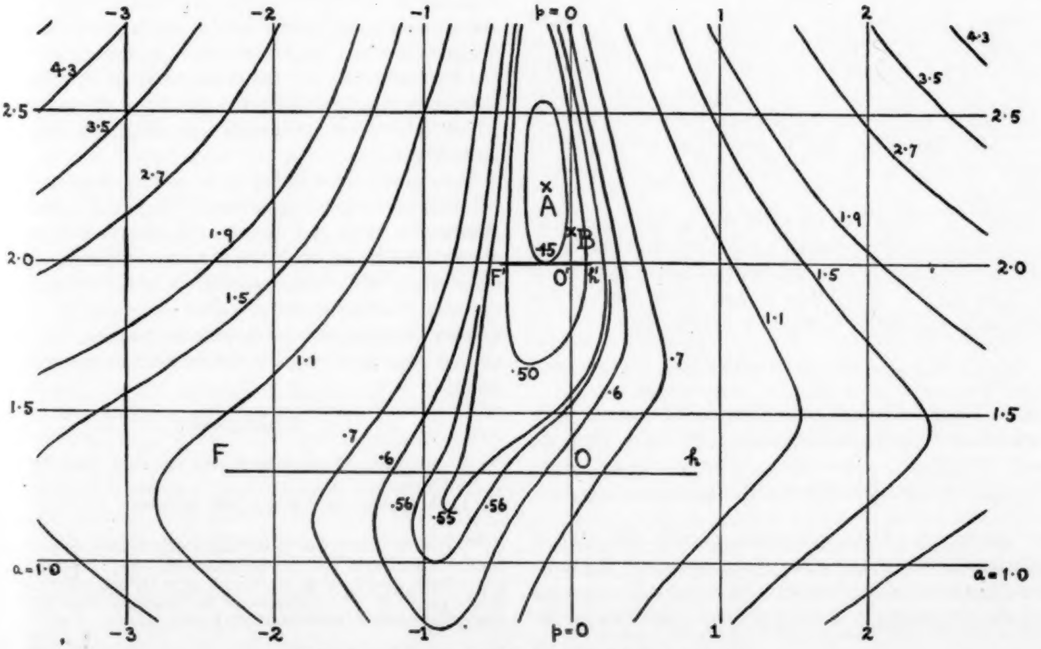

FIG. 2. Level curves for $(e^*)^{\frac{1}{2}}$ as a function of a and p.

and an adopted spectral range $F-h$, which is the most commonly used range of the astrographic spectrum. Then, by (28), the variation in p corresponding to this spectral range is

$$356(1.54011-1.53123)=3.16. \tag{29}$$

If a horizontal linear segment, of fixed length equal to 3.16 units, is moved into a position on Fig. 2 which makes $(e^*)^{\frac{1}{2}}$ as small as possible throughout the segment, then the common ordinate a of its points gives the optimum radius r_0 of the neutral zone on the plate by means of the equation

$$a=2r_0^2/R^2, \tag{30}$$

while the optimum value of N can be read off in the following way. To each point of the movable segment corresponds a particular value of n, these values running linearly from $n_F=1.53123$ at the left-hand end of the segment to $n_h=1.54011$ at its right-hand end. By (12) and (25), the value of n which falls on the line $p=0$ in Fig. 2 corresponds to the wave-length for which the system is axially stigmatic; the appropriate choice of N is therefore equal to this value.

To make $(e^*)^{\frac{1}{2}}$ as small as possible over the whole of the linear segment, it is sufficient to move the segment horizontally until the value of $(e^*)^{\frac{1}{2}}$ is balanced at its two end-points, and then, keeping this balance, to slide the segment up or down until the value of $(e^*)^{\frac{1}{2}}$ at the two end points is a minimum. The selected position of the segment is shown as FOh on the graph.

This method of balancing the aberrations is best suited to systems intended for use as spectrograph cameras. With systems intended solely for direct photography, it would be possible to proceed in a more refined way by taking into account the varying density of the photographic spectrum along the adopted wave-length range and trying to minimise the weighted mean of e^* over this range. But so much elaboration hardly seems appropriate in a discussion of the present character.

From Fig. 2 it is seen that, for this system, the 'best' values of a are those between 1.2 and 1.5, and that there is little to choose between different values in this range, provided that N is suitably chosen in each case. The effective image radius in F and h light is then

$$\tfrac{1}{2}(e^*/2)^{\frac{1}{2}}K\mu^3\varphi_0^2=0.136(e^*)^{\frac{1}{2}}=0.12 \text{ second of arc.}$$

As a second example, consider an $f/1$ camera with obstruction ratio $\frac{1}{3}$, working over a 19° field. Here we have

$$\varphi_0=\tfrac{1}{6},\quad p=(n-N/0.55)\cdot 6^2=65.44(n-N),$$

and the length of the p-segment corresponding to a variation 0.00888 in the value of n is now only 0.6 unit. This shortening of the segment, by a factor 5 compared with the first example, is the graphical expression of the much smaller importance, in the second system, of chromatism relative to the monochromatic aberrations.

In this case the selected position of the segment, shown as $F'O'h'$ on the graph, gives

$$a=2.0,\quad N=1.5383$$

as the optimum values; then $(e^*)^{\frac{1}{2}}=0.52$ and the effective image radius is $31.66(e^*)^{\frac{1}{2}}=16.5$ seconds of arc. The value $a=2.0$ corresponds to a plate with its neutral zone at the edge of the aperture.

It will be seen that in the $f/3.5$ system of the first example the effect of the monochromatic errors is merely to displace the best choice of 'stigmatic wave-length' some way from the center towards the violet end of the effective range, and that even for the unusually wide field of 8° the best value of a is substantially the same as that which optimises the axial image.***

Besides indicating optimum values of a and N in numerical cases, Fig. 2 provides answers to one or two questions of a more general character. For example, the 'best monochromatic plate,' represented on the graph by the point A at which $(e^*)^{\frac{1}{2}}$ attains its least value 0.43, is the plate with

$$a=2.25,\quad p=\frac{n-N}{n_0-1}\frac{1}{\varphi_0^2}=-0.18,$$

that is,

$$a=2.25,\quad N=n+0.10\varphi_0^2.$$

The term $0.10\varphi_0^2$ indicates the axial undercorrection required to balance the monochromatic errors of the system over the given field. For a monochromatic Schmidt in which the corrector plate is designed to give axial stigmatism, the optimum value of a is 2.1; this system is represented on the graph by the point B at which $(e^*)^{\frac{1}{2}}$ takes its least value along the line $p=0$, namely 0.46.

More generally still, Fig. 2 shows that in astronomical Schmidt cameras of focal ratio $f/3$ or $f/3.5$ and with obstruction ratio not exceeding $\frac{1}{2}$, the monochromatic aberrations are of small importance compared with the color-error, while the opposite is true for large-field systems working at focal ratios near to $f/1$. An $f/2$ system occupies an intermediate position, in which neither type of aberration can be said to dominate the other.

Bibliography

(1) B. Strömgren, Vierteljahresschrift der Astr. Ges. **70**, 65–89 (1935).
(2) E. H. Linfoot, M.N.R.A.S. **109** (in press).

*** The effective radius of the axial image is least when $a=4/3$. This follows from (26) on substituting for p its value (25) and setting $\varphi_0=0$, when we obtain $E^*=\frac{1}{8}K^2\mu^6(n-N)^2/(n_0-1)^2 \times(a^2-8a/3+2)$. The diameters of the color-confusion circles are least when $a=3/2$ (Strömgren (1), p. 81).

JOURNAL OF THE OPTICAL SOCIETY OF AMERICA VOLUME 39, NUMBER 9 SEPTEMBER, 1949

Lorentz-Type Transformations as Derived from Performable Rod and Clock Operations

HERBERT E. IVES
32 Laurel Place, Upper Montclair, New Jersey

(Received May 9, 1949)

Transformations of the Lorentz-type are derived in terms of distance and time measurements made by rods and clocks subject to the Fitzgerald-Larmor-Lorentz contractions by their motion through the ether. These transformations contain terms involving the self-measured velocity of a transported setting clock which must be used to establish times at distant points. When the setting clock velocity is small the expressions approximate to the original Lorentz transformations.

INTRODUCTION

IN an earlier paper on "The Measurement of the Velocity of Light by Signals Sent in One Direction,"[1] it was indicated that the derivation of the Lorentz transformations and of the Special Theory of Relativity should be reviewed in the light of the results there found. In the present communication this is done. The relations between the read coordinates of an "event" as measured on relatively moving platforms, which are the objective of the Lorentz transformations, are developed entirely in terms of operations with rods and clocks subject to the Fitzgerald-Larmor-Lorentz contractions. The resulting transformations contain terms in "q," the "rod-clock-quotient" of the clock which must be moved to the locus of the "event" in order to establish its local time.

HISTORICAL

The Lorentz transformations, as first developed by Voigt, in a discussion of the Doppler effect, were a mathematical device calculated to leave the optical equations unchanged in form from one moving body to another. Lorentz, in his independent development, introduced the "local time" as a mathematical convenience, relating it to no physical operation by which it might be obtained. Einstein, in the derivation of the Lorentz transformations which has been frequently interpreted as basing these on rod and clock operations, actually bases his whole development on his "definition" that the velocity of light, for signals *sent in one direction*, is constant, and equal to "c," the velocity of light, as ordinarily measured, by *out and back* signals. As pointed out in the preceding paper, these are two different experiments, and the ascription to one of the result of the other is not legitimate, and, from the findings of that paper, not true.

No historical note on the Lorentz transformations is complete without reference to the work of Larmor, who, while he did not formulate the Lorentz transformations, made the contractions of length and clock rate experienced by motion through the ether the basis of his work on the invariance of electromagnetic phenomena in moving systems. All the material necessary for the development which follows may be found in Larmor's "Aether and Matter" of 1900.[2]

GROUNDWORK

The groundwork for deriving the Lorentz-like transformations which are the subject matter of this paper is the same as that of the previous paper, which should be referred to. Important features are the formulation of all distances, times, and velocities primarily by reference to invariant quantities in the radiation transmitting ether; the distinction between "velocity" which is used only for length and time relations in the ether, and "rod-clock-quotient," which is a measurement made with rods and clocks experiencing the F.L.L. contractions; and the specification that clocks at a distant point are to be set by a transported clock whose rod-clock-quotient is in terms of time *as indicated by the clock itself*.

In the preceding paper, which was concerned primarily with the measurement of the velocity of light, the signal was sent along the axis of motion of the observing platform. For the present problem the direction of motion of the signal or particle must be made more general. Most of the work will be done in polar coordinates, appropriate since the setting clock experiences its retardation by traversing the path of the signal or particle. For a mathematically complete treatment the analysis should be carried through in three dimension. Since this introduces only trigonometrical complexity, without adding to the information obtained, the simpler case of particle motion in the same plane as the platform motion is studied.

We shall follow essentially the same sequence of argument here as in the preceding paper. In Fig. 1, 0 indicates the point from which the moving platform starts at time zero to move along the axis at velocity W. From the same origin a particle is projected along the path R at the angle Θ, to reach the point E on the observation platform at the time T. Since any "event" may be correlated with the arrival of a particle from the origin with an appropriate velocity, we shall consider our

---

[1] H. E. Ives, J. Opt. Soc. Am. 38, 879 (1948).

[2] J. Larmor, *Aether and Matter* (Cambridge University Press, London, 1900).

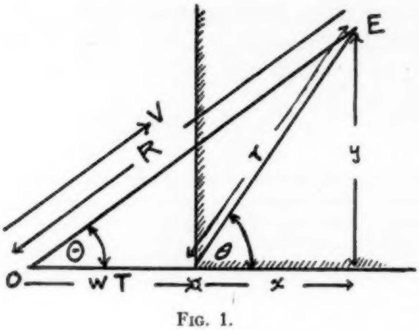

FIG. 1.

problem entirely in terms of such a particle, which, if its velocity is c, becomes a light signal.

The trace of the path R on the moving platform is given by $0-E$, which we shall designate r, which lies at an angle θ with the axis. Our problem is to discover how r, θ, and the arrival time T of the particle will be measured on different platforms, moving at different W's. The procedure is the same as that in the preceding paper, except that the relations of sides and angles of oblique plane triangles are involved, instead of straight lines alone. Denoting the read values by primed letters, and using for the moment Cartesian coordinates for convenience of calculation, we put $r^2=x^2+y^2$, and from the relation $x'=x/[1-(W^2/c^2)]^{1/2}$ we easily derive from the right triangle relations

$$r=r'[1-(W^2/c^2)\cos^2\theta']^{1/2}$$

$$\cos\theta=\frac{\cos\theta'[1-(W^2/c^2)]^{1/2}}{[1-(W^2/c^2)\cos^2]^{1/2}\theta'}$$

$$r'^2=r'^2\sin^2\theta'+r'^2\cos^2\theta'. \qquad (1)$$

By following the same steps as in the preceding paper we obtain for the amount Δ by which a clock moved along r is set back when moved at the rod-clock-quotient q, the expression

$$\Delta=\frac{r'}{q}\left\{[(1+(q^2/c^2))^{1/2}-1]+\frac{Wq\cos\theta'}{c^2}\right\}. \qquad (2)$$

For the measured time of transit t' of a particle in terms of T

$$T=\frac{t'+(Wr'\cos\theta'/c^2)+(r'/q)\{[1+(q^2/c^2)]^{1/2}-1\}}{[1-(W^2/c^2)]^{1/2}} \qquad (3)$$

and for the velocity of the particle with respect to the platform,

$$V=\frac{Q_2[1-(W^2/c^2)\cos^2]^{1/2}\theta'[1-(W^2/c^2)]^{1/2}}{1+(WQ_2\cos\theta'/c^2)+(Q_2/q)\{[1+(q^2/c^2)]^{1/2}-1\}} \qquad (4)$$

where Q_2 is as in the preceding paper, the observed rod-clock-quotient when the distant clock is set by a setting clock moved at the self observed rod-clock-quotient q. These equations differ from those previously given (Eqs. (12)–(14), l.c.) by the factor $\cos\theta'$, and become identical with these when $\cos\theta'=1$.

THE VELOCITY OF LIGHT

Of special interest is the rod-clock-quotient obtained for a light signal. The velocity of the trace of the light signal on the moving platform is given by the relation

$$V^2+2VW\cos\theta+W^2=c^2$$

from which

$$V=-W\cos\theta\pm(W^2\cos^2\theta-(W^2-c^2))^{1/2}.$$

Substituting the value of $\cos\theta$ in terms of $\cos\theta'$ from (1), this gives

$$V=\frac{[1-(W^2/c^2)]^{1/2}}{[1-(W^2/c^2)\cos^2\theta']^{1/2}}[c-W\cos\theta']. \qquad (6)$$

Putting this in (4) we get

$$Q_2=\frac{c}{1-(c/q)\{[1+(q^2/c^2)]^{1/2}-1\}}, \qquad (7)$$

which is identical with the result obtained in the previous paper.

The important thing to note is that, since this expression does not contain W, the velocity of the platform, we get the same value for the two-clock rod-clock-quotient for light, no matter what the motion of the platform. That is, the same provided the same value is used for the rod-clock-quotient q of the setting clock. Also note that while, as discussed in the previous paper, we also get the "same" value for the one-clock rod-clock-quotient (namely c) no matter what the motion of the platform, these "sames" are not identical. (They are in the terminology of semanticists "same$_1$" and "same$_2$.") It is to the false identification of these "sames" that the formulae of the Special Theory of Relativity owe an apparent simplicity and elegance which give place to more complicated expression when the description of the necessary operations of measurement is introduced, as shown below.

THE LORENTZ-TYPE TRANSFORMATIONS

Consider two observation platforms, both starting from the origin together, one moving with the velocity W_1, the other at the velocity W_2. We wish to describe the arrival of a particle starting from the origin at the same instant, in terms of the r', t', and $\cos\theta'$ of each platform. We shall designate these quantities r_1', r_2', t_1', t_2', $\cos\theta_1'$, $\cos\theta_2'$.

From Fig. 2 we have

$$r_2\cos\theta_2=r_1\cos\theta_1-(W_2-W_1)T. \qquad (8)$$

Substituting from the relations (1) and (3) for r_1, r_2, $\cos\theta_1$, $\cos\theta_2$, and T (in terms of t_1'), and utilizing the relation

$$\left(1-\frac{W_1^2}{c^2}\right)\left(1-\frac{W_2^2}{c^2}\right)=\left(1-\frac{W_1W_2}{c^2}\right)^2-\frac{(W_2-W_1)^2}{c^2} \quad (9)$$

we get an equation for $r_2'\cos\theta_2'$ involving observed quantities and the quotient

$$(W_2-W_1)/(1-W_1W_2/c^2).$$

We put this quotient in terms of the rod-clock-quotient of platform 2 as observed from platform 1 by using the relation (4), putting $\cos\theta'-1$, and $V=W_2-W_1$. Calling this rod-clock-quotient Q_P we have

$$\frac{W_2-W_1}{1-(W_1W_2/c^2)}=\frac{Q_P}{1+(Q_P/q)\{[1+(q^2/c^2)]^{\frac{1}{2}}-1\}}. \quad (10)$$

In the interest of typographic economy we shall, except when the full expressions are needed in the development, put for the expressions (10) the symbol P; and for the quantity $\{[1+(q^2/c^2)]^{\frac{1}{2}}-1/q\}$, which comes in because of the use of the setting clock, we shall use the symbol k.

With these symbols the expression for $r_2'\cos\theta_2'$ is

$$r_2'\cos\theta_2'=\frac{r_1'[\cos\theta_1'-Pk]-Pt_1'}{[1-(P^2/c^2)]^{\frac{1}{2}}}. \quad (11)$$

Since $r_2'^1=r_2'^2\sin^2\theta_2'+r_2'^2\cos^2\theta_2'$, and $r_2'\sin\theta_2'=r_1'\sin\theta_1'$, we have for r_2'

$$r_2'=\left(r_1'^2\sin^2\theta_1'+\frac{[r_1'(\cos\theta_1'-Pk)-Pt_1']^2}{1-(P^2/c^2)}\right)^{\frac{1}{2}}. \quad (12)$$

$\text{Cos}\,\theta_2'$ we get by dividing (11) by (12); it is

$$\cos\theta_2'=\frac{r_1'[\cos\theta_1'-Pk]-Pt_1'}{\{r_1'^2(1-Pk)^2\sin^2\theta_1'+[r_1'(\cos\theta_1'-Pk)-Pt_1']^2\}^{\frac{1}{2}}}. \quad (13)$$

From (3) we have

$$T=\frac{t_1'+(Wr_1'\cos\theta_1'/c^2)+r_1'k}{[1-(W_1^2/c^2)]^{\frac{1}{2}}}=\frac{t_2'+(W_2r_2'\cos\theta_2'/c^2)+r_2'k}{[1-(W_2^2/c^2)]^{\frac{1}{2}}}.$$

Solving for t_2' in terms of t_1' we have

$$t_2'+r_2'k=\frac{t_1'-(Pr_1'\cos\theta_1'/c^2)+r_1'k}{[1-(P^2/c^2)]^{\frac{1}{2}}}, \quad (14)$$

in which for r_2' is to be taken the value from (12).

The relations (12)–(14) are the exact Lorentz-type transformations describing any event (particle arrival) entirely in terms of observed rod and clock readings on two relatively moving platforms. The presence in the formulae of "c," the rod-clock-quotient for light, as obtained from one-clock out-and-back measurement, is a constant reminder that the rod and clock behaviors involved are functions of their motions through the ether.

LIGHT SIGNALS

The relations (12)–(14), assume relatively simple forms if the particle is a light signal. From (7) we have

$$r_1'/t_1'=c/(1-ck)=r_2'/t_2'. \quad (15)$$

Substituting these we obtain

$$r_2'=\frac{r_1'-[Pt_1'\cos\theta_1'/(1-ck)]}{[1-(P^2/c^2)]^{\frac{1}{2}}}, \quad (16)$$

$$t_2'=\frac{t_1'-\{Pr_1'\cos\theta_1'[1-ck]/c^2\}}{[1-(P^2/c^2)]^{\frac{1}{2}}}, \quad (17)$$

$$\cos\theta_2'=\frac{\cos\theta_1'-(P/c)}{1-(P/c)\cos\theta_1'}. \quad (18)$$

THE LORENTZ-TYPE TRANSFORMATIONS IN CARTESIAN COORDINATES

As an aid to the comparison and correlation of these transformations with the original Lorentz transforma-

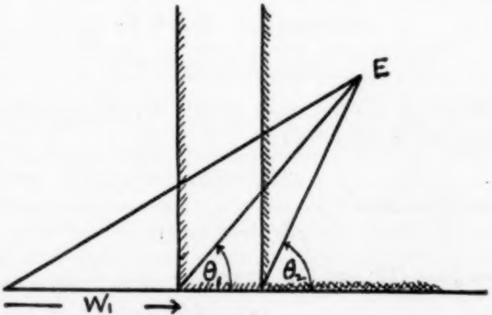

FIG. 2.

tions, the equations will now be expressed in Cartesian coordinates.

Going back to Eq. (11), on putting $r_1' \cos\theta_1' = x_1'$, $r_2' \cos\theta_1' = x_2'$, we get

$$x_2' = \frac{x_1' - Pt_1' - r_1'Pk}{[1-(P^2/c^2)]^{\frac{1}{2}}}, \tag{19}$$

to which we may add from relations (1)

$$y_2' = y_1', \quad r_1' = (x_1'^2 + y_1'^2)^{\frac{1}{2}}, \quad r_2' = (x_2'^2 + y_2'^2)^{\frac{1}{2}}.$$

Going back to Eq. (14) we get for t_2'

$$t_2' + r_2'k = \frac{t_1' - (Px_1'/c^2) + r_1'k}{[1-(P^2/c^2)]^{\frac{1}{2}}}. \tag{20}$$

Inspection of these equations shows that they are of the form of the original Lorentz transformations, except for the terms in k, that is in $\{[1+(q^2/c^2)]^{\frac{1}{2}}-1\}/q$. Now on expanding we get

$$k \cong \tfrac{1}{2}(q/c^2) + \cdots,$$

showing that if q is zero the transformations are of the original Lorentz form. This however means that the setting clock would not be moved, and the operation of measurement could not be performed. What can be said legitimately is that when q is *small* the equations *approximate* to the Lorentz form. This is the practical case; the attainable speed of a setting clock would always be small compared with c. We are here concerned however not with practical approximations, but with obtaining rigorous expressions.

SPECIAL CASES

Two special cases are of interest to investigate. The first is where the particle whose arrival time constitutes the "event" travels along the axis of platform motion. In this case $r_1' = x_1'$, and we have on substitution in (19) and (20), and reverting to the use of Q_P,

$$x_2' = \frac{x_1' - Q_P t_1'}{[(1+Q_P k)^2 - (Q_P^2/c^2)]^{\frac{1}{2}}}, \tag{21}$$

$$t_2' = \frac{t_1'(1+2Q_P k) - (x_1' Q_P/c^2)[1-k^2c^2]}{[(1+Q_P k)^2 - (Q_P^2/c^2)]^{\frac{1}{2}}}. \tag{22}$$

Now call the rod-clock-quotient for the particle as measured on platform 1

$$x_1'/t_1' = (Q)_1,$$

and on platform 2

$$x_2'/t_2' = (Q)_2;$$

then from (21) and (22) we get

$$(Q)_2 = \frac{(Q)_1 - Q_P}{1 - [Q_P(Q)_1/c^2](1-k^2c^2) + 2Q_P k}. \tag{23}$$

This is the exact formula for what is termed in the Special Theory of Relativity the "composition of velocities."

Now consider the origin on platform 2. At this point $x_2' = 0$, or, from (21),

$$x_1' = Q_P t_1'.$$

Put this value in (22) and we have

$$t_2' = t_1'[(1+Q_P k)^2 - (Q_P^2/c^2)]^{\frac{1}{2}}, \tag{24}$$

or, since

$$k^2 = \frac{\{[1+(q^2/c^2)]^{\frac{1}{2}}-1\}^2}{q^2} = \frac{1}{c^2} - \frac{2k}{q}, \tag{25}$$

$$t_2' = t_1'\left(1 + 2Q_P k - \frac{2Q_P^2 k}{q}\right)^{\frac{1}{2}}. \tag{26}$$

Now if $Q_P = q$, then $t_2' = t_1'$. This gives a confirmation of the formulae developed, since a clock on the origin on platform 2 traveling at rate q is identical with the setting clock used to establish clock settings on platform 1.

The second special case is that of light signals. Here we use the relations (15) and our Cartesian coordinate equations become

$$x_2' = \frac{x_1' - P/(1-ck)}{[1-(P^2/c^2)]^{\frac{1}{2}}}, \tag{27}$$

$$t_2' = \frac{t_1' - [Px_1'(1-ck)/c^2]}{[1-(P^2/c^2)]^{\frac{1}{2}}}. \tag{28}$$

If we put

$$P/(1-ck) = \mathfrak{W}, \tag{29}$$

and write

$$Q_L = c/(1-ck), \tag{30}$$

these equations become

$$x_2' = \frac{x_1' - \mathfrak{W}t_1'}{[1-(\mathfrak{W}^2/Q_L^2)]^{\frac{1}{2}}}, \tag{31}$$

$$t_2' = \frac{t_1' - (\mathfrak{W}x_1'/Q_L^2)}{[1-(\mathfrak{W}^2/Q_L^2)]^{\frac{1}{2}}}. \tag{32}$$

These transformations, which have the form of the Lorentz transformations, illustrate a remark made in the preceding paper, that the Lorentz transformations are "properly expressed in terms of Q_2." In order to do this it is not sufficient to merely replace the "c" in the Lorentz transformations by Q_2, for light signals, but to use the appropriate expression ($\mathfrak{W}$) to describe the relative velocity of the measuring platforms.

SOME OBSERVATIONS ON PREVIOUS DERIVATIONS OF THE LORENTZ TRANSFORMATIONS

The concluding remark of the last section emphasizes a point in regard to the Voigt-Lorentz original derivation of the Lorentz transformations, namely, that being primarily a mathematical artifice to meet the condition of invariance of form in optical equations, they are not the only equations which could accomplish this. The Eqs. (31) and (32) meet the requirement of invariance, but at the same time, through (10), (29), and (30), the expressions for platform and light signal rod-clock-quotients are operationally defined, while the "c" and "V" of the original formulations were not.

Certain steps in the usual derivation of the Lorentz transformations in the Special Theory of Relativity, which purports to obtain these from the consideration of operations, without reference to the radiation transmitting medium, may now be critically examined.

An initial step in this derivation is to consider the value of x_1' when $x_2'=0$. Then, according to the usual procedure,[3] it is stated that

$$x_2'=0$$

and

$$x_1'-Vt_1'=0$$

are equations of identical meaning, and the relation

$$x_2'=a(x_1'-Vt_1') \tag{33}$$

is used for substitution in further work.

Now from our solution, with the particle moving in any direction, we have from (19) that the relation is, when $x_2'=0$, (Q_P being equivalent to V)

$$x_1'-[Q_P/(1+Q_Pk)][t_1'-r_1'k]=0,$$

so that the substitution (33) is not valid.

The reason for this is not difficult to see; it depends on the fact that the measured distances and times are determined not solely by the motion of the platform (described by Q_P), but by the motion of the setting clock along the path of the particle (described by q) which in general is in a direction different from that of the platform.

The next step is to set down the relations

$$x_1'^2+y_1'^2+z_1'^2-S_1'^2t_1'^2=0,$$
$$x_2'^2+y_2'^2+z_2'^2-S_2'^2t_2'^2=0,$$

where S_1' and S_2' are the observed velocities of the particle on the two platforms. These equations are also declared to be of identical meaning. In order to solve them the number of unknown quantities is reduced by the substitution above discussed (33), and by putting "c" in place of both S_1' and S_2', since this is by definition the same in both systems. This last substitution implicitly assumes that in the expressions for x_2' and t_2' in terms of x_1' and t_1', the coefficients of the latter shall be the same no matter what the particle considered, so that as obtained for a light signal ($S_1'=S_2'=c$), they apply to any particle. Explicitly they are assumed to be functions of V alone.

Referring now to Eqs. (19) and (20) and putting

$$S_1'=r_1'/t_1',$$
$$S_2'=r_2'/t_2',$$

we have

$$x_2'=\frac{x_1'(1+Q_Pk)-Q_Pt_1'(1+S_1'k)}{[(1+Q_Pk)^2-(Q_P^2/c^2)]^{\frac{1}{2}}}$$
$$t_2'=\frac{t_1'[(1+S_1'k)(1+Q_Pk)/(1+S_2'k)]-[Q_Px_1'/c^2(1+S_2'k)]}{[(1+Q_Pk)^2-(Q_P^2/c^2)]^{\frac{1}{2}}},$$

from which we see that the coefficients in question are functions (when q is finite) of the observed particle velocities (S_1' and S_2'), and the assumption that they are functions of Q_P alone, which can be found for any particle by considering only a light signal, is invalid.

If in these equations the terms in k (that is the terms involving the setting clock) are eliminated, the assumptions in question would hold. This analysis therefore shows that the assumptions used in the Special Theory of Relativity derivation exclude the use of clocks for setting "times" at a distant point. Clocks can be used only for measuring duration or interval at a given point, not for fixing an epoch. For the latter recourse must be made to light signals giving their indication by fiat, not confirmable by the readings of any physical measuring instrument.

The existence of this limitation is further brought out by the observation that the Special Theory of Relativity treatment leads to an internal inconsistency if clocks are admitted for distant time setting. For, from the expressions for x_1', x_2', etc., it is a regular step to derive a variation of clock rate with "V." If one then proceeds to use a moved clock to establish the setting of a distant clock (the procedure is parallel to that here used), the outcome is to show that the "velocity of light" as measured by a signal sent in one direction is different from "c." This however is contrary to the basic "definition," which says it is always "c."

The Lorentz transformations as derived in the Special Theory of Relativity are thus, in the light of the present analysis, an approximation, owing their simplicity of form to the exclusion of clocks in the determination of epoch. They are practically valid to the order of accuracy that the difference between c and

$$\frac{c}{1-(c/q)\{[1+(q^2/c^2)]^{\frac{1}{2}}-1\}}$$

may be disregarded.

---

[3] The treatment given by O. W. Richardson in *The Theory of Electrons* (Cambridge University Press, London, 1914), p. 297, is here followed, but with an amplified discussion of the assumptions involved in each step.

JOURNAL OF THE OPTICAL SOCIETY OF AMERICA VOLUME 39, NUMBER 9 SEPTEMBER, 1949

A Study of the Mechanism of Modified Rayleigh Scattering*

D. H. RANK AND J. P. MCKELVEY
Physics Department, Pennsylvania State College, State College, Pennsylvania

(Received May 12, 1949)

A study of the mechanism of modified Rayleigh scattering has been attempted by more detailed considerations of the "moving mirror" model. A calculation has been made which yields the order of magnitude of the amplitude of the hypersonic waves in liquids. The small amplitude obtained is used to explain the persistence of the modified Brillouin components in glycerine when the macroscopic viscosity is so high that the hypersonic vibrations should no longer be propagated according to the classical hydrodynamic equations.

THE novel idea proposed by Brillouin[1] concerning the nature and mechanism of Rayleigh scattering has had considerable success in predicting the fine structure of Rayleigh scattering.

This picture of Rayleigh scattering predicts a Doppler effect in the light scattered from liquids and crystals which behaves in essentially the same fashion as though the scattered light were reflected from moving mirrors having a very small relative index of refraction, and moving with the velocity of sound. The elastic disturbances which are responsible for the above mentioned phenomenon are considered to be the Debye waves.

The Brillouin picture does not predict the existence of the central unmodified component, and in the case of crystals, no central component appears.

Landau and Placzek[2] have demonstrated by means of a thermodynamic argument that both the Doppler components and the central unmodified component will appear in the case of a liquid, and that the relationship existing between these will be:

$$I_c/2I_B=\gamma-1, \tag{1}$$

where I_c is the intensity of the central unmodified component, and I_B the intensity of the modified component.

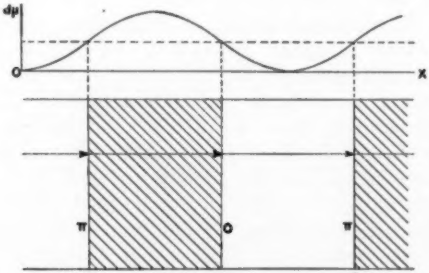

FIG. 1. Plot of $d\mu$ against distance along the wave train, and schematic diagram of the replacement of the continuous variation of refractive index by discrete plates of refractive index $\mu_0+d\mu_0$ corresponding to the condensations of the Debye waves. Reflections take place at boundaries indicated by Figs. 1–3. Phase changes due to reflections at these boundaries are shown.

γ is the ratio of the specific heat at constant pressure to the specific heat at constant volume.

Gross[3] has given a derivation of this so-called Landau-Placzek formula. A derivation following Gross' method can be found in a monograph on light scattering by Rousset.[4]

A quite rigorous discussion of the fine structure of Rayleigh scattering by means of statistical methods has been given in a monograph by Ketel.[5] The end result of Ketel's statistical treatment of the density fluctuations in the liquid is a derivation of the Einstein formula for scattering, and also the Landau-Placzek formula for the intensity distribution between modified and unmodified fine structure components.

The moving mirror picture of the origin of the Doppler components of the fine structure of Rayleigh scattering yields quantitatively correct answers for the wavelength shift with frequency, velocity of sound, and angle of scattering. In addition, this simple picture also predicts the correct state of polarization for the modified Brillouin components.

It has occurred to us that it is a relatively simple matter to follow the moving mirror picture somewhat further than has been done in the past, in order to make an attempt to extract further information from this useful model.

Let us inquire into the energy directly associated with the existence of the modified Doppler components on the moving mirror picture. We shall assume a volume containing the liquid which is scattering the light to contain the Debye waves, which are present with all the permitted frequencies, and propagated in all possible directions. Since the Debye waves are propagated throughout the volume in all possible directions, we can sort out a group of these waves for study by applying a proper set of conditions to a selected set of these waves.

The Rayleigh constant, i.e., the ratio of the amount of light scattered at right angles, to the amount of light incident, per unit length traversal of incident light, has been measured for a number of substances.

---

* This research was carried out on Contract N6onr-269, Task V of the ONR.

[1] L. Brillouin, Ann. de physique **17**, 88 (1922).

[2] L. Landau and G. Placzek, Physik. Zeits. Sowjetunion **5**, 172 (1934).

[3] E. Gross, Acta Physicochemica U.R.S.S. **20**, 459 (1945).

[4] A. Rousset, *La Diffusion de la Lumière par les Molécules Rigides*, Centre National de la Récherche Scientifique, Paris (1947).

[5] R. S. Ketel, *Theorie van het Rayleigh-Verstrooiingstriplet van Vloeistoffen*, Martinuius Nijhoff, 'S-Gravenhage (1946).

Let us assume a unit cube of scattering liquid. The incident light will be normal to one face of the cube. The scattered light will be observed normal to a face of the cube which is at right angles to the incident face. We shall imagine a set of Debye waves to be traversing the cube in such a manner that the planes formed by the condensations and rarefactions of this wave train will be at an angle of 45° with the incident and scattered rays. These condensations and rarefactions will, of course, have an index of refraction different from the mean index of the liquid, and thus will act as moving mirrors. We shall further assume that we have two mirrors per wave-length of sound, spaced π radians apart. The reflecting power of these mirrors which will be calculated arises from the differential index of refraction produced by the passage of the sound wave. For convenience, we shall call the index of the liquid at the rarefaction μ_0, and the condensation will have an index of $\mu_0+d\mu_0$. A schematic diagram of this model is shown in Fig. 1.

The condition which must be fulfilled for the appearance of scattered radiation of appreciable intensity from such a system of moving mirrors will be that given by the familiar Bragg equation for x-rays:

$$\lambda=2\mu_0\lambda_s\sin\theta, \qquad (2)$$

where λ is the wave-length of the incident light, λ_s the wave-length of the sound waves, μ_0 the gross refractive index of the material, and θ the glancing angle. For any other values of θ, the scattered rays are mutually extinguished.[6]

When the scattering takes place through an angle of 90°, i.e., $\theta=45°$, since μ, the relative index of refraction at the condensations, must closely approach unity, it is easily seen that the familiar Fresnel formulas show the polarization to be nearly complete. Thus the parallel component of the scattered light has vanished, and we must only deal with the perpendicular component. (The practically complete polarization of the modified Brillouin components is an experimental reality for 90° scattering.[7–9])

The relative index of refraction, μ, will vary sinusoidally as a function of the phase angle of the vibratory disturbance. There will be a continuous distribution of variation of index throughout a wave-length. We have chosen the separation of our hypothetical mirror surfaces in a reasonable though somewhat arbitrary fashion. The result of our choice of separations is that when the phase change in reflection of the perpendicularly polarized light is taken into account, we obtain complete constructive interference from pairs of mirrors observed in depth.

It is easy to see that if the reflectivity is very small, only first reflections will be of significance. We shall make a further easily justifiable assumption that there is no significant loss of intensity in the incident beam, due to reflections at the moving mirrors.

The problem now remains, to determine the manner in which the reflections from the system of moving mirrors must be summed. We are considering the problem of the total flux reflected from our moving mirrors. It is obvious that the flux reflected from such a longitudinal array of mirrors of infinitesimal size will be proportional to the number of these mirrors. This problem is analogous to the case of a plane diffraction grating in that the total flux arising from the uniformly illuminated grating must be proportional to the width of the grating. It is not immediately obvious how to treat the reflections from the arrays of mirrors in depth.

The Rayleigh constant R is experimentally independent of the illuminated volume. In order to measure this constant it is necessary to make use of an extended volume of liquid, and, in general, an extended source of light. The rays incident upon the liquid on the face of our cube will in general have arisen from different parts of the source, and thus disturbances reflected from widely separated mirrors arranged in depth cannot interfere. However, it is necessary to have constructive interference in order to apply the Bragg equation to our phenomenon. We shall make the arbitrary assumption that disturbances reflected from neighboring mirrors arranged in depth will be coherent, making it necessary to add amplitudes arising from pairs of mirrors. This last assumption is probably too strict, since interference from more than two mirrors is probably possible, in view of the close spacing of these mirrors. However, since intensities arising from pairs of mirrors will be added pair to pair, the Rayleigh constant will remain independent of the depth of the liquid. The effect of this stringent interference condition will be to make the calculated value of the amplitude of the hypersonic oscillations a maximum value.

Thus it can be seen that for any incident bundle of rays of cross-sectional area $dydz$, the number of pairs of mirrors encountered by this incident bundle in passing through a unit-length of material will be:

$$n=\cos\theta/\lambda_s. \qquad (3)$$

It is easy to demonstrate that the reflectivity α, of a mirror having an index of refraction μ, very closely approaching unity, and illuminated with perpendicular polarized light at a 45° angle of incidence, will be given by the expression:

$$\alpha=(\mu-1)^2. \qquad (4)$$

The expression which represents the reflectivity of a single surface from the system of moving mirrors in our cube will be,

$$\frac{R}{\gamma}=\frac{2\sqrt{2}}{\lambda_s}\alpha=\frac{2\sqrt{2}}{\lambda_s}\left(\frac{d\mu_0}{\mu_0}\right)^2. \qquad (5)$$

---

[6] J. Frenkel, *Kinetic Theory of Liquids* (Clarendon Press, Oxford, 1946), p. 237.

[7] B. V. R. Rao, Proc. Ind. Acad. Sci. **2**, 236 (1935).

[8] K. Birus, Physik. Zeits. **39**, 80 (1938).

[9] Rank, McCartney, and Szasz, J. Opt. Soc. Am. **38**, 287 (1948).

TABLE I.

Substance	$d\mu_0$	dP, dyne/cm²	A, cm	E_t, erg/cm³	$(V_q)^{\frac{1}{3}}$ A
Water	5.72×10^{-6}	1.86×10^{5}	2.84×10^{-11}	1.55	310
Methanol	8.51×10^{-6}	1.32×10^{5}	4.44×10^{-11}	1.70	273
Ethanol	9.62×10^{-6}	1.38×10^{5}	4.43×10^{-11}	1.81	271
Ethyl Ether	12.0×10^{-6}	1.06×10^{5}	5.54×10^{-11}	1.74	258
Acetone	10.2×10^{-6}	1.47×10^{5}	4.71×10^{-11}	2.06	260
Carbon Tet.	12.2×10^{-6}	1.72×10^{5}	3.89×10^{-11}	2.16	244
Benzene	18.7×10^{-6}	2.08×10^{5}	5.36×10^{-11}	4.53	214

The gross index of refraction of the liquid is μ_0. The relative index, μ, due to the fluctuation of density from the passage of the sound waves will be given by the following expression:

$$\mu=\frac{\mu_0+d\mu_0}{\mu_0}=1+\frac{d\mu_0}{\mu_0}. \tag{6}$$

The adiabatic compressibility, B, the density, ρ, the volume of a unit mass, V, and the pressure, P, are connected by means of the following expression:

$$dP=1/B\cdot dV/V. \tag{7}$$

For small changes in μ_0 and ρ, $(\mu_0-1)/\rho=K$. $\rho=1/V$. Making use of Eqs. (5)–(7), and considering the fact that the plus and minus Doppler components arise from waves being propagated in opposite directions, we obtain:

$$dP=\frac{\mu_0\cdot 2^{\frac{1}{2}}}{4KB\rho}\left(\frac{R\lambda_s}{\gamma}\right)^{\frac{1}{2}}. \tag{8}$$

From the classical theory of elastic waves, the amplitude, A, is given by:

$$A=dP/(2\pi\nu c\rho), \tag{9}$$

where ν is the frequency, and c the propagation velocity. The energy, E, per unit volume, for each of the progressive density waves is:

$$E=2\pi^2A^2\nu^2\rho. \tag{10}$$

If we make the substitutions:

$$c=(1/B\rho)^{\frac{1}{2}},\quad \lambda_s=\lambda/(\mu_0\sqrt{2}),\quad (I_c/2I_B)_{\text{obs.}}=r$$

where γ is replaced by $r+1$, Eq. (9) becomes,

$$A=\frac{\lambda\sqrt{2}}{16\pi(\mu_0-1)}\left(\frac{R\lambda}{\mu_0(r+1)}\right)^{\frac{1}{2}}. \tag{11}$$

Note that Eq. (11) should yield the amplitude of the Debye waves in question under conditions where the Landau-Placzek law is violated. It should be observed that R is not strictly constant, but classically must depend on the wave-length in the well-known manner.

Making use of Eqs. (10) and (11), the energy per unit volume E_t associated with the observed disturbance will be,

$$E_t=\frac{R\lambda\rho c^2}{16(r+1)}\cdot\frac{\mu_0}{(\mu_0-1)^2}. \tag{12}$$

If we assume that the Debye waves exist in quanta, of energy $h\nu$, where h is Planck's constant, the average volume per quantum, V_q, will be given by:

$$V_q=\frac{16h(r+1)(\mu_0-1)^2\sqrt{2}}{R\rho c\lambda^2}. \tag{13}$$

We have tabulated values for $d\mu_0$, dP, A, E_t, and $V_q^{\frac{1}{3}}$ for a number of common liquids in Table I. These values were calculated using the formulas given above. The values used for R were taken from the work of Peyrot[10] and from Bhagavantam.[11] Values of R were corrected by means of the inverse fourth power law for $\lambda=4078$A. Probably the most striking result of the calculations is the large value obtained for dP. It can be seen that E_t and $V_q^{\frac{1}{3}}$ remain sensibly constant for the liquids investigated.

By far the most significant calculation is that of the amplitude of the hypersonic oscillations. This amplitude is of the same order of magnitude as the molecular vibrations, and probably furnishes insight into the anomalous behavior of the Brillouin effect in viscous liquids.

Venkateswaran[12] has found that the modified Brillouin components are observable in glycerine at temperatures as low as 0°C. He has also observed that the velocity of sound in glycerine as measured by the Brillouin effect is considerably larger than would be expected for a normal liquid. This anomalous velocity behavior has been interpreted by Venkateswaran as due to a quasi-crystalline behavior of the viscous liquid.

Classically, according to hydrodynamics, plane sound waves propagated through a viscous liquid suffer a diminution of amplitude in the ratio of $1/e$ in traversing a number of wave-lengths $3c\lambda_s\rho/8\pi^2\eta$, where η is the viscosity coefficient of the liquid. It is easy to demonstrate that no propagation of the hypersonic disturbance is to be expected when the viscosity has reached a value as high as about one poise. (At 0°C glycerine has a viscosity of approximately 120 poises.)

Leontowitsch[13] has calculated the effect of viscosity on the intensity of the Brillouin components. The observation of modified Brillouin satellites in viscous glycerine has been interpreted as evidence of the incorrectness of Leontowitsch's theoretical calculations.

We have not as yet been able to make quantitative calculations concerning the effect of viscosity on the intensity of the modified Brillouin components in viscous liquids. However, it is immediately obvious from the order of magnitude calculations of the amplitude of the hypersonic vibrations that the classical macroscopic viscosity must have little to do with the attenuation of the elastic disturbances. (It is apparent that at amplitudes of only a few thousandths of an angstrom unit no viscosity bonds are broken by the elastic disturbance.) The phenomenon of decrease of viscosity at high rates of shear demonstrated theoretically by Grunberg and Nissan[14] does not give any aid in the solution of the present problem. The theory of Grunberg and Nissan also would demand considerable amplitude in order to have the rate of shear have an appreciable effect on the viscosity.

---

[10] P. Peyrot, Comptes Rendus **203**, 1512 (1936).

[11] S. Bhagavantam, *Scattering of Light and the Raman Effect* (Chemical Publishing Company, Inc., Brooklyn, New York, 1942), p. 84.

[12] C. S. Venkateswaran, Proc. Ind. Acad. Sci. **15**, 362 (1942).

[13] M. Leontowitsch, Zeits. f. Physik **72**, 247 (1931).

Qualitatively, if one considers the effect of viscosity as loosely bonding the molecules in the liquid into large molecular aggregates, it seems reasonable that even at very small amplitudes, the displacement of molecules thus loosely bound to their neighbors may cause absorption of the hypersonic waves, and conversion of this energy into unmodified scattering. Conversely, in a crystal where we have strict organization of the structure, no absorption occurs, and only the modified Brillouin components appear in the scattered light.

It might be interesting to remark that the small value for absorption observed for frequencies of the order of magnitude of 5×10^9 cycles per second is completely different from the behavior of the absorption of sound at 5×10^7 cycles per second.

Hall[15] has theoretically explained the high values of absorption of sound in water for these ultrasonic frequencies.

We are indebted to Dr. D. W. E. Axford for many helpful discussions and suggestions concerning this work.

---

[14] L. Grunberg and A. H. Nissan, Nature **156**, 241 (1945).

[15] L. Hall, Phys. Rev. **73**, 775 (1948).

Book Review

Comparative List of Color Terms. Compiled by Sidney M. Newhall and Josephine G. Brennan. A Report of the Inter-Society Color Council, 96 multilithed pages, available at $2.00 from the Secretary, Inter-Society Color Council, Box 155, Benjamin Franklin Station, Washington 4, D. C.

It may come as a shock to members of the Optical Society of America that as many as 1500 English terms are required for expressing ideas about color and for transmitting color information. These terms and their definitions have been compiled and compared in an alphabetical list as one of the regular projects of the Inter-Society Color Council, a preliminary compilation having been issued in 1939. The present list comprises about 440 terms from our own Society, about 200 terms from the American Psychological Association, 170 from the Illuminating Engineering Society, 160 from the American Artists Professional League, 110 from the Society of Motion Picture Engineers, 80 from the American Association of Textile Chemists and Colorists, and about 200 from seven other member bodies of the Inter-Society Color Council. In addition there are 200 terms from the Colour Group of the Physical Society (London).

This list is not intended as a final report on definitions of color terms; instead, it is meant to provide the basis for a thorough study of the subject. The reader will find that the alphabetical arrangement of the main list makes it easy to compare the various usages of color terms and throws into strong relief the many minor and the relatively few major inconsistencies in this usage among the various scientific, technological and artist groups contributing to the list. The various definitions of a given term supplied are simply given verbatim one after the other. Discrepancies between these definitions are so many stumbling blocks to efficient exchange of color ideas and information between workers of different backgrounds and training. The Inter-Society Color Council has performed a signal service in its appropriate field by bringing into the open the heretofore hidden basis for argument and misunderstanding among color workers.

As an example of such discrepancy we may cite the definition of *color* itself. The OSA and IES define color as "the characteristics of light other than spatial and temporal inhomogeneities," but all other groups disagree. The APA calls this idea *color stimulus*. Color they take to be "a sensory or perceptual component of visual experience . . .," the concept called *color perception* by the OSA. The ASTM defines color as an "aspect of the appearance of objects. . . ." The AAPL gives three meanings for color: (1) a property of visible phenomena, (2) a sensation, and (3) pigment. The corresponding OSA terms would be: (1) *color perception*, (2) *color sensation*, and (3) *colorant*.

The CGPS likewise has three definitions (1) "that characteristic of the visual sensation which enables the eye to distinguish differences in its quality . . ., (2) same as (1) but applied to the stimulus, and (3) "that property of an object or stimulus, or quality of a visual sensation, distinguished by its appearance of redness, greenness, etc. in contradistinction to whiteness, greyness, or blackness." The corresponding OSA terms would be: (1) *color sensation*, (2) *color*, and (3) *chromaticity* applied to an object or stimulus, or *chromaticness* as applied to a visual sensation.

Other color terms present equally knotty problems, ***brightness***, ***shade***, and ***tint***, being examples. Furthermore, there are some color terms well known and much used in certain fields that might give many a color expert pause. Try these on your friends: barre, downhand, isopaque curve, minus color, tri-color ratio, wash-back, characteristic curve, bloom, blushing, cast, masstone, tint tone, under-tone, alychne, high, ghosting, amaurosis, colored hearing, episcotister, Horner's law, phosphene, yellow spot, chatters, crock, duochroism, dichroism, duotonic, hungry, level, mealy, overhand, nicks, picking-off, resist, snaps, throwster colors, timber, distemper, gouache, juicy color, reticence, rutilant, scumbling, shot color, tender, truculent, upper register, valuable discord, and skitteriness.

In preparing, assembling, and editing a work of this magnitude, some errors are to be expected. The reviewer is glad of an opportunity to call attention to an error arising from his own neglect to supply a definition of *Munsell hue* according to OSA usage. This definition should be something like: "Expression of one aspect of an object color on arbitrary scales defined in terms of its Y-value (luminous reflectance or luminous transmittance) and its chromaticity coordinates (x, y). *Note:* The Munsell hue scales have approximately uniform perceptual steps; under ordinary observing conditions Munsell hue of a specimen correlates well with the hue of the color perceived to belong to the specimen."

The definition included in the list wrongly implies that Munsell hue is a perceptual quality. Since Munsell hue may be computed from the Y-value and chromaticity coordinates of a color, OSA usage makes it (like Munsell value and Munsell chroma) an attribute of color (psychophysical) rather than an attribute of color perception (psychological).

Other errors that this reviewer has detected are quite minor, and the compilers are to be congratulated on a difficult job well done. The format is attractive and convenient, and the printing legible. The list forms a valuable reference book that everyone dealing with people in more than one specialized field of color should have.

Deane B. Judd, *Chairman,*
OSA Representatives on the
Inter-Society Color Council

JOURNAL OF THE OPTICAL SOCIETY OF AMERICA VOLUME 39, NUMBER 9 SEPTEMBER, 1949

The Coefficient of Specific Resolution of the Human Eye for Foucault Test Objects Viewed through Circular Apertures[*]

HOWARD S. COLEMAN, MADELINE F. COLEMAN, DAVID L. FRIDGE, AND SAMUEL W. HARDING
The Optical Research Laboratory of The University of Texas, Austin 12, Texas

(Received May 11, 1949)

A study has been made of the resolving power of the human eye for Foucault test objects of different inherent contrast viewed through circular artificial pupil stops ranging from 0.30 of a millimeter to 7.0 millimeters in diameter. Two methods were used to make the resolution measurements. The first consisted of viewing the test objects through circular apertures in 10-mil blackened brass shim stock disks placed about 3 millimeters from the observer's eye. Provision was made for illuminating the test objects both with tungsten lamps and with mercury arcs. The second method involved the use of test objects viewed in collimated light by means of a telescopic system for which the exit pupil could be varied from 0.40 of a millimeter to 2.0 millimeters. Both methods used equipment embodying the basic principles of the K.D.C. apparatus. The study included resolution measurements for rectangular and square Foucault test objects consisting of straight parallel black and white bands having an inherent contrast of approximately 94 percent. The coefficient of specific resolution was computed for test objects having lower values of inherent contrast. The resolution measurements, totaling over 100,000, were made by thirty-two different observers ranging from 18 to 76 years in age. The coefficient of specific resolution was found to be practically independent of age and observer for artificial pupil stops less than 0.75 of a millimeter in diameter. This suggests an effective consistency of the contrast threshold of the human retina as far as resolution measurements are concerned and indicates that the diffraction of light at the pupil stop is the primary factor controlling resolution. For artificial pupil stops of larger diameter, the coefficient of specific resolution was found to depend upon the individual observer but only with a maximum variation among the observers used of 30 percent. The composition of the test object was found to influence the coefficient of specific resolution to a certain extent with an indication that the best resolution was obtainable with test objects having the greatest number of elements.

INTRODUCTION

IN using nearly any form of a visual aid to study the fine detail of objects, the limit to which such detail may be seen is, in the final analysis, generally controlled by the limitations imposed by the human eye. It is therefore of interest to study the behavior of the eye under conditions simulating those encountered in the use of visual aids. In a visual optical system used to study the fine detail of objects, there is generally an effective stop located near or at the eye. This stop is sometimes larger than the natural pupil of the eye, but generally it is smaller. Such a stop may be located somewhat in front of the eye or it may be located (optically) inside the eye, depending upon the location of the exit pupil of the optical system being used. Since the size and position of this stop frequently control the fraction of the pupil of the eye actually used in making an observation using an optical system, it is of value to determine the manner in which such stops influence the visibility of objects (or images) viewed through them. On the basis that the fine detail visible by means of an optical system (including the photosensitive receptor) is closely related to its resolving power, a study was made of the resolution of the human eye using Foucault test objects viewed through artificial pupil stops. Foucault test objects were used because of the simplicity of making quantitative measurements using them and the fact that they can be made to closely simulate many common situations of interest. Two types of pupil stops were used. One type was located about 3 millimeters from the pupil and the other type placed optically in the pupil corresponding to two general locations of the stops mentioned above.

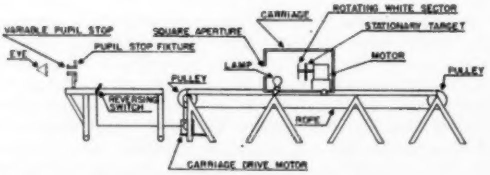

FIG. 1. Schematic diagram of the pupil stop apparatus.

FIG. 2. The pupil stop apparatus.

It is the purpose of this paper to describe the methods used and the results obtained in the study of the resolution of Foucault test objects viewed through artificial circular pupil stops.

THE APPARATUS

Two types of apparatus were used in the resolving power studies described in this paper. The first is re-

---

[*] The work described in this paper was performed in part under terms of Contract NOrd-10222 and NOrd-10403 between the Bureau of Ordnance of the Navy Department and The University of Texas and under terms of ORSD Contract OEMsr-1197 at The Pennsylvania State College.

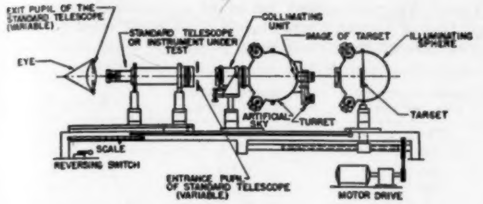
EXIT PUPIL OF THE STANDARD TELESCOPE (VARIABLE)
STANDARD TELESCOPE OR INSTRUMENT UNDER TEST
COLLIMATING UNIT
IMAGE OF TARGET
ILLUMINATING SPHERE
EYE
ARTIFICIAL SKY
TURRET
TARGET
SCALE
REVERSING SWITCH
ENTRANCE PUPIL OF STANDARD TELESCOPE (VARIABLE)
MOTOR DRIVE

FIG. 3. Schematic diagram of the K.D.C. apparatus Model 7 used to measure the resolving power of the human eye.

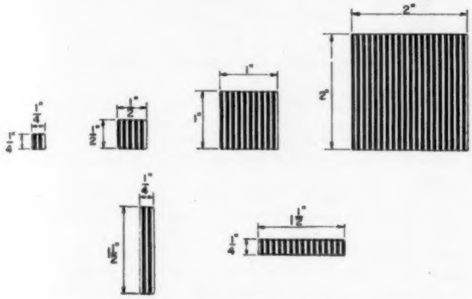

FIG. 4. Form of Foucault test objects used in the pupil stop apparatus.

ferred to as "the pupil stop apparatus" and the second is referred to as "the kinetic definition chart apparatus."[1]

TABLE I. Minimum angle of resolution for a Foucault test object of a 94 percent inherent contrast *vs.* the diameter of an artificial pupil stop placed 3 mm from the pupil of the human eye.

Pupil stop (millimeters)	Minimum angle of resolution (radians ×10⁵) for five observers No. 1	No. 2	No. 3	No. 4	No. 5
0.41	144	133	133	137	133
0.46	129	122	125	125	125
0.76	81	76	80	79	77
1.02	67	63	64	60	60
1.27	58	55	55	51	49
1.52	52	51	48	45	45
1.78	49	49	45	44	42
2.03	51	48	45	38	41
2.29	51	47	45	41	39
2.54	49	47	44	39	38
3.05	49	45	44	41	36
5.08	49	44	42	39	38

TABLE II. Minimum angle of resolution of a Foucault test object of 94 percent inherent contrast as a function of the exit pupil of a high grade telescopic system.

Exit pupil (millimeters)	Reciprocal of exit pupil	Minimum angle of resolution for two observers (radians ×10⁵) No. 1	No. 2
0.39	2.6	143	149
0.60	1.7	94	92
1.6	0.62	44	46
3.0	0.33	38	41
4.6	0.22	37	40

The pupil stop apparatus consists of an illuminated Foucault test object mounted on a track and provided with a mechanism by means of which the distance between the test object and the observer can be varied continuously. The test object is viewed by the observer through circular apertures of different diameters formed in 10-mil blackened brass shim stock diaphragms placed approximately 3 millimeters from the pupil of the eye. The angular separation between the elements of the test object is varied by varying the distance between the observer and the test object. The arrangement of the pupil stop apparatus is shown in Figs. 1 and 2. The pupil stop apparatus includes a series of thirty circular apertures (referred to as artificial pupil stops) ranging from 0.3 of a millimeter to 7 millimeters. The apparatus is used in a darkened room such that the

TABLE III. The coefficient of specific resolution for a Foucault test object of 94 percent inherent contrast *vs.* age of the observer.

Designation of observer	Observer's age	K.D.C. scale reading	Coefficient of specific* resolution ×10⁵
1	22	10.5	60.0
2	24	10.7	59.0
3	24	10.5	60.0
4	24	10.8	57.6
5	24	10.7	59.0
6	26	10.8	57.6
7	26	10.9	57.6
8	27	10.7	59.0
9	27	10.8	57.6
10	28	10.5	60.0
11	28	10.7	59.0
12	30	10.5	60.0
13	32	10.7	59.0
14	33	11.0	56.5
15	40	10.8	57.6
16	76	10.5	60.0

* Coefficient of specific resolution is defined here as the product of the minimum separable angle (in radians) between the elements of the test object and the aperture (in mm).

TABLE IV. Computed values of the coefficient of specific resolution of Foucault test objects of different inherent contrast viewed through an artificial pupil stop 0.4 of a mm in diameter.

Inherent contrast (C_o) in percent	Apparent contrast (C_a) in percent	$\overline{R}$ (mm-rad. ×10⁵)
100	100	56.0
90	90	56.5
80	80	56.9
70	70	57.4
60	60	57.9
50	50	58.5
40	40	59.5
30	30	60.8
20	20	63.2
10	10	69.5
7	7	78.2
3.1	3.1	∞

Notes:

(1) The contrast threshold ($C_{\dagger}$) of the photosensitive receptor is 3.1 percent.

(2) Contrast rendition ($C.R.$) = 100 percent.

(3) Apparent contrast (C_a) = inherent contrast (C_o) × contrast rendition ($C.R.$).

(4) A coefficient of specific resolution ($\overline{R}$) of 56.0 millimeter-radians ×10⁵ is equivalent to a relative resolving power (*RRP*) of 100 percent.

---

[1] H. S. Coleman and S. W. Harding, J. Opt. Soc. Am. **37**, 263 (1947).

Table V. Computed values of the coefficient of specific resolution of Foucault test objects of different inherent contrast viewed through an artificial pupil stop 0.6 of a mm in diameter.

Inherent contrast (C_o) in percent	Apparent contrast (C_a) in percent	$\overline{R}$ (mm-rad. ×10^5)
100	92.6	56.4
90	83.3	56.8
80	74.0	57.2
70	64.7	57.7
60	55.5	58.2
50	46.3	59.0
40	37.0	60.0
30	27.8	61.4
20	18.5	63.9
10	9.3	71.2
7	6.5	77.4
3.3	3.1	∞

Notes:

1. The contrast threshold ($C_\dagger$) of the photosensitive receptor is 3.1 percent.
2. Contrast rendition (*C.R.*) = 92.6 percent.
3. Apparent contrast (C_a) = inherent contrast (C_o) × contrast rendition (*C.R.*).
4. A coefficient of specific resolution ($\overline{R}$) of 56.0 millimeter-radians ×10^5 is equivalent to a relative resolving power (*RRP*) of 100 percent.

Table VI. Computed values of the coefficient of specific resolution of Foucault test objects of different inherent contrast viewed through an artificial pupil stop 0.7 of a mm in diameter.

Inherent contrast (C_o) in percent	Apparent contrast (C_a) in percent	$\overline{R}$ (mm-rad. ×10^5)
100	75.0	57.0
90	67.5	57.5
80	60.0	57.9
70	52.5	58.3
60	45.0	59.1
50	37.5	59.8
40	30.0	60.9
30	22.5	62.6
20	15.0	65.6
10	7.5	74.3
5	3.8	97.2
4.1	3.1	∞

Notes:

1. The contrast threshold ($C_\dagger$) of the photosensitive receptor is 3.1 percent.
2. Contrast rendition (*C.R.*) = 75.0 percent.
3. Apparent contrast (C_a) = inherent contrast (C_o) × contrast rendition (*C.R.*).
4. A coefficient of specific resolution ($\overline{R}$) of 56.0 millimeter-radians ×10^5 is equivalent to a relative resolving power (*RRP*) of 100 percent.

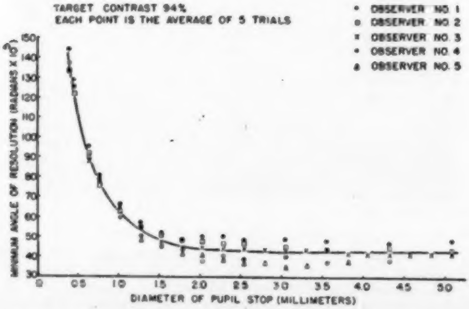

Fig. 5. The minimum angle of resolution for the human eye *vs.* the diameter of the pupil stop used in the pupil stop apparatus.

Table VII. Computed values of the coefficient of specific resolution of Foucault test objects of different inherent contrast viewed through an artificial pupil stop 0.8 of a mm in diameter.

Inherent contrast (C_o) in percent	Apparent contrast (C_a) in percent	$\overline{R}$ (mm-rad. ×10^5)
100	36.2	60.0
90	32.6	60.6
80	29.0	61.1
70	25.4	61.8
60	21.7	62.8
50	18.1	64.0
40	14.5	66.0
30	10.9	68.6
20	7.2	75.0
10	3.6	104.0
8.6	3.1	∞

Notes:

1. The contrast threshold ($C_\dagger$) of the photosensitive receptor is 3.1 percent.
2. Contrast rendition (*C.R.*) = 36.2 percent.
3. Apparent contrast (C_a) = inherent contrast (C_o) × contrast rendition (*C.R.*).
4. A coefficient of specific resolution ($\overline{R}$) of 56.0 millimeter-radians ×10^5 is equivalent to a relative resolving power (*RRP*) of 100 percent.

Table VIII. Computed values of the coefficient of specific resolution of Foucault test objects of different inherent contrast viewed through an artificial pupil stop 1.0 mm in diameter.

Inherent contrast (C_o) in percent	Apparent contrast (C_a) in percent	$\overline{R}$ (mm-rad. ×10^5)
100	24.9	62.0
90	22.4	62.6
80	19.9	63.3
70	17,4	64.4
60	15.0	65.6
50	12.5	67.3
40	10.0	69.8
30	7.5	74.2
20	5.0	83.9
12.4	3.1	∞

Notes:

1. The contrast threshold ($C_\dagger$) of the photosensitive receptor is 3.1 percent.
2. Contrast rendition (*C.R.*) = 24.9 percent.
3. Apparent contrast (C_a) = inherent contrast (C_o) × contrast rendition (C.R.).
4. A coefficient of specific resolution ($\overline{R}$) of 56.0 millimeter-radians ×10^5 is equivalent to a relative resolving power (*RRP*) of 100 percent.

Table IX. Computed values of the coefficient of specific resolution of Foucault test objects of different inherent contrast viewed through an artificial pupil stop 1.5 mm in diameter.

Inherent contrast (C_o) in percent	Apparent contrast (C_a) in percent	$\overline{R}$ (mm-rad. ×10^5)
100	8.2	73.5
90	7.4	74.5
80	6.6	76.8
70	5.7	80.4
60	4.9	85.2
50	4.1	91.6
40	3.3	109.1
38	3.1	∞

Notes:

1. The contrast threshold ($C_\dagger$) of the photosensitive receptor is 3.1 percent.
2. Contrast rendition (*C.R.*) = 8.2 percent.
3. Apparent contrast (C_a) = inherent contrast (C_o) × contrast rendition (*C.R.*).
4. A coefficient of specific resolution ($\overline{R}$) of 56.0 millimeter-radians ×10^5 is equivalent to a relative resolving power (*RRP*) of 100 percent.

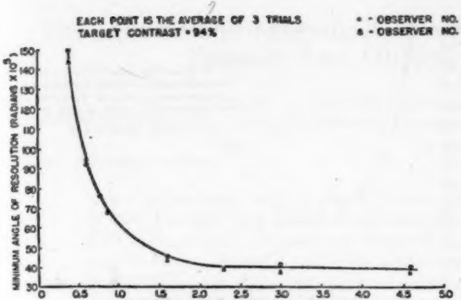

FIG. 6. The minimum angle of resolution of the human eye *vs.* pupil stop diameter obtained using the K.D.C. apparatus Model 7.

TABLE X. Computed values of the coefficient of specific resolution of Foucault test objects of different inherent contrast viewed through an artificial pupil stop 2.0 mm in diameter.

Inherent contrast (C_0) in percent	Apparent contrast (C_a) in percent	$\bar{R}$ (mm-rad.$\times 10^5$)
100	4.8	88.0
90	4.3	90.4
80	3.8	96.4
70	3.4	112.4
65	3.1	∞

Notes:

(1) The contrast threshold ($C_\dagger$) of the photosensitive receptor is 3.1 percent.

(2) Contrast rendition (*C.R.*) = 4.8 percent.

(3) Apparent contrast (C_a) = inherent contrast (C_0) × contrast rendition (*C.R.*).

(4) A coefficient of specific resolution ($\bar{R}$) of 56.0 millimeter-radians $\times 10^5$ is equivalent to a relative resolving power (*RRP*) of 100 percent.

pupil of the observer's eye is approximately at its maximum value. A shield is provided which prevents the light from the illumination system of the test object from reaching the observer's eye except through the pupil stop. The pupil stops are mounted in a mechanical assembly resembling an eyepiece of a conventional optical system. Targets are illuminated to a brightness level of approximately 500 foot lamberts.

The Kinetic Definition Chart apparatus (abbreviated to K.D.C. apparatus)[1] is shown schematically in Fig. 3. This apparatus is used in a darkened room and is essentially the same as the pupil stop apparatus except for the use of optical parts and the fact that the apparent distance between the test object and the observer does not change. The test object is viewed through the exit pupil of a high grade telescopic system as shown in Fig. 3. The method used to vary the diameter of the pupil stop was to change the entrance pupil (and hence the exit pupil) of the part of the apparatus designated as "the standard telescope" shown in Fig. 3.

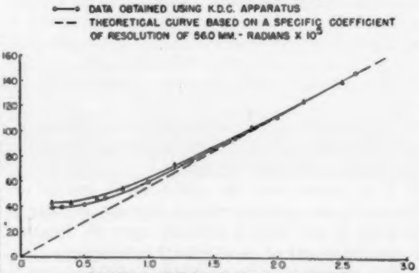

FIG. 7. The minimum angle of resolution *vs.* the reciprocal of the diameter of the artificial pupil stop for the human eye.

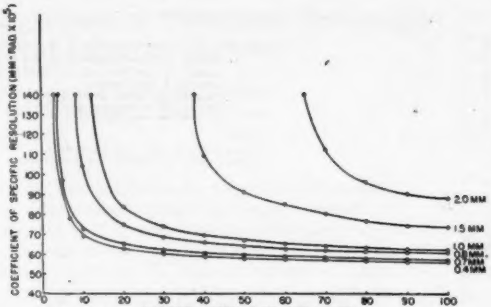

FIG. 8. The coefficient of specific resolution *vs.* inherent contrast of Foucault test objects viewed through artificial pupil stops of various sizes.

THE PROCEDURE

Two procedures were followed in measuring the resolving power of the human eye, depending upon the particular type of apparatus used. In using the pupil stop apparatus, resolution measurements were made for Foucault test objects of different shapes and sizes, using light from tungsten lamps and light from mercury arcs. The form of the test objects used are shown in Fig. 4. The sixteen observers used in making resolution measurements with the pupil stop apparatus consisted of seven males and nine females ranging from 20 to 32 years in age.

In using the K.D.C. apparatus, resolution measurements were made in which the Foucault test objects

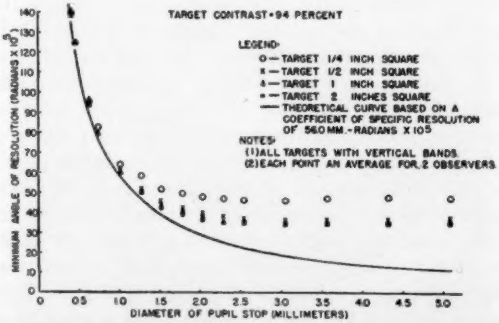

FIG. 9. The minimum angle of resolution *vs.* the artificial pupil stop diameter for Foucault test objects in the form of different size squares.

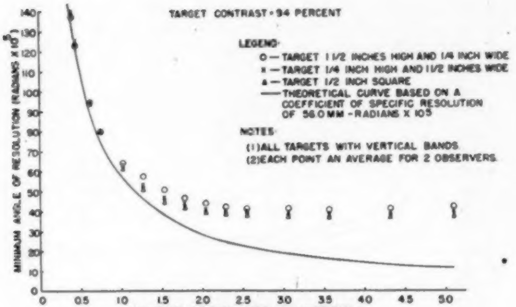

FIG. 10. The minimum angle of resolution *vs.* the artificial pupil stop diameter for Foucault test objects of different composition.

were illuminated from tungsten lamps to a brightness level of approximately 500 foot lamberts. Sixteen different male observers ranging from 22 to 76 years in age were used in these measurements.

The minimum angles of resolution obtained by the two methods described for different pupil stop sizes for Foucault test objects of 94 percent inherent contrast,[2] were used to calculate the angles of minimum resolution for Foucault test objects of less contrast using the methods described in a previous paper.[2] The values of the coefficient of specific resolution were computed as the product of the minimum angle of resolution in radians and the diameter of the artificial pupil stop in millimeters.

THE DATA

The data obtained in the study of the resolving power of the human eye are shown in Tables I to X inclusive and Figs. 5 to 11 inclusive. The tables show the basic data obtained and the computed values of the apparent contrast that a 94 percent contrast test object would appear to have as a result of the aberrations of the eye and the diffraction of the light by the artificial pupil stop. Figures 5 and 6 show sample data obtained for the minimum angle of resolution for the two methods used to vary the size of the pupil stops. Figure 7 shows the comparison of the minimum angle of resolution obtained using the two methods used to vary the diameter of the pupil stops. Figure 8 shows the computed coefficients of specific resolution of the human eye for Foucault test objects of different inherent contrast. Figure 9 shows the influence of the size of a Foucault test object on the minimum angle of resolution. Figure 10 shows the influence of the composition of a Foucault test object on the minimum angle of resolution. Figure 11 shows the values obtained for the minimum angle of resolution using a Foucault test object illuminated with the light from a mercury arc and viewed through a green filter placed in the pupil stop apparatus.

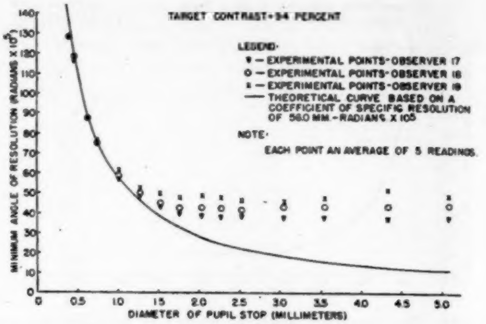

FIG. 11. The minimum angle of resolution *vs.* artificial pupil stop diameter for Foucault test objects illuminated with green mercury light.

DISCUSSION AND CONCLUSIONS

A study of the data presented in this paper indicates that the ability of the human eye to resolve Foucault test objects viewed through circular aperture stops depends upon the artificial pupil size, the test object contrast, the wave-length of light used to illuminate the test object, the test object shape, the test object size, and appears to be independent of the sex and age of the observers as well as the method used to vary the diameter of the pupil stop and its distance from the pupil of the eye. In addition to these general observations, the following specific conclusions may be drawn:

(1) It is evident that the minimum resolvable angle for Foucault test objects of 94 percent inherent contrast range from 1 to 5 minutes for artificial pupil stops ranging from 0.4 of a millimeter to 7.0 millimeters in diameter.

(2) It is evident that the minimum angle of resolution for Foucault test objects occurs at an artificial pupil stop diameter of 2.5 millimeters.

(3) It is evident that the resolution of the human eye is somewhat improved by the use of an artificial pupil stop of 2.5 millimeters in diameter.

(4) It is evident that for artificial pupil stops smaller than approximately 0.75 of a millimeter, the diffraction of light is the controlling factor for resolution rather than the aberrations of the human eye.

(5) It is evident that it is easiest for the human eye to resolve Foucault test objects for those objects having the greatest number of elements.

(6) It appears that the minimum angle of resolution for Foucault test objects viewed through circular aperture stops is somewhat less for targets illuminated with green mercury light than with light from incandescent tungsten filaments. This is somewhat contrary to diffraction theory and is likely explainable on the basis of the spectral response of the human eye.

(7) It is evident that no particular correlation exists between the coefficients of specific resolution obtained for the different observers and their ages.

(8) It is evident that the coefficients of specific resolution of Foucault test objects viewed through circular artificial pupil stops do not depend critically upon the location of the stop from the pupil up to at least 3 millimeters.

(9) It is evident that the coefficients of specific resolution of Foucault test objects viewed through circular artificial pupil stops are substantially the same whether they are viewed in collimated light or diverging light from objects located at distances greater than one meter from the observer.

---

[2] H. S. Coleman and M. F. Coleman, J. Opt. Soc. Am. 37, 572 (1947).

JOURNAL OF THE OPTICAL SOCIETY OF AMERICA VOLUME 39, NUMBER 9 SEPTEMBER, 1949

The Influence of Magnification on Resolving Power of Telescopic Systems for Foucault Test Objects of Different Inherent Contrast*

Howard S. Coleman, Madeline F. Coleman, and Samuel W. Harding
The Optical Research Laboratory of The University of Texas, Austin, Texas

(Received May 12, 1949)

A study has been made of the variation in resolving power with magnification for telescopic systems used to view Foucault test objects of different inherent contrast. The study included the use of a form of the K.D.C. Apparatus. The results of the study indicate the existence of an optimum magnification that can be used to resolve Foucault test objects and that the optimum value of the magnification depends upon the inherent contrast of the test object. As the test object contrast decreases, the optimum amount of magnification decreases. For test objects having an inherent contrast of approximately 100 percent, an optimum amount of magnification was found to be approximately 70× for each 25.4 mm of aperture of the telescopic system under consideration. For objects of 10 percent inherent contrast, the optimum magnification was found to be approximately 30× for each 25.4 mm of aperture.

INTRODUCTION

In using optical systems to study fine detail of objects, the amount of magnification used often controls the amount of detail that can be seen. Although "rules of thumb" have existed for selecting the amount of magnification to be used, it is generally recognized that such "rules" have relatively little scientific foundation and hence the procedure one generally follows is that of trial and error in selecting the amount of magnification to be used for a particular task. It is evident, however, that it would be helpful to have some guidance as to the order of magnitude of the magnification that should produce optimum results for common cases of interest. In order to explore the possibility of establishing this order of magnitude, a study was conducted in which the resolving power of a number of telescopic systems was measured using different amounts of auxiliary magnification and Foucault test objects of different inherent contrast as subjects. It is the purpose of this paper to describe the results obtained in this study for four telescopic systems of different degrees of design complexity. In the study, nine different observers were used. Three of these were males and six were females. The observers used had 20/20 vision, or better, and ranged in age from 20 to 32 years. The study involved over 20,000 precision resolution measurements.

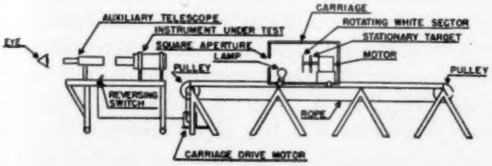

Fig. 1. Schematic diagram of the Kinetic Definition Chart Apparatus Model 2.

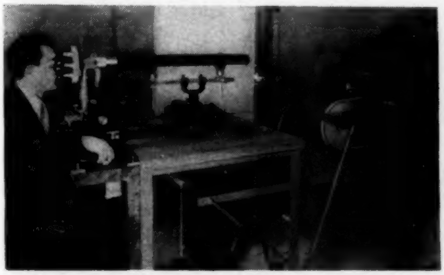

Fig. 2. The Kinetic Definition Chart Apparatus Model 2.

THE APPARATUS

The apparatus used to study the influence of magnification on resolving power of telescopic systems is referred to as the Kinetic Definition Chart Apparatus

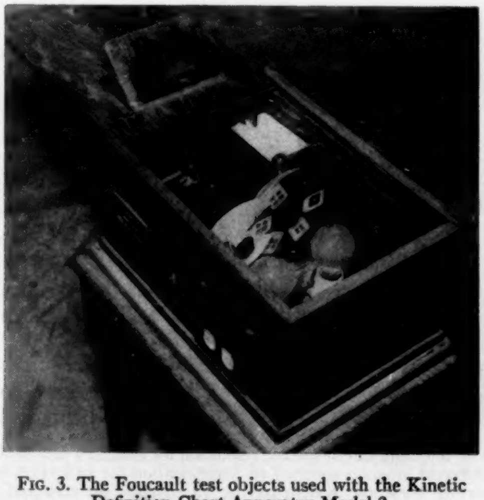

Fig. 3. The Foucault test objects used with the Kinetic Definition Chart Apparatus Model 2.

---

* The work described in this paper was performed in part under terms of Contract NOrd-10403 between the Bureau of Ordnance of the Navy Department and The University of Texas, and under O.S.R.D. Contract OEMsr-1197 at The Pennsylvania State College.

TABLE I. Coefficient of specific resolution for Foucault test objects of different inherent contrast *vs.* magnification for an $F/17.1$ lens inverting telescopic system having 6 air-glass surfaces and an aperture of 7.12 mm.

Magnification of telescopic system	Coefficients of specific resolution for Foucault test objects of different inherent contrast (mm-rad. ×10⁶) 50 percent	40 percent	30 percent	20 percent	10 percent
2.4×	110	119	123	133	174
4.8×	69.6	71.2	77.5	79.0	90.4
6.4×	67.8	69.5	69.7	76.7	89.0
9.6×	63.6	64.3	65.8	73.3	77.5
14.4×	61.7	63.4	65.0	66.8	81.2
24.0×	62.3	65.9	65.3	73.3	89.6

TABLE II. Coefficient of specific resolution for Foucault test objects of different inherent contrast *vs.* magnification for an $F/11.5$ lens inverting telescopic system having 12 air-glass surfaces and an aperture of 25.4 mm.

Magnification of telescopic system	Coefficients of specific resolution for Foucault test objects of different inherent contrast (mm-rad. ×10⁶) 95 percent	50 percent	30 percent	10 percent
6×	130	157	196	250
15×	69.5	89.6	87.3	111
30×	59.3	68.5	70.0	102
60×	58.5	66.3	68.0	90.0
90×	59.3	65.2	68.8	96.7

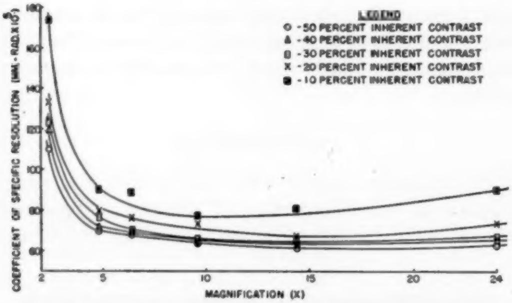

FIG. 4. Coefficient of specific resolution for Foucault test objects of different inherent contrast *vs.* magnification for an $F/11.5$ lens inverting telescopic system having 6 air-glass surfaces and an aperture of 7.12 mm.

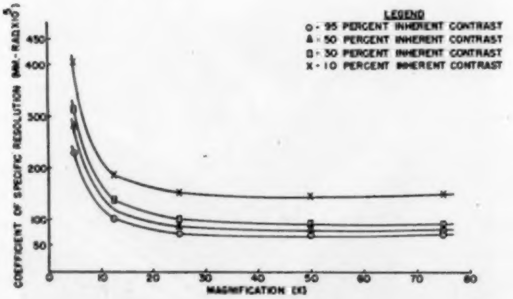

FIG. 5. Coefficient of specific resolution for Foucault test objects of different inherent contrast *vs.* magnification for an $F/11.5$ lens inverting telescopic system having 12 air-glass surfaces and an aperture of 25.4 mm.

TABLE III. Coefficient of specific resolution for Foucault test objects of different inherent contrast *vs.* magnification for an $F/5.0$ lens erecting telescopic system having 34 air-glass surfaces and an aperture of 21.7 mm.

Magnification of telescopic system	Coefficients of specific resolution for Foucault test objects of different inherent contrast (mm-rad. ×10⁶) 95 percent	50 percent	30 percent	10 percent
6.95×	113	137	158	199
13.9×	71.6	88.2	94.3	163
18.5×	69.5	82.1	90.4	157
27.8×	62.5	73.4	80.0	154
41.7×	62.2	71.5	79.5	173
69.5×	61.9	71.2	80.0	216

TABLE IV. Coefficient of specific resolution for Foucault test objects of different inherent contrast *vs.* magnification for an $F/4.0$ lens erecting telescopic system having 28 air-glass surfaces and an aperture of 35.0 mm.

Magnification of telescopic system	Coefficients of specific resolution for Foucault test objects of different inherent contrast (mm-rad. ×10⁶) 95 percent	50 percent	30 percent	10 percent
5.0×	230	287	314	407
12.5×	102	96.6	137	188
25.0×	72.5	88.0	102	154
50.0×	71.0	84.5	90.5	145
75.0×	71.4	83.5	92.0	150

Model 2 (abbreviated to K.D.C. Apparatus).[1] The K.D.C. Apparatus is essentially a resolving power chart in which the angular subtense between the elements of the test objects, with respect to an observer, can be varied continuously. The apparatus is provided with a mechanism by means of which the contrast between the elements of the test object and the background against which they are viewed can be varied as desired. As may be seen from Figs. 1, 2, and 3, the K.D.C. Apparatus Model 2 consists of a test object, referred to as the target, a mechanism for varying the distance between the target and the optical system under test, a rotating

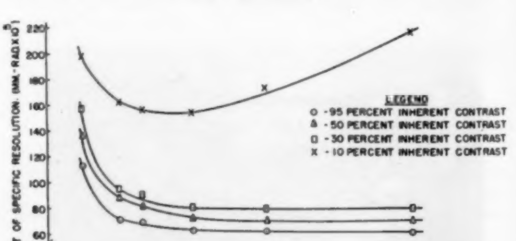

FIG. 6. Coefficient of specific resolution for Foucault test objects of different inherent contrast *vs.* magnification for an $F/5.0$ lens erecting telescopic system having 34 air-glass surfaces and an aperture of 21.7 mm.

---

[1] Howard S. Coleman, and Samuel W. Harding, Methods for Making Precise Resolution Measurements, J. Opt. Soc. Am. 37, 263–271 (1947).

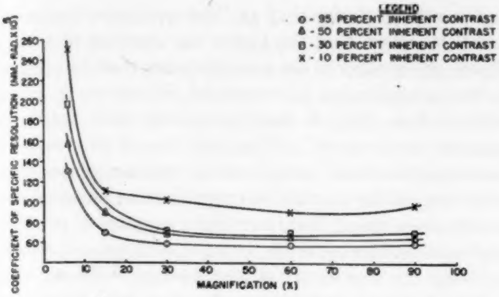

Fig. 7. Coefficient of specific resolution for Foucault test objects of different inherent contrast *vs.* magnification for an $F/4.0$ lens erecting telescopic system having 28 air-glass surfaces and an aperture of 35.0 mm.

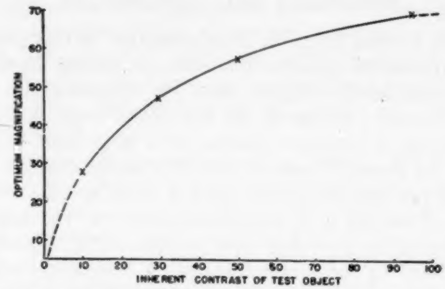

Fig. 8. Optimum magnification per 25.4 mm of aperture for the resolution of Foucault test objects using telescopic systems.

white sector assembly for controlling the target contrast, and a device designated as the auxiliary telescope.

The target is an illuminated reflection type Foucault test object consisting of four sets of straight alternately black and white parallel bands. The bands in the four sets are oriented in different directions and are viewed "through" rotating white sectors of different angular subtense. These sectors make the target appear to have various inherent contrasts depending upon the angle of the particular sector used. The details of this unit are shown in Fig. 3.

The mechanism for varying the subtense of the elements of the target with respect to the entrance pupil of the optical system under test, consists of a motor driven carriage which moves the target along a fifty-foot tract such that it always lies along the extension of the optical axis of the system under consideration. The motion of the carriage is controlled by a reversing switch assembly and is operated by the observer.

The auxiliary telescope is a high grade telescopic system consisting of an achromatic objective which is moved along its axis for focusing purposes and has a turret of six Ramsden eyepieces of different effective focal lengths. The different eyepieces are used to vary the magnification of the auxiliary telescope from unity to approximately 30×.

THE PROCEDURE

In the study of the influence of magnification on the resolution of Foucault test objects by means of telescopic systems, four different designs of optical systems were used. Two of these were simple astronomical telescopes and two were relatively complex terrestrial lens erecting designs. The optical systems studied were of average quality, from a resolving power point of view, and were selected as being typical specimens of their designs.

The procedure consisted of having each observer determine the maximum distance at which he could resolve the elements of a given test object using a particular instrument under consideration and a definite amount of auxiliary magnification. Each observer made at least 100 readings for each of these conditions but not more than five successive readings for any one condition.

In making the resolution measurements, the criterion used for the limit of resolution was the distance at which the direction of any one of the four sets of the test object elements no longer could be specified. This distance is referred to hereafter as "the limiting distance of resolution." The criterion used is somewhat arbitrary and may not yield the highest possible resolution values for the optical systems considered. It does, however, insure the consistency of a criterion in the present study.

The average values of limiting distances of resolution obtained by the different observers and the distances between adjacent white bands of the test objects were used to compute the minimum angle of resolution for each of the conditions of observation. These angular values and the apertures of the telescopic systems under test were used to compute the coefficients of specific resolution for each of the observation conditions.

THE DATA

The data obtained for the resolving power of the telescopic systems studied are presented in Tables I to IV inclusive. These tables show the values of the coefficient of specific resolution obtained for each of the test objects used and the total magnification of the optical system involved. The total magnification was computed as the product of the magnification of the optical system under test and the magnification of the auxiliary telescope. The values of the coefficient of specific resolution were computed as the product of the apertures of the telescopic system under test, expressed in millimeters, and the minimum angles of resolution, expressed in radians. To facilitate in the comparison of the data, graphs have been prepared in which the coefficients of specific resolution are presented as functions of total magnification for selected test object contrasts for each of the four instruments studied. These are shown in Figs. 4 to 8 inclusive.

DISCUSSION AND CONCLUSIONS

It is evident from the data presented in this paper, that the resolving power of a telescopic system depends, to a considerable degree, upon the magnification and the inherent contrast of the test object used. A study of graphs of the data plotted on a large scale shows that, for Foucault test objects of inherent contrast up to 100 percent, there exist minima in the specific coefficient of resolution *vs.* magnification curves. The magnification values at which these minima occur, appear to be related to the target contrast in a regular fashion when expressed per unit of aperture as shown in Fig. 8. This figure can be interpreted as indicating an upper limit to the magnification that should be used for maximum resolution of objects of a particular contrast and has been designated as "the optimum magnification." It is seen that the higher the contrast of the test object, the greater is the magnification that can be used so far as resolution is concerned. However, it is also evident from Fig. 8 that no matter how small the inherent contrast of a Foucault test object may be, some magnification is required for maximum resolution even though the amount of magnification required may be relatively small. This fact has a number of practical applications. For example, in the use of microscopes for studying the fine detail of low contrast objects, relatively small amounts of magnification may render the fine detail in objects more visible than the greater amounts of magnification inherent in the design of common microscopic systems.

JOURNAL OF THE OPTICAL SOCIETY OF AMERICA VOLUME 39, NUMBER 9 SEPTEMBER, 1949

On Some Aspects of White, Gray, and Black*

Ralph M. Evans
Eastman Kodak Company, Rochester, New York

(Received May 18, 1949)

In any system which defines color on the basis of the non-spatial, non-temporal properties of light it is shown that white, gray, and black are not colors. The perception of white is shown to be caused by a physical property of the object not associated with its selectivity. This property is the diffusion of light. White is shown to be one extreme of a series starting at clear and passing through various degrees of pale white to a maximum. Gray is shown to be the perception of the relative visual effectiveness of the light from two areas and cannot be seen unless at least two areas are present. Black is considered the extreme in lack of relative effectiveness.

THE Report of the Colorimetry Committee of the Optical Society of America defines color as a psychophysical entity. This entity involves only the non-spatial and non-temporal aspects of the light reaching the observer's eyes and evaluates this in terms of a standardized observer. Tristimulus values or the derived values of dominant wave-length, excitation purity, and luminance constitute a complete description.

When the word color is used in connection with the appearance of an object, considerable care must be taken if one is to avoid implications beyond the concept as defined in this manner. The Report notes that color as seen in daily life in connection with objects is normally seen as a property of the objects rather than of the light coming from them. It points out, however, that little is gained by referring the color to the object and that it tends to obscure the separation of the object's true properties. Thus such a reference tends to confuse the color with the selective absorption which causes it and which is not an observable property to the unaided eye. In addition, the practice tends to include in color such properties as gloss and the like which are better handled separately. The Report points out that there are four ways, or "modes," in which perception can take place and that each of these modes has the possibility of possessing certain "attributes." Thus glossiness is an attribute of the object mode of perception. Color can be seen in any mode and has only the attributes of hue, saturation, and brightness.

In addition to these facts, color is so defined that it does not take into account either the environment in which the color is seen or any change in the condition of the eye from the standardized conditions under which the basic accepted psychophysical data have been obtained. It follows that the visual correlate to the color uniquely described by any computation based on the definition can be seen with certainty only under these conditions, namely, a single patch of light seen in the aperture mode, and completely homogeneous in respect to each of the three attributes. Such a condition is approximated by the field of a good photometer *when the fields are exactly matched*, since this is the condition under which the data were obtained. In its pure form the stimulus completely fills the field of view. In either case, color as so perceived cannot possess two characteristics which are referred to as colors in everyday speech. Color seen in the aperture mode does not contain either white or gray. We are forced to the conclusion, therefore, that white and gray are not colors under the definition. The purpose of the present paper is to attempt to clarify the situation by the introduction of a number of concepts somewhat different from those usually stated in the literature. In the discussion it will be necessary to consider also the perceptual attributes "black" and "clear."

---

* Delivered in substance as a paper before the meeting of the Optical Society of America in New York, New York, on February 22, 1947.

It has been customary to think of white, gray, and black as forming a single continuous series of appearances as exemplified by any set of reflection standards. Such a series may be described physically by the statement that the areas are non-selective or neutral or achromatic and by giving their percent reflectances.

Accompanying this concept, of course, there has been the realization that gray and black are not unique to this reflection series but are to be found as well in series of clear liquids. Such a series of appearances also runs through gray to black but has at its head not white but clear.

It has generally been realized also that between the white, which is at the top of one of the series, and the clear, which is at the top of the other, there is a large and important difference. The two, however, are connected by a continuous unbroken series. From white to clear there is a series of appearances important enough to have a whole group of common speech names for its description. Such words as hazy, foggy, turbid, milky indicate fairly well-defined regions, each shading into the other.**

In terms of the accepted nomenclature this is a continuous transition in the object mode from a clear through a cloudy volume to an opaque liquid surface. Such a transition from volume to surface is not necessary, however. The same series may be obtained by spraying white paint on a clear glass surface in varying amounts or by grinding the surface of a polished metal to varying degrees. This will again give the transition from clear through varying degrees of white to a maximum opaque white.

This intermediate or connecting series between clear and opaque exists also for all chromatic series and for all shades of gray. That is, for every color specification regardless of its origin there corresponds one of these series. In a sense, therefore, it represents a sort of fourth-dimensional no-man's land between the concepts of a chromatic series arising from matte surfaces, such as those of the Munsell System and from clear, transparent objects such as might be constructed from clear gelatin filters. It is this region which it is hoped may be clarified in the present paper.

For achromatic objects four concepts are involved, namely, clear, white, gray, and black. For simplicity of argument each of these will be considered separately and then the suggestion made that the same concepts may be extended to the chromatic members also. Specifically, the attempt will be to show that gray and white are independent variables.

Consider first the concept called "clear." If one looks at a clear achromatic object in recognizable surroundings, it is at once apparent that the expression "clear and achromatic" must necessarily involve an object if it is to refer to a direct perception. A real object or at least real material has to be assumed in order to give the term meaning as a direct perception. We are dealing, therefore, with the properties of objects. The perceptions, clear and achromatic, in combination at least, require the presence of an object which is visible in some other way, usually through its edges or because it refracts the light.

A similar situation exists for the perception of clear, chromatic objects. One can see both the color and the clear objects. The perceptions of color are associated with the effect of the objects but again the fact that they are clear depends on the way in which the light is affected by them.

When we say that an object has certain characteristics, what is meant by the term? It seems that it can mean only that after we have lived with that object for a while, have walked around it and seen it under a number of conditions, perhaps have picked it up and turned it over or around, we have come to believe that *as an object* it possesses certain properties. Under these conditions the term "shiny," for example, means that the object has certain fundamental surface properties which we believe to be inherent in the object and not a product of its environment. Such characteristics may be called the "residual" properties of the object. They are the "residual" perceptions (memories) retained in the mind after walking away from the object and its environment. These residual properties, or more accurately the residual perceptions of these properties, are what seem to be specified by the word attributes. Thus shape is an attribute of the object mode of perception.

As a residual perception, "clear" as applied to objects means that the objects do not diffuse the light, that is, that diffusion is not one of their properties. In an achromatic object introduction of diffusion produces "whiteness" and decreases the "clarity," thus forming the earlier mentioned series from clear to white. Such a series also illustrates the point that it is possible to have varying degrees of whiteness from no white to pure white. The term which should be used for chromatic objects is not so apparent but the same sort of series is generated when any clear object is made to diffuse the light in increasing amounts.

It is necessary at this point to consider somewhat more completely the manner in which the perception of a clear object originates. Basically the perception of "clear" requires the perception of some other object

---

** After this manuscript was finished, Dr. Deane B. Judd called the writer's attention to a somewhat similar scheme involving a larger number of attributes which he had prepared some time before for the O.S.A. Colorimetry Committee but had never published. It is not in conflict with the present material and the writer is glad to recognize Dr. Judd's priority. The writer feels, however, that too little attention has been paid to the nature of the variables discussed.

beyond and seen through the clear one. That is, it is perceived that the clear object does not obscure the more distant one. Its reality is attested by its boundaries and its clearness is attested by its lack of effect on the distinctness with which the more distant objects are seen. Similar considerations apply to front surface mirrors and it seems logical for present purposes to extend the meaning of the term "clear" to cover this case also since it will be found that the conclusions reached are the same as for transparent objects.† The object may refract the light so that objects appear displaced or distorted, it may reflect it so that they appear in a different position, or it may have selective absorption which changes the color of the light. The requirement is that it not diffuse it. If diffusion is present, one tends to see the object itself rather than the one beyond and the object approaches opacity as the diffusion increases. At least in achromatic objects this is seen as an increase in whiteness and a similar sort of perceptual change occurs for chromatic objects.

In the perception of a piece of clear glass, a clear reflecting mirror, or a clear selectively reflecting surface such as polished brass, the fact that the transmitted or reflected light is attributed to objects other than the clear one produces the perception that the object itself is clear. Its position is determined by the edges of the surface. In the case of the polished brass the selectivity of the surface is perceived directly as a property of the surface.

It follows from these considerations, of course, that in order for a clear object to appear clear it must be possible for the observer to see whether or not the light does originate at the object. It is relatively easy to arrange a situation in which this condition is not met.

If a mirror reflects a large, uniformly lighted area of white paper which is not visible to the observer, the mirror is readily made to appear like a piece of white paper in a frame. Under these conditions some other criterion is necessary before the direct perception of clear can again occur. In this case movement of the observer's head may be sufficient for parallax to indicate that the reflected white surface and the mirror itself are at different distances. In other words the perception "clear" requires the presence in adequate amount of both depth and object perception, since both of these determine the extent to which the "residual" properties of the object are perceived directly.

Consider now the conditions under which "white" is seen and the directions in which it may vary. The most common condition for observing a white is probably some such situation as a piece of high reflectance, nonselective paper lying on a darker ground.

Such a subject may be modified in various ways and still remain white. First, consider a glossy surface on the paper. Two perceptions are involved now instead of one. The paper is seen as white and the surface as shiny. It is suggested that what is seen is white paper through a *clear* surface layer, or perhaps a white paper *with* a clear reflecting surface, this surface being seen, of course, because of the reflected light sources. Again, we may surround the paper by both a light and a dark background. This will demonstrate another property of white, namely, that it can vary in intensity even though it remains white. Suppose we now eliminate all the objects from the background and leave only an area out of the center of the paper, surrounded by a black paper. We shall have destroyed neither the object character of the paper nor its whiteness.

This approach may be extended and refined to the point of imaging a clear area sharply on a white screen by projection. In this case it can be argued that it is this white screen which is seen as white. However, the existence of the screen is not a necessary condition. If, instead of projecting a clear area on the white screen, a hole is viewed with an illuminated white screen at *any* distance behind it, it would look exactly the same, provided the light from the screen filled the area completely for both eyes and provided the observer thought it was a white screen. It would not matter whether the eyes were focused on the hole or the true screen. In fact, the physical stimulus reaching the eyes would be the same in all cases. The requirement is that the light can appear to come from a completely diffusing area, seen as localized and object in character. (If the area is isolated and is the sole cause of the existing eye adaptation, it may be seen as light and *not* as an object.)

Now the common ingredient of all these conditions, the fact which applies to all of them alike, is that the light from the area considered as white has appeared to *originate* from that area. Physically this means that the cones from each point of the area to each of the eyes have been filled with the same amount of light. It has been what is ordinarily called "diffused" light, that is, it has been diffusely reflected, transmitted or radiated from the perceived object. It is suggested that the perception to which we apply the term "whiteness" is the perception of the light leaving the area under consideration more or less uniformly in all directions, at least as far as the observer can see. In other words, "white" as an object characteristic means diffusion associated with high relative brightness and an achromatic object.

Taking diffusion as a variable, therefore, note that what happens when the diffusion of a white is decreased is the production of a surface series from white to clear such as was noted at the start. The central members of this series can only be described by some such term as "pale" whites. These intermediate steps are perceived as white and not gray in the great majority of cases although research is needed to establish this as a valid generalization. They illustrate the point that white can vary in strength in a way which is not accounted for by its simple absorptance or reflectance but which is directly attributable to its degree of diffusion.

---

† This extension makes the word "clear" analogous to the word "glossy" for reflecting objects.

The concept involved is very similar to that of the "contrast ratio" as used in specifications for paper‡ and of the "covering power" of paints. Contrast ratio is defined as the ratio of reflectance of the paper when measured in contact with a perfectly absorbing black surface to that measured in contact with a perfectly reflecting white. It is the ratio of reflected to the reflected plus the doubly transmitted light. It will be seen later that absorption, if present, plays a different kind of role.

To summarize to this point, then, white can be perceived only when achromatic light originates or appears to originate from a definite object, whether by diffuse reflection, diffuse transmission, or by radiation. This white can vary in intensity (or brightness) and it can also vary in strength in the sense of the words "pale" and "pure." Note also that the color perceived from near whites can depart from achromatic whites in possessing a recognizable hue, and two near whites having the same hue can depart from white by differing saturations of that hue.

No one of these directions leads toward what is called the "scale of grays." For this reason it is necessary to inquire into the nature of the perceptions gray and black and their relationship to white.

The common situation in which a gray is seen is that of a gray surface. Because this is the usual situation there is a tendency to forget the fact that this same perception of gray applies also to many other situations. That is, a gray is not always an opaque object. Transparent filters may occur in a series of grays as may a series of clear liquids. The grayness of an object appears as (looks like) a fairly permanent characteristic of that object and the tendency is to think of gray as corresponding to some physical property of that object. As a matter of fact, it does not so correspond except under rather rigidly defined conditions.

Gray is actually the quality of the perceptual response produced by the brightness of an object *relative to the other objects* which can be seen at the same time. This is quite easy to demonstrate. If a photograph of a gray object be taken in such a way that when projected it is the brightest area on the screen, it will ordinarily appear white. It can be made to appear gray again by introducing a lighter area.

This perception of the lightest surface as white is so strong that use is made of it in color photography to brighten the colors seen. If objects which are to appear white are actually gray under normal conditions but are the lightest objects in the scene as photographed, they will appear white on the screen.

These same considerations, of course, apply equally to gray transparent materials, although situations in which such effects occur are more difficult to produce. A clear absorbing material is visible only by virtue of its absorption (which changes the appearance of objects seen through it), by reflection from its surface, or by the appearance of its edges. All three of these give a direct comparison between the clear object and the background.

If these three conditions are removed, then transparent grays immediately appear as diffusing grays, necessarily ceasing to be visible as clear objects since the requirements are identical for the two perceptions.

The extreme effect of this sort is produced when gray filters are simply projected on a screen in a darkened room. In this case the filter may or may not be seen as such but the gray content depends entirely on what else is being projected at the same time. If a brighter border be projected around the image of the filter, it will always make the filter area appear gray.

We see, therefore, that gray as such, is the perception of a lesser brightness. It has no physical counterpart in an object unless the conditions of observation are such that a higher reference brightness is *also* visible. Under these conditions the gray correlates with the reflectance or transmittance as the case may be, *relative* to that which is being seen as white.

We have considered now white, clear, and gray as they relate to simple situations. When more complex situations are considered, however, an anomaly is encountered. It is a well-known fact in psychology that a stimulus can be seen as white and at the same time can be seen to be *less bright* than another. This is sometimes caused by simultaneous contrast as noted earlier, but is more frequently due to the so-called "brightness constancy" effect.

Take two white cards with identical gray central areas, and so place them that one is in shadow and the other is not. Both cards will continue to appear white, yet the one in shadow will be obviously less bright. It is easy so to arrange matters that the light reaching the eye from the shaded white is the same as that from the gray patch on the white card in full light. As a matter of fact, the light from the shaded white may be decreased far below that from the lighted gray without any loss of its whiteness. When matters are carried to extremes, a point is reached where many people are able to see the shaded white card either as white or as gray. If the intention is to see the nature of the card, that is, if an *object directed attitude* is adopted toward the shaded card, it will appear white. However, if instead of this, one looks critically to compare the stimulus from the shaded and unshaded cards, that from the shaded one will tend to appear gray. In fact many observers report being able to see the card in shadow as a white containing a gray. The situation is sometimes described as seeing the *shadow* as a gray *lying on* a white surface. In the case of a white wall with a shadow falling across it the shadow may always be seen as gray.

A similar phenomenon exists for clear gray objects, although it does not seem to have received any attention in the literature. Thus a clear gray filter held in the hand, so that objects may be seen through it, is perceived as a

---

‡ Official Method of the Technical Association of the Pulp and Paper Industry for Determination of Opacity of Paper (No. T425m).

uniform gray. This is exactly the equivalent of seeing a white surface as continuous and white across the edge of a shadow. Both *can* be seen as non-uniform if one directs the attention toward the light rather than the object.

Note that in all cases these changes can be voluntary on the part of the observer. They depend on what he is looking for. In particular they depend on whether attention is directed toward the object, or toward the light by which the object is seen. These can be called the object-directed and the stimulus-directed attitudes. The two perceptions are called respectively "lightness" and "brightness" in the O.S.A. Report of the Colorimetry Committee.

Gray, then, when this phenomenon is taken into account, is found to be either relative brightness or relative lightness depending on the circumstances and on the attitude of the observer. When a low reflectance surface in shadow is seen to be approximately the same as an identical surface in full illumination, we are concerned with relative lightness. This is the situation also in the Munsell scale of value when illuminance is changed. When a shadow on a white wall is seen as gray, however, the situation is reversed and we are dealing with relative brightnesses. It is necessary to say, therefore, when the illumination is non-uniform, that gray is the perception of relative brightness *or* lightness, whichever is sought by the observer. They become identical in *uniform* illumination. This raises the interesting question as to whether gray can be a perception in other than the object mode. Aside from the obvious statement already made that it cannot appear in any *homogeneous* field, however, the subject is considered outside the scope of this paper.

One further point is necessary. It was noted that the conventional object series of brightnesses or lightnesses are usually described as white or clear through gray to black. The implication is obvious that they are all aspects of the same phenomenon. It has been shown, however, that white is necessarily associated with diffusion and that gray is the perception of relative lightness or brightness. This leaves the question: "What is black?"

Imagine a piece of white paper with a black spot in the center made by a very dense deposit of a blue pigment. Why is it black? The answer seems fairly obvious and yet it is not the one most frequently given. The spot appears black because the stimulus reaching the eyes from the spot is not adequate to produce a sensation of light under the conditions in which it is seen. If the conditions are altered but not the spot, the stimulus may become adequate. If a piece of black material with a hole smaller than the spot is placed over the paper and illuminated by very bright light, the chances are that the stimulus will become adequate and the light from the spot will be seen as blue.

Black, then, may be considered as the perception of a boundary from within which the stimulus is not adequate to produce a visible light response. Black is seen when, for any reason, the stimulus is ineffective in producing the eye response which we call the sensation of light, but the area itself is clearly defined by its edges. This does not mean that the perception is not positive, it *is*, but it is a perception based on a lack of effective light stimulus over a particular area. Earlier the perception of gray was called that of relative lightness or brightness. It could just as well, however, have been called the perception of the *relative effectiveness* of the light in producing a visual response. When considered in this manner the relationships between gray and black become apparent. Black occurs when the light is ineffective and gray when it is only partially so.¶

If we now return to consideration of the variables of white, we find ourselves in a peculiar situation. It was noted that a white can vary in brightness and remain white and it was also noted that gray is caused by the relative lightnesses or brightnesses of two stimuli. Furthermore, an achromatic diffusing object may be seen as white, gray, or black without any change in either the object or the light reaching the observer's eye from the object. The conclusion is almost inescapable that white and gray are independent perceptions. Gray is the aspect of light produced by the relation of the area under consideration to the scene as a whole, that is, it is a perception based on the spatial characteristics of light under particular circumstances.

If gray and white are to be considered as independent, however, the interesting question is raised as to whether addition of diffusion to a clear, chromatic object adds white perceptually.

Consider a clear, chromatic object such as a Wratten filter. Imagine this bound up with a series of sheets of diffusing material with increasing diffusion. As you look along the series there is an increase in diffusion and a decrease in the quality clear. The question is whether or not the obvious difference may be described as a difference in white content of the resulting perception. No attempt will be made to answer the question here, although in some colors such as yellows and light pinks the answer must be "yes." It is a question, however, which would well deserve psychological investigation.

The importance of this question comes from the fact that the color specification of all the filters of the series as described by any of the known systems would all be alike. The ICI System would make no distinction at all. The Munsell System would apply directly to the one with maximum diffusion and a transparency system such as the Lovibond would apply directly to the one with none. The nearest description would be the same in all cases although the samples would look quite different. There is no system specifically for the large class of materials represented by the ones in the central part of the series. The appearances of the different members of the series are so different, however, that matches between the different ones are often difficult and sometimes impossible to make.

¶ In this section we are dealing primarily with light at the photopic level. At the threshold of vision under total dark adaptation all observers report gray. Some contrast appears to be necessary. We must "see" that the light is ineffective to perceive black. The phenomenon is associated with adaptation level nonetheless. There is nothing quite so black as a completely dark room entered from high illuminance.

In any case, whether or not diffusion always adds white as a perceptual increment in chromatic objects, it has now been shown that the perception of a slightly chromatic diffusing object may vary in four principal attributes from its original state. These four attributes are hue, saturation, brightness, and whiteness. The same four general directions are possible for all chromatic objects. They may vary in hue, saturation, brightness, and amount of diffusion. The first three of these are defined as the perceptual attributes of color. The fourth might be called whiteness if investigation showed it appropriate for all objects but might otherwise be called by some term derived from diffusion such as "diffuseness" or the like.

The perceptions produced by the great bulk of objects encountered in daily life would be clarified at the psychophysical level if, instead of specifying or describing only the color in terms of dominant wave-length, excitation purity, and luminance, a term were added specifying its luminous diffusion (perhaps diffusance). Such a term might be expressed in units based on an equivalent of the paper contrast ratio.

One interesting sidelight of the above discussion warrants specific statement. Since gray and white are independent and neither of them is related to brightness *as such*, it follows that the achromatic scale of material standards is not *color as defined*. In other words Munsell value or Ostwald shade are not coordinates of color perception. They are based on an equal spacing of grays from white to black in matte, diffusing materials. The brightness attribute of color perception relates to the amount of the illumination (the illuminance) even though modified by reflectance, and not to the perceived *relative* reflectance. The brightness scale produced by color is that of the aperture series, varying from just perceptible to intolerable over a range of one to a million or so in luminance. The material scales run their gamuts in little over 40 to 1 and contain white, gray, and black, no one of which is visible in the aperture mode. To be sure, the reflectance scales do produce brightnesses, but they are *different* for every level of illumination, while a single step is moderately well placed on the reflectance scales over a large range of illuminances.

It should be added also that while white, gray, and black have here been considered in relation to a non-spatial and non-temporal definition of color, the properties which have been adduced for these perceptions are not *consequences* of such a definition. White and gray are independent variables under *any* definition of color. They are each perceptions of spatial (or occasionally temporal) variables of light and are produced by independent physical relationships. Clear is the antithesis of white and black that of the perception of light as such.

In conclusion it seems desirable to attempt to state the main points intended. This is made desirable by the necessarily discursive nature of the main text and in spite of the evident danger from the varying contexts of the words which must be used.

1. White, gray, and black are not colors under any non-spatial, non-temporal definition of color.
2. White may be perceived at varying brightnesses.
3. White may exist in all degrees from zero at "clear" through various "pale" or "thin" whites to maximum whiteness.
4. White is the perception produced by the diffusion of light by an object. It is seen typically in a high reflectance, opaque, and achromatic object.
5. Gray is the perception of the relative effectiveness of the light from two areas, the effectiveness being construed to mean "effective for a given purpose." Thus under proper circumstances it may be seen either in connection with the relative reflectances of objects or the relative illumination of objects, whichever is sought. Black is considered the extreme in lack of relative effectiveness, although it is not seen near the absolute threshold of vision. Gray excludes color perception partially and black excludes it completely.
6. White, gray, black, and clear are attributes of the object mode of perception (although their necessary restriction to this mode is not intended). Their explicit consideration as such would greatly clarify many discussions.

JOURNAL OF THE OPTICAL SOCIETY OF AMERICA VOLUME 39, NUMBER 9 SEPTEMBER, 1949

Use of Polytrifluorochloroethylene in Infra-Red and Raman Spectroscopy*

J. S. KIRBY-SMITH AND ERNEST A. JONES
K-25 Research Laboratories, Carbide and Carbon Chemicals Corporation, Oak Ridge, Tennessee

(Received May 20, 1949)

Methods of fabricating Raman scattering tubes and infra-red absorption cells of chemically resistant polytrifluorochloroethylene are described. Curves showing the infra-red transmission of the material are given. Approximate values for the visible and ultraviolet transmission are also included.

THE recent development of polytrifluorochloroethylene[1] now makes available a new material for absorption and scattering cells of superior chemical resistance. The advantages of this material over the fully fluorinated compound (Teflon) are optical transparency, availability of a chemically resistant sealing wax[2] and the thermoplastic properties of the material which allow it to be welded. Raman and infra-red spectra of many fluorine compounds that have been impossible to handle in the past may now be successfully studied.[3] Some methods of fabricating Raman tubes and infra-red cells from this polymer are outlined below:

The construction of Raman tubes is described in the following paragraphs. Cylinders of the plastic are first machined as shown at *T* in Fig. 1. The milky, translucent material is then polished, and optical clearing of the polymer carried out by heating to approximately 200°C in an oil bath. Above this temperature the milkiness disappears and the material becomes very clear and transparent. It is then quenched by immersion in liquid nitrogen or a CO_2-trichloroethylene bath after which it retains most of its optical clarity. The material is given a final polish and is ready for fabrication into Raman tubes.

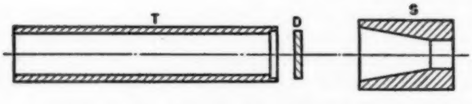

FIG. 1. Details of sealing fluorothene windows.

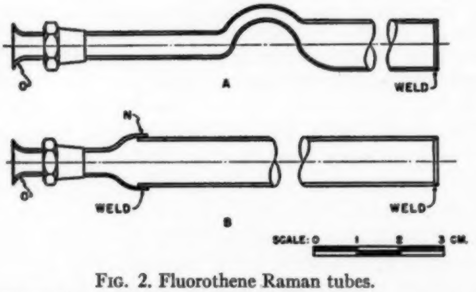

FIG. 2. Fluorothene Raman tubes.

Completed tubes fabricated by two different methods are shown in Fig. 2. The first (Fig. 2A) is made in the conventional form by heating and drawing one end of the polished cylinders to the desired shape. This drawing process is difficult and it is not always possible to obtain the smooth curves desired. A polished window (D, Fig. 1) of the clear polymer is placed in the shoulder at the end of the tube. A reasonably tight fit is desirable. Sealing is accomplished by pressing the end of the Raman tube inside a tapered metal plug (S, Fig. 1) heated to the required welding temperature (approximately 250 to 300°C).

Tubes of a second design (Fig. 2B) have proved very satisfactory, and since this type is easier to fabricate, it has been adopted for most of the work in this laboratory. The tapered section (N, Fig. 2B) is welded to the body of the tube by the method given above for sealing windows. A close fitting metal support is temporarily introduced at the point N during this process in order to keep the tube from collapsing. The front window is then sealed in place. The flared ends (O, Fig. 2) are formed with the usual flaring tools heated to the softening point of the polymer. Both welded seals and flared joints may be made vacuum tight without the use of additional sealing compounds.

These Raman tubes have been fabricated for use with liquid samples only and are relatively small, with out-

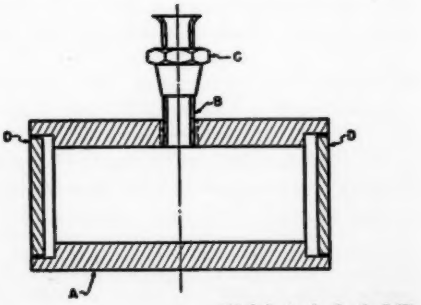

FIG. 3. Fluorothene infra-red absorption cell.

---

* This document is based on work performed for the AEC by Carbide and Carbon Chemicals Corporation at Oak Ridge, Tennessee.

[1] At present, the material is being manufactured by Carbide and Carbon Chemicals Corporation at Oak Ridge, under the name of Fluorothene. Inquiries should be addressed to the Atomic Energy Commission, Oak Ridge, Tennessee.

[2] Known locally as fluorothene-W. This is partially polymerized trifluorochloroethylene, m.p. 70–90°C.

[3] Jones, Parkinson, Murray, J. Chem. Phys. 17, 501 (1949). P. J. H. Woltz and E. A. Jones, J. Chem. Phys. 17, 502 (1949).

side diameters in the range 1 to 2 cm and a length of 10 to 15 cm. Wall thickness is approximately 1.5 mm. The tubes have been exposed to temperatures from 80°C to −170°C under operating conditions with no mechanical failures. The polymer has sufficient tensile strength and resistance to flow at 80°C to allow pressures of at least 2 atmospheres absolute to be used over long periods in tubes of the above dimensions. No appreciable flow has been noted after exposures of 4 hours under these conditions. At lower temperatures, tubes of much larger dimensions can be used at higher pressures. Tubes of larger size (2 to 5 cm diameter×20 cm long) should allow the Raman spectra of corrosive compounds to be observed in the vapor phase.

The design of an infra-red cell is shown in Fig. 3. The body of the cell (A, Fig. 3) and the inlet tube C are machined from solid bars. The inlet tube is flared on one end for connection to a valve and threaded into the cell at B. A vacuum seal is obtained at B by coating the threads with fluorothene-W. The optical windows D are placed in the shoulders at the ends of the cell and fluorothene-W applied to the surface of contact. A vacuum-tight seal is obtained around the windows by gently heating in an oven until the wax flows.

Because of the poor infra-red transmission of polytrifluorochloroethylene at the longer wave-lengths, (Fig. 4), crystalline halide windows may be necessary in many cases. Both NaCl and KBr have shown good corrosion resistance to many fluorine compounds. No difficulties have been encountered in sealing these window materials to the cells.

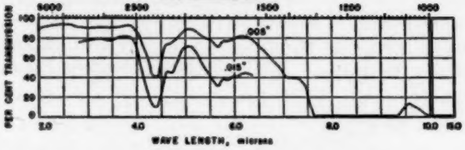

FIG. 4. Infra-red transmission of fluorothene.

The transmission of the cleared polymer is high throughout the visible spectrum and extends into the ultraviolet, dropping smoothly from 90 percent at 4000A to 30 percent at 2500A for a thickness of $\frac{1}{16}$ of an inch. To date, the most serious objectionable optical property of the material has been its optical inhomogeneity. This arises from strains introduced during the clearing process and has prevented any quantitative polarization measurements of Raman lines. Work now in progress by the Plastics Sections, Engineering Development Division, Plant K-25, indicates that these strains may be minimized by appropriate heat treatment.

We should like to acknowledge numerous suggestions on the handling of this material and measurements of its physical properties which have been given us by individuals throughout the K-25 Research and Engineering Development groups.

Table of Sines and Cosines to Fifteen Decimal Places at Hundredths of a Degree

The National Bureau of Standards has just issued a ninety-five page booklet of tables of sines and cosines to fifteen decimal places at hundredths of a degree. The booklet is now available from the U. S. Government Printing Office at forty cents per copy. Its page size is $10\frac{1}{4}''\times7\frac{3}{4}''$.

JOURNAL OF THE OPTICAL SOCIETY OF AMERICA VOLUME 39, NUMBER 9 SEPTEMBER, 1949

Visibility on Cathode-Ray Tube Screens: Viewing Angle*

STANLEY B. WILLIAMS**
Psychological Laboratory, The Johns Hopkins University, Baltimore, Maryland

(Received May 23, 1949)

Thresholds of visual detectability were determined for signals on a modified 7BP7 cathode-ray tube. Thresholds were determined in units of signal voltage for three pip sizes, all relatively small, and for four screen brightnesses at each of several positions from the line of binocular regard to 20 degrees out from it. The purpose was to determine the limits within which chance eccentricity of view could be a factor in radar detection. The range of impairment from zero to twenty degrees of eccentricity was about 17 db of signal voltage. The course of the impairment is probably not quite linear, with the optimal scope brightness (about 0.16 footlambert for this phosphor), but the slope is a function of scope brightness. For very small pips the data show no region of equal visibility, even within the fovea; direct fixation is required for maximal detection. There being no data based on optically precise stimuli available for comparison with the radar thresholds, an estimate was made of the luminances of the pips and their backgrounds. As estimated, the visual threshold probably varies up to one-log unit or greater over a range of 20 degrees of viewing angle, for the optimal scope background.

INTRODUCTION

CONSIDERING the structure of the retina and the greater photopic sensitivity in its central region, we should expect that the visibility of traces on a radar scope might steadily deteriorate with eccentricity of view. This expectation, of course, assumes that the scope is operating in the photopic response range of the eye, which it will be if it is a properly adjusted tube of the PPI (Plan Position Indicator) type, with rotatory scan, employing a P7 phosphor screen. Tubes of this type, we have found,[1] have an optimum visibility range of approximately 0.05 to 0.5 footlambert, with a peak at very near 0.16 footlambert. At this value, very weak signals are detected best. At lower brightness the eye is inefficient and at higher brightness the cathode-ray tube is inefficient.

To what extent differential sensitivity is impaired in using extrafoveal vision cannot be forecast from previous studies, because relevant data are noticeably lacking. The absolute threshold has been determined in various parts of the retina,[2,3] as has visual acuity.[4] But the only reference that seems available on the differential threshold as a function of retinal position is that of Wallace[5] whose paper has never been published. In private correspondence, Wallace reports his recollection that there was a steady drop in differential sensitivity from fovea to periphery, roughly paralleling the decrease in density of the cone population. This result would fit in with the visual acuity data and furnish the best clue to a rationale for the radar problem. However, we are still left with no very definite expectation as to the exact amount of stimulus energy that might be required for varying degrees of eccentricity or viewing angle. Furthermore, the practical problem of visually detecting radar pips may be so confounded with other factors—for example, the changing gradient of light emission, binocular viewing, the Stiles-Crawford effect—that one hesitates to apply data from studies made with optical devices, monocular fixation and immobilized or artificial pupils.

TABLE I. Brightness of field adjacent to pip, in footlamberts.

Bias in volts from VRI*	Brightness of field
−2.5	0.003
−4.5	0.05
−5.5 (optimal)	0.16
−6.5	0.36

* The minus sign of the bias voltage refers to visual reference intensity (see reference 1), a value at which the sweep line is barely visible.

TABLE II. Approximate angles subtended at the eye by pips at half-radius.

Size of pip on scope		Visual angle at 12 inches	
Horizontal	Vertical	Horizontal	Vertical
½ microsec.	1 degree	1′ 43″	7′ 31″
1 microsec.	1 degree	3′ 29″	7′ 31″
3 microsec.	3 degrees	10′ 25″	22′ 29″

---

* This research was carried out under Contract N5-ori-166, Task Order I, between Special Devices Center, ONR, and The Johns Hopkins University. This is Report No. 166-I-92, Project Designation No. NR-784-001, under that contract.

** Now at the College of William and Mary, Williamsburg, Virginia.

[1] Williams, Bartlett, and King, "Visibility on cathode-ray tube screens: screen brightness," J. Psych. **25**, 455 (1948).

[2] L. L. Sloan, "Rate of dark adaptation and regional threshold gradient of the dark-adapted eye: physiologic and clinical studies," Am. J. Opthal. **30**, 705–720 (1947).

[3] W. J. Crozier, and A. H. Holway, "Theory and measurement of visual mechanisms. I. A visual discriminometer. II. Threshold stimulus intensity and retinal position," J. Gen. Physiol. **22**, 362 (1939).

[4] W. H. Howell, *Textbook of Physiology* (W. B. Saunders Company, Philadelphia, 1947), see Chapter 23, "Vision," by T. C. Ruch.

[5] S. R. Wallace, Jr., "Intensity discrimination in the peripheral retina," Psych. Bull. **37**, 552 (1940).

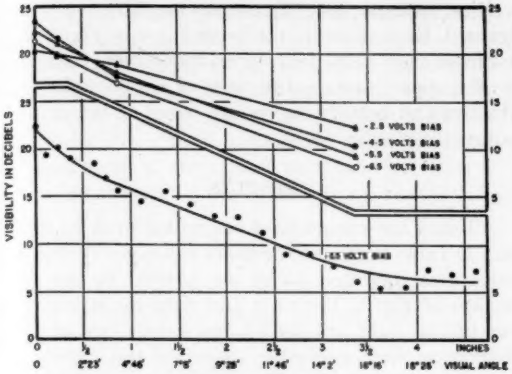

FIG. 1. Relative visibility as a function of distance from fixation point, measured in inches on the scope face. Visibility units are decibels of attenuation of an eight-volt signal required for an appearance threshold. The curve in the lower section is for the optimally biased tube (brightness about 0.16 footlambert). Curves in upper section are at higher biases (lower brightness) and a lower bias. All data are based on the binocular observation, by two subjects, of a small pip 1 μsec. in radial dimension and 1° in azimuth, subtending about 3′ 29″ by 7′ 31″ at the eye.

After undertaking the present experiment, it came to our attention that Craik and MacPherson[6] had already investigated the problem, using a simulated radar apparently very much like ours. However, their report failed to specify, even approximately, the brightness of the viewing screen or the dimensions of the artificial echo, both critical variables. They did make detectability tests at points 1° to 16° from the line of sight on four different observers. Sensitivity loss over that range was only about five db of signal strength in one observer and as much as 12 db in another, suggesting individual differences too great to fit a single curve to all the data.

In the present experiment, detectability thresholds were measured on two highly trained observers at several positions deviating from the binocular line of regard. Especial care was taken to control screen brightness and pip size; four values of the former and three of the latter were tested. The data show a progressive decline in differential sensitivity from the fovea to parafoveal regions.

EXPERIMENTAL METHODS

The general method employed is the same as that used in the earlier studies of this series.[1, 7, 8] In order to obtain accurate data, a long development of methods of monitoring tube voltages had been found necessary. This work, carried out by the staff of the Electrical Engineering Section of the Systems Research Laboratory, made possible the precise control of relevant parameters in the experiment. The radar indicator finally used was realistic in visual appearance only; in other respects it was complete transformation of a standard PPI into a precision instrument. The viewing screen was the bare surface of a 7BP7 cathode-ray tube. The tube face itself was shielded from external light by a tightly fitting, dull-surfaced viewing hood which kept the observer's head fixed so that his eyes were 12 inches from the center of the scope.

The grid-bias was either the visual optimum or a known departure from it. The pip was always placed on the screen at half-radius, either at West or at East. It was generated by a square pulse which was also gated rectangularly in azimuth, in contrast to the common triangular gating. This was necessary in order to provide a pip with sharp borders and definable area. Local tests had shown also that variations in brightness and area of the pip could be made independently, so that the parameter of pip size could safely be introduced. For threshold determinations, the intensity of the pip was varied by a decibel attenuator on the signal generator.

All observation was binocular. Fixation points for the observer were provided by dots of black ink placed directly on the glass face of the scope but there was never more than one dot at a time. Dots were separated from the pip by steps of ⅛ or ¼ inch and these separations, rather than pip location on the scope, became the actual independent variable in the experiment. Although dot placements would cause slight head shifting and introduce slightly the variables of absolute dis-

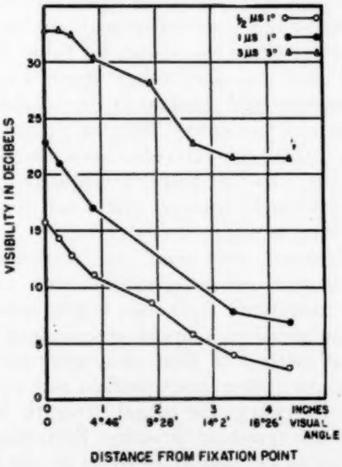

FIG. 2. Visibility as a function of distance from fixation point for pips of three different sizes. All pips are small by operational standards. Optimal bias used throughout. Visual angles subtended by pips are given in Table II.

---

[6] K. J. W. Craik, and S. J. MacPherson, "The effect of certain operating conditions on the visibility of P.P.I. radar echoes," Med. Res. Council, UAP, Cambridge, England, No. 16, December 3, 1945.

[7] S. B. Williams, and N. R. Bartlett, "Visibility on cathode-ray tube screens: problems and methods," J. Psych. 25, 401–417 (1948).

[8] R. M. Hanes, and S. B. Williams, "Visibility on cathode-ray tube screens: the effects of light adaptation," J. Opt. Soc. Am. 38, 363–377 (1948).

TABLE III. Visibility as a function of viewing angle*

Inches	db
0	22.4
$\frac{1}{8}$	19.4
$\frac{1}{4}$	21.1
$\frac{3}{8}$	19.0
$\frac{5}{8}$	18.5
$\frac{7}{8}$	15.6
$1\frac{1}{8}$	14.4
$1\frac{3}{8}$	15.6
$1\frac{5}{8}$	14.3
$1\frac{7}{8}$	12.9
$2\frac{1}{8}$	12.8
$2\frac{3}{8}$	11.3
$2\frac{5}{8}$	9.0
$2\frac{7}{8}$	9.0
$3\frac{1}{8}$	7.8
$3\frac{3}{8}$	6.1
$3\frac{5}{8}$	5.4
$3\frac{7}{8}$	5.5
$4\frac{1}{8}$	7.4
$4\frac{3}{8}$	6.9
$4\frac{5}{8}$	7.3

* Mean visibility thresholds are in decibels of attenuation of eight-volt signal. Higher values represent lower thresholds. Each mean is based on eight data. Grid bias is optimal (−5.5 volts), providing an effective screen brightness of about 0.16 footlambert. Distance from fixation point is given in inches but calculated visual angles are shown in Fig. 1. The pip is 1 microsecond by 1 degree.

tance and convergence of the eyes, these contaminations were regarded as far less serious than those introduced by the procedure of Craik and MacPherson, varying the position of the pip on the scope, for very drastic changes in both size and brightness of the pip accompany the latter. In fact, it is all but impossible to duplicate exactly at far range a pip of given visual dimensions at close range. Only horizontal displacements were used.

Four values of grid bias were tested; their probable corresponding screen brightnesses are given in Table I. The values are calculated from a previous calibration.[7] Three sizes of pip were tested with the optimal bias (−5.5 volts). These are shown in Table II. Besides grid bias and pip size, other significant electrical parameters were held constant at the following values: rotation rate of "antenna," 20 r.p.m.; pulse repetition frequency, 1000 pps; no video noise except residual tube and line noise; all supply voltages as specified by tube manufacturer; focus of sweep line, sharpest possible by visual setting.

Two observers were used, one female essentially emmetropic and one male, myopic with appropriate refractive correction.[9] Both were highly proficient and had had hundreds of hours of observational practice. A modified method of limits was used to determine thresholds. An appearance threshold was obtained by gradually increasing the signal strength in one-db steps from sub-threshold intensity. Each datum, then, is a number of decibels attenuation of the eight-volt signal; means of these were plotted directly on the vertical ordinate, insignificant observer differences being ignored. Each point on the lower curve of Fig. 1 is the mean of eight data, four by each observer; each point on the upper curves is the mean of ten data. In Fig. 2 the top and bottom curves are based on ten data per point; the middle, on 18.

RESULTS

All data are summarized in graphic form in Figs. 1 and 2. Table III shows the mean values for the optimal brightness condition which are plotted in the lower section of Fig. 1. Both left and right deviations from the line of sight are pooled, since over this area the differences were negligible. None of the curves was fitted mathematically. For optimal scope brightness there is no substantial area of equal visibility; an impairment occurs as soon as the fixation point is left and it increases in proportion to the amount of the departure. The rapidity of the decline with angular distance from line of sight probably is, however, a function of the brightness of the scope. The upper section of Fig. 1 shows that the impairment curves are nearly parallel for the three brightest fields but that the slope of the curve for the dimmest field is definitely less. Here we could say that within two to three degrees of eccentricity the impairment is slight enough to be almost insignificant.

In the case of the optimal grid bias, visibility deteriorates about three db for the first degree of deviation from the fixation point and then apparently continues its deterioration at a lesser rate, one db or less per degree, out to the limit tested. In the case of the dimmest scope, the total deterioration is only about seven db. Even dimmer scopes would have been tested except for the difficulty encountered in providing a visible fixation point. The dimmest scope tested, however, is of a brightness in the region of the rod-cone break and it is doubtful, therefore, whether any useful purpose would have been served by data in the twilight-to-dark region. Obviously if the scope were completely dark, the pip would show up best some degrees parafoveally.

In Fig. 1 only one pip size is used, the 1 μsec.×1° pip. In Fig. 2 are shown data for the smallest pip available as well as for a slightly larger one. All three, however, are small compared to the pips customarily encountered in operation and are in the general range of those produced by schnorkel echoes on some radars. Within these limits, pip size appears to be approximately a constant factor in visibility as evidenced by the nearly parallel positions of the curves. It is to be noted, however, that for the largest pip there is an area of one to two degrees of equal visibility. This is still within the foveal region and as soon as the approximately two degree foveal region is left, visibility becomes impaired. It is especially to be noted that the largest pip is, in visual angle, *far smaller* than the width of the fovea and *far smaller* also than the width of the area of equal visibility. It is, in fact, little more than one-third of a degree in its greater dimension, the vertical, and it is only about one-sixth of a degree in the horizontal dimension. Since the rate of initial decrement within the fovea is some inverse function of pip size, it is conceivable that it is due to what Stiles[10] calls the directional sensitivity of the retinal receptors, but this, of course, is speculative.

---

[9] The writer is indebted to Mrs. Beverly Richards and Mr. Hamilton Mowbray for their services as observers.

DISCUSSION

It is difficult to translate decibels of signal voltage into light values but we can do it approximately. The difficulty arises from the non-linear response of the phosphor screen to electronic stimulation. Calibration curves are cumbersome and the most we have accomplished is to measure the light output occasionally and not simultaneously with visual observation. From these measures, however, we can get a very approximate idea of the size of the differential threshold in brightness units.

Taking the optimal bias as an effective screen brightness of 0.16 footlambert and a curve of light emission published earlier,[7] we can calculate the difference threshold equal to a 0.5-volt signal (24-db attenuation of eight-volt signal) to be about 0.09 footlambert. (This is slightly smaller than the foveal threshold as indicated in Fig. 1 but we are making approximations here.) This means the difference threshold is about 0.56 of the background brightness, a value which checks fairly closely (by interpolation) with the data of Blackwell[11] on minimal contrasts for objects of similar size. At 16 to 20 degrees peripherally, a four-volt signal is required for threshold; this should produce a light value of about 1.75 footlamberts or a contrast of 11. Since neither Blackwell nor anyone else but Wallace has tested this threshold at parafoveal points, we can only guess that this value is in the right range.

If we can accept these values tentatively, we can see that the total increase in the differential threshold, from center to 20 degrees peripherally, is on the order of a log unit or better. Likewise for minimal contrast, it is on the order of 1.5 log units of brightness. We could have guessed this from two facts: (1) the total range in signal voltage (17 db) is nearly a log unit of energy, and (2) light output is a decreasing function of signal voltage at this brightness level. Therefore we can be fairly safe in asserting that the total loss in differential brightness sensitivity in 20 degrees of parafoveal vision is greater than one log unit. The data are not considered sufficiently exact to warrant any conclusions as to the curvature of the decline. The best they can do is point up the need for precise measures of this important visual function.

SUMMARY

Thresholds of visual detectability have been determined for weak signals appearing on the face of an intensity-modulated radar scope. The signal strength required for threshold steadily increased as the pip's location was moved peripherally from the binocular line of sight. In this peripheral impairment of visibility, both scope brightness and pip size are variables. For optimal scope brightness (about 0.16 footlambert for this P7 phosphor), the signal voltage for threshold at 20 degrees eccentricity must be about 17 db greater than at zero degrees. In light units, this difference is probably greater than one log unit.

---

[10] W. S. Stiles, "The directional sensitivity of the retina and the spectral sensitivities of the rods and cones," Proc. Roy. Soc. London, **127B**, 64–105 (1939).

[11] H. R. Blackwell, "Contrast thresholds of the human eye," J. Opt. Soc. Am. **36**, 624–643 (1946).

JOURNAL OF THE OPTICAL SOCIETY OF AMERICA VOLUME 39, NUMBER 9 SEPTEMBER, 1949

A Low Temperature Infra-Red Transmission Cell*

H. O. McMahon, R. M. Hainer, and Gilbert W. King
Arthur D. Little, Inc., Cambridge 42, Massachusetts

(Received May 26, 1949)

A versatile apparatus is described which allows the infra-red absorption spectra of materials to be obtained at temperatures down to that of liquid helium 4.2°K. The observed spectrum is the usual transmission measurement obtained in the normal way without disturbing the optics of the spectrometer.

Samples can be observed which are solid, liquid, or gas at ordinary temperatures. Solids and liquids are suitably supported and are surrounded by helium gas at the temperature of liquid helium in order to provide for heat removal from the sample by both gaseous conduction and convection. The temperature rise of the sample due to absorbed radiation is thus very small. Condensible gases may be deposited onto one side of the vacuum tight infra-red transparent windows bathed on the inner side by cold helium gas. Observations have been made for periods of forty-five minutes using a single charge of approximately 200 cc of liquid helium. Detailed features of construction and operation conform to the exacting requirements of very low temperature work.

THE possibility of obtaining new information concerning the molecular properties of certain materials by observing their infra-red absorption spectra at very low temperatures has led to the construction of a transmission cell which maintains a specimen at temperatures down to 4.2°K, the boiling point of helium. For several reasons it is desirable that the sample be interposed simply and directly into the infra-red beam without modification of the excellently designed optics of the present-day infra-red spectrometer. This is desirable partly because of the difficulties involved in the modification of infra-red optics and partly because of the important advantages which exist in favor of a simple transmission type of measurement. An alternative technique that has been used in the past for low temperature measurements has followed the practice of Rubens and Hertz[1] for measuring reststrahlen reflections from cold solids. This method consists of reflecting the infra-red beam from a cold metallic mirror upon which the sample has been deposited and has been adopted[2-4] primarily, because of the difficulty of devising a transmission cell with assurance that the sample would be maintained at the low temperature while being irradiated by an infra-red beam.

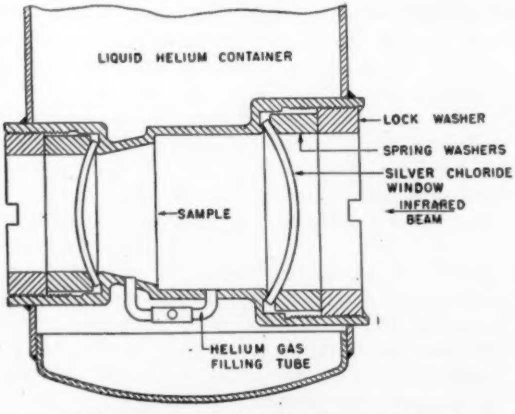

FIG. 1. Cross section of low-temperature infra-red transmission cell: sample chamber.

Obviously the reflection-double-transmission measurement is unable to distinguish between radiation which penetrates and passes through the sample twice and that which is reflected from the sample surface with no penetration. Strong reflection is therefore interpreted as high transmission. It is well known that powerful absorption is accompanied by strong reflection. This of course may lead to very serious errors. Thus, in the case of a silica glass film, for example, a 50 percent reflectivity occurs at 9.6μ which would be interpreted as high transmission although the true transmission is substantially zero even for exceedingly thin films. If low temperatures sharpen absorption bands this effect will increase.

Reflections also play a role in simple transmission measurements, but the effects are in general minor and are never such as to obscure structure.[5]

A transmission cell is, therefore, desirable for low temperature work, but means must be provided for satisfactorily maintaining the sample at the low temperature. This difficulty can be overcome by devising infra-red transparent windows capable of holding a high vacuum while at the same time being able to withstand cooling to very low temperatures.

Considerable effort has been expended in finding a suitable solution to this problem and has finally resulted in the described apparatus. The principal element is a vacuum-tight cell containing the sample bathed in helium gas, and fitted with infra-red transparent windows. It is surrounded by a very high vacuum for good thermal isolation, a requirement which is essential

---

* This work was done in part under a Grant-in-Aid from the American Cancer Society upon recommendation of the Committee on Growth of the National Research Council.

[1] H. Rubens and G. Hertz, Ber. d. Ber. Akad. (1912) p. 256.

[2] Conn, Lee, Sutherland, and Wu, Proc. Roy. Soc. **A176**, 484 (1940).

[3] W. H. Avery and C. F. Ellis, J. Chem. Phys. **10**, 10 (1942).

[4] W. H. Avery and J. R. Morrison, J. App. Phys. **18**, 960 (1947).

[5] W. C. Price and K. S. Tetlow, J. Chem. Phys. **16**, 1157 (1948).

for liquid helium experimentation and desirable also in order to minimize drift problems which would be introduced if large temperature gradients were allowed to develop in the spectrometer housing.

DESCRIPTION OF APPARATUS

Figures 1 and 2 show the construction of the low-temperature transmission cell. The cell itself has the form of a truncated cone aligning axially with the beam of infra-red energy and having the same cross section. The cell is sealed through a cylindrical container into which liquid helium or any other refrigerant may be poured. The two ends of the sample chamber are fitted with transparent silver chloride windows[6], † compressed around their rims by means of a suitable arrangement of spring loaded washers and nuts. It is necessary that the closures formed by these windows be absolutely vacuum tight at all temperatures since the interior of the cell is filled with helium gas to establish a heat transfer medium, and the exterior is highly evacuated to provide thermal isolation. Fortunately the physical properties of rolled silver chloride[7] windows make this material almost ideally suited to the application at hand. At room temperature silver chloride has properties very similar to those of metallic lead. It can be deformed readily and will flow without cold working and without the necessity of frequent annealing. It retains its high degree of infra-red transparency even after considerable cold working. Its undesirable properties are its high coefficient of thermal expansion, its ease of marring, and its ready corrosion when in contact with other than noble metals. This large thermal expansion requires stiff back-up springs to hold the window against its seat and at the same time to allow for the necessary differential thermal expansion between the silver chloride and metal sample cell in the direction of change of thickness of the window. Differential expansion in the plane of the window is also troublesome since this tends to cause the silver chloride to slide on its seat as the temperature is lowered. If sliding is allowed to occur, the two sealing surfaces no longer mate exactly and sufficient leakage occurs to spoil the vacuum. If satisfactory seating is obtained by compression on rounded lands, the circumference cannot move on cooling and circumferential or radial cracks develop as the result of the bulk shrinkage. Failures of this type have been eliminated by using a domed rather than a flat window, so that as a temperature change occurs the height of the dome changes but the strains developed do not exceed the elastic limit of the material. During this development a number of different shapes of windows and seats were tried before a completely successful combination was found; for a window of 1.25 in. diameter a radius of curvature of $\frac{7}{8}$ in. for the window is found to be satisfactory. The windows were formed in a hand-lapped, high quality monel metal die on a hydraulic press capable of 15,000 lbs. per square inch. The use of monel metal for all components in contact with silver chloride reduces markedly the effects of corrosion. Silver has been used for the washer in contact with the silver chloride window in order to eliminate corrosion but the use of silver for the whole sample container is needlessly expensive.

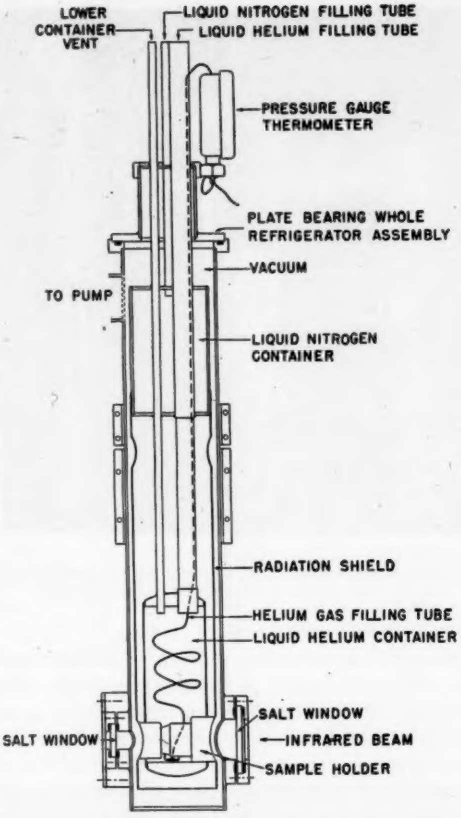
LOWER CONTAINER VENT
LIQUID NITROGEN FILLING TUBE
LIQUID HELIUM FILLING TUBE
PRESSURE GAUGE THERMOMETER
PLATE BEARING WHOLE REFRIGERATOR ASSEMBLY
VACUUM
TO PUMP
LIQUID NITROGEN CONTAINER
RADIATION SHIELD
HELIUM GAS FILLING TUBE
LIQUID HELIUM CONTAINER
SALT WINDOW
INFRARED BEAM
SALT WINDOW
SAMPLE HOLDER

FIG. 2. Cross section of low temperature infra-red transmission cell: total assembly.

The interior of the sample cell communicates directly with the outside of the apparatus by means of a thin-walled stainless-steel capillary tube. This tube serves to fill the sample cell with helium gas and is also attached to a pressure-vacuum gauge so that the resulting combination serves as a helium gas thermometer enabling the operator to know the temperature of the sample quite accurately. The function of the helium gas is to remove energy absorbed by the sample and transfer it to the walls of the sample cell, which in turn are immersed in the liquid helium or other refrigerant.

---

[6] A vacuum tight infra-red transparent cell for use near room temperature has been used by R. M. Fuoss, Rev. Sci. Inst. 16, 154 (1945).

† *Note added in proof:* Recently quartz windows held between silver chloride gaskets have been used successfully at liquid nitrogen temperature; this extends the use of the apparatus to the visible and ultraviolet region.

[7] H. C. Kremers, J. Opt. Soc. Am. 37, 337 (1947).

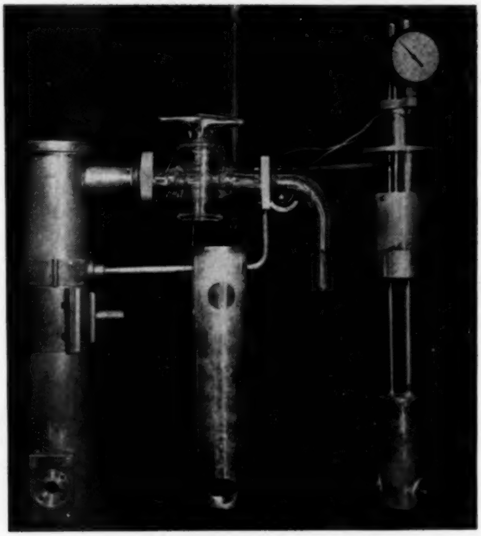

FIG. 3. Low temperature infra-red transmission cell separated into major components with radiation shield removed.

In general, it is extremely difficult to remove energy from a thin film which is absorbing radiation and is surrounded by a vacuum. Even if the film is a good conductor of heat, which it generally is not, and it is in good contact with the metal sink, it is usually so thin that extremely large temperature gradients would be required to conduct the absorbed energy any appreciable distance, e.g., along a radius, or to radiate sufficient energy to the surroundings. When the film is surrounded by helium gas, however, it is easy to show that the quantity of energy absorbed could not raise the film temperature above that of the ambient by more than one degree at most. The heat transfer rate for free convection around a vertical plane, such as the absorbing film, depends primarily upon the volumetric expansion coefficient, the thermal conductivity and the viscosity of the ambient medium. For helium gas at 4.2°K an unusually favorable condition prevails since the expansion coefficient is of course enormous, the thermal conductivity is high and the viscosity is very low. Thus a slight rise in temperature of the film sets up powerful convection currents which effectively prevent any further rise. The energy to be dissipated can be estimated from the temperature of the infra-red source and aperture of the system, times the area of the source visible at the sample. It was measured directly in our spectrometer, for an average absorbing sample (polystyrene) by the increased rate of evaporation of helium on opening the shutter exposing the sample to radiation. The increased rate was 2.0 liters per minute of gas at room temperature, corresponding to 0.13 watts in agreement with calculation.

In order to protect the liquid-helium pot and its associated sample chamber from the thermal radiation of the room temperature surroundings, a copper radiation shield which completely envelops the very low temperature region has been soldered to an auxiliary pot which is cooled with liquid nitrogen. This liquid-nitrogen pot is mounted directly above the liquid-helium pot, coaxially with it, and is of a somewhat larger diameter. The radiation shield is silver plated in order to reduce the emissivity. The helium pot is supported by means of two very thin-walled stainless steel tubes which serve as filler tubes and, on account of their low heat conductivity as partial thermal isolators. These tubes are run through the liquid-air pot which then acts as a heat station for the liquid-helium region making the problem of thermal isolation somewhat easier. The liquid-nitrogen pot is also suspended by two filler tubes and these, as well as the helium-filler tubes, pass up through the covering plate of the whole vacuum-jacketed assembly. The area where the four filling tubes are brought through the lid is thermally isolated from the rest of the lid area by means of a raised stainless steel hat of low thermal conductivity. This design avoids transferring excessive amounts of refrigeration to the neoprene gasket or the outer shell of the vacuum jacket during refrigerant transfer operations. The entire assembly is inserted into a brass shell which has a connection to a vacuum system.

The inner assembly rests on a specially designed neoprene gasket which is recessed into a suitable flange attached to the upper rim of the brass jacket. The inner assembly aligns the sample cell with two rocksalt windows provided in the brass shell so that the infra-red beam may traverse the entire apparatus. The rocksalt windows are sealed with neoprene gaskets. The liquid-helium pot acts as an extremely effective trap for all gases except helium. Thus, in the absence of gaseous helium, the only heat loss from the outer jacket is to the radiation shield at 77°K and the sample cell at 4°K. This being negligible, the salt windows and outer jacket remain at room temperature and do not cause temperature drifts in the spectrometer or in the detector.

Nearly all the component parts of this apparatus are silver brazed together to give strength and durability. Several parts, e.g., the sample cell and the radiation shield, however, are soft soldered in place in order to allow for easy modification from time to time. Materials for construction are chosen for their thermal properties, chemical properties, or ease of fabrication. They include: brass for most pieces, copper for the radiation shield, stainless steel for heat insulation, and monel for the sample cell to reduce the corrosion with silver chloride.

Figure 2 shows the cross-section of the assembled cell indicating clearly: the sample cell of approximately 10 cc volume; the liquid-helium pot of 220 cc volume; the liquid-nitrogen pot of 240 cc volume; the radiation shield; the four filling tubes for the two containers, one for the lower pot being large enough to accept the liquid-helium transfer tube from the Collins helium cryostat; the external shield with its salt windows; and the connections to the vacuum system. Figure 3 shows a photograph of the low temperature cell, separated into the major components with the radiation shield removed. Figure 4 is a photograph of the assembled cell in the operating position of a Perkin-Elmer spectrograph and attached to the 20 mm Pyrex glass stopcocks of the high vacuum system. These stopcocks allow for the removal of the low temperature cell from the pumping system in order to fill it with liquid helium without loss of vacuum and for quick resumption of the dynamic vacuum on returning the cell to the spectrograph.

SAMPLES

The design of this low temperature apparatus allows the mounting of the sample in the sample cell either as a solid film or as a liquid (or solution) in an appropriate liquid cell made of two silver chloride plates; rock salt cannot be used because of the high probability of cracking on cooling. This liquid cell can be much like the conventional liquid cell made with salt windows and a spacer, or it can be made from silver chloride plates with a shallow recess pressed into them, and sealed face to face by fusing them together around the periphery to form a fixed thickness cell without spacer. Such a cell can be filled by a hollow needle inserted into a hole drilled through the fused rim. In addition, the low temperature dewar allows the study of spectra of gases and liquids with appreciable vapor pressure. These samples are prepared by letting the gas or vapor into the vacuum system from which it deposits on the cold silver-chloride windows of the lower pot, the upper pot and shield being maintained at room temperature or at a temperature such that the vapor pressure of the sample is high. In addition the way is open for further generalization of the sampling by vacuum sublimation or molecular distillation of the sample onto the windows.

OPERATION

The apparatus can be operated at the temperature of liquid nitrogen as long as desired by occasional filling of the lower pot from a small portable Dewar. For runs at liquid-helium temperatures transfer of helium is made directly from the cryostat. The heat of vaporization of liquid helium is only 5 cal. per gram, so intermediate transfer equipment would waste considerable quantities of liquid helium during the cooling. The time for observation of spectra, without refilling, is limited to the dissipation of the stored refrigeration by losses from radiation, metallic conduction and gaseous conduction by the residual helium in the vacuum system. The latter factor can be quite large if the pressure of the helium in the vacuum system is not sufficiently low because of small leaks, a poor pumping rate, a poor ultimate vacuum, or a combination of these troubles. Since liquid helium has a small heat of vaporization and a density of only 0.13 grams per cc, the 220 cc capacity of the liquid helium container provides only 150 calories of refrigeration at 4°K. The heat losses either with or without the infra-red beam's falling on the sample can be accurately measured by metering the helium vaporized and exhausted through the filling tubes. Approximately 160 liters of helium gas is exhausted at standard conditions from a full charge of liquid. Losses with the infra-red's falling on a sample mounted before the entrance slit amount to approximately 4 liters per minute, twice the rate without radiation, so that operation for 40 minutes can be expected. In practice 45-minute runs have been obtained.

The difficulties experienced with this apparatus in the measurement of the low temperature spectra of a number of materials have been due to unsatisfactory vacuum conditions or failure of the silver chloride windows. Minor vacuum troubles can be tolerated so long as the rate of loss of coolant does not become so great that the time of observation is cut severely. However, the cracking of a silver chloride window immediately terminates low temperature operation. With the present apparatus this failure has not been frequent. For samples introduced in the gas phase, where the silver chloride windows do not need to be removed to change sample, eight successive low temperature determinations with warming to room temperature in between have been made without difficulties of any sort. Factors

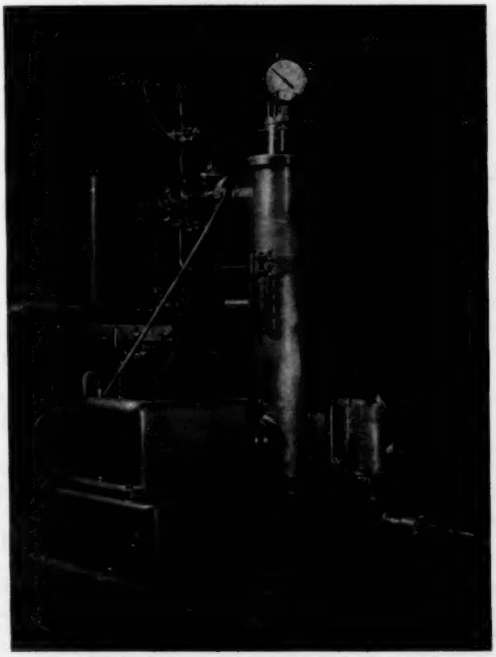

FIG. 4. Assembled low temperature infra-red transmission cell in operating position of a Perkin-Elmer spectrograph.

which limit this performance have not as yet been ascertained.

The use of the external pressure-vacuum gauge connected to the sample cell via the capillary tubing allows accurate measurement of the temperature of the helium gas in the cell and indirectly the temperature of the sample bathed in helium gas. The use of a gas flow meter allows accurate measure of the rate of dissipation of the coolant. The use of a gas displacement meter allows accurate measure of the accumulated energy losses. From these measurements considerable understanding about the rate and equilibrium conditions for the heat loss from an absorbing sample is forthcoming. For example, on exposing a sample to radiation the gauge shows no change in the gas temperature of 4°K, within the precision of measure. In addition, a very rapid response is observed on the rate of evaporation of helium on exposure of the sample to radiation, showing the heat absorbed by the sample is rapidly removed.

The attenuation of infra-red radiation by the cell is only that of the optical materials (two rock salt and two silver chloride windows), and the sample. The metal components including locking rings and pressure nuts do not intersect the light path provided the cell is used immediately in front of the entrance slit of 1.2 cm height and with an optical system of aperture 4.5. Modification has been made recently to preserve these optical specifications and allow the apparatus to be also used at a focus in the system.

The authors wish to acknowledge the careful machine work and soldering done by Messrs. Alfred L. Wright and Herman Lerch.

Errata: Sunlight and Skylight as Determinants of Photographic Exposure.* I. Luminous Density as Determined by Solar Altitude and Atmospheric Conditions

[J. Opt. Soc. Am. 38, 123 (1948)]

Loyd A. Jones and H. R. Condit
Eastman Kodak Company, Rochester, New York

On p. 142, second line of footnote *k*, the word "footcandles" should be changed to "footlamberts."

In Table IV, p. 147, the number in the fifth row of the fourth column should read "4910" instead of "3910."

The heading "Luminance density" in Table XIII, p. 170, should be "Luminous density."

II. Scene Structure, Directional Index, Photographic Efficiency of Daylight, Safety Factors, and Evaluation of Camera Exposure

[J. Opt. Soc. Am. 39, 94 (1949)]

On p. 109, column 2, Eq. (37) and the line preceding it should be changed to read, "the ratio of E_s to E_m,

$$RW_s = E_s/E_m. \qquad (37)\text{''}$$

On p. 110, omit the word "relative" from the abscissa of Fig. 33.

In column 2, p. 112, omit all material following Eq. (41) through Eq. (43) and substitute the following:

"If the two curves, J and J', are so plotted that the luminous intensities of the two sources of radiant energy are equal, as given by

$$K\int_0^\infty J_\lambda T_\lambda d\lambda = K'\int_0^\infty J_\lambda' T_\lambda d\lambda, \qquad (42)$$

then the photographic efficiency of the radiant energy coming from the overcast sky relative to that of the photographic unit, is given by the ratio, W' to W, as defined in Eq. (35). This leads to the following expression for the relative photographic efficiency:

$$RW' = \frac{\int_0^\infty J_\lambda' C_\lambda T_\lambda d\lambda}{\int_0^\infty J_\lambda C_\lambda T_\lambda d\lambda} \cdot \frac{K'}{K}. \qquad (43)\text{''}$$

On p. 114, first column, line 14, the sentence beginning "The ordinates of the two curves . . ." should be changed to read, "The ordinates of the two curves, *B* and *D*, are so adjusted that the two sources of radiant energy have equal luminous intensities."

On p. 115, first column, line 6 of the second paragraph, the sentence beginning, "In all cases shown in Figs. 37 . . ." should read, "In Figs. 37, 38, and 39, the curve for the blackbody associated with a given phase of natural light is so plotted that these two sources of radiant energy have equal luminous intensities."

Note.—Confusion has arisen because of the use of two different concepts of photographic efficiency without distinction of terminology. The first, and more fundamental concept, was defined by Eq. (35) of the original paper and is the photographic response per unit of radiant energy of a prescribed spectral distribution. The second concept is an outgrowth of the traditional expression of photographic "speed" in terms of photometric units—usually meter-candle-seconds. American Standard Speed is based on the spectral distribution as well as the photometric intensity of the international unit of photographic intensity. It does not countenance an evaluation of "speed" based on any other spectral distribution. If, however, an analogous procedure, Fig. 33, is carried out for some photographic material, using any other spectral distribution, a number can be obtained which bears a ratio to the ASA speed of that material which is commonly considered to be the photographic efficiency of the non-standard light source relative to the international standard source.

The efficiencies implicit in this procedure are photographic responses per unit of luminous energy, and are not equivalent to photographic efficiency as defined in the original paper, Eq. (35). We propose to restrict the unqualified term ***photographic efficiency*** of radiant energy to the concept defined by Eq. (35), the photographic response per unit of radiant energy. We suggest that the distinctive term ***photo-luminous efficiency*** be applied to the photographic response per unit of luminous energy, corresponding to ASA speed and analogous quantities. The relative photo-luminous efficiency of two sources may be computed by omitting the factor K'/K from Eq. (43) above, retaining condition (42) as stated.

---

* *Communication No. 1155 from the Kodak Research Laboratories.*

JOURNAL OF THE OPTICAL SOCIETY OF AMERICA VOLUME 39, NUMBER 9 SEPTEMBER, 1949

The Spectral Dispersion of Birefringence, Especially of Birefringent Plastic Sheets

C. D. West and A. S. Makas
Polaroid Corporation, Cambridge, Massachusetts

(Received June 6, 1949)

It is shown apparently for the first time how dispersion of birefringence (retardation, phase difference or ellipticity) can be measured through the visible spectrum by the use of a Martens type of polarization photometer and monochromator. Dispersion curves are given for several organic thermoplastic sheets including those with both normal and abnormal dispersion of birefringence, and possible uses for such sheets are suggested.

INTRODUCTION

PROBABLY the most complete account of spectral dispersion of birefringence of crystalline materials is found in a paper by Ehringhaus.[1] This writer found it useful to employ a function N, given by $N=(\Delta n(D)/(\Delta n(F)-\Delta n(C))$, to classify his material into two main groups: when $|N|$ is large, say greater than 30, the specimen is said to have normal dispersion, whereas when $|N|$ is small, say less than 30, the dispersion is abnormal. In this expression $\Delta n(D)$ denotes the birefringence n_1-n_2 of the crystal section for sodium light, etc. Otherwise stated, the birefringence of normal materials is essentially constant with wave-length between the C and F lines. A wedge cut from such a material and viewed in a polariscope exhibits a normal sequence of interference colors, whereas wedges cut from abnormal materials may exhibit very strange sequences of colors indeed.

A kind of abnormal dispersion of especial interest occurs when Δn is not constant, but varies so as to be directly proportional to wave-length, or $\Delta n=k\lambda$. In this case the ***phase difference*** δ introduced by passage of polarized light through the specimen is constant with the wave-length, and the material is suitable for the preparation of achromatic retardation plates. The N value necessary to give achromatic interference is thus

$$N=\frac{589}{486-656}=-3.46.$$

The relations employed in this work are

$$\Delta n=\frac{\Gamma}{t}=x\frac{\lambda}{t}=\frac{\delta}{2\pi}\frac{\lambda}{t},$$

where Γ is the path difference expressed in the same units as thickness t and wave-length λ; and x is the same thing expressed in fractions of a wave-length.

The Fresnel rhomb employing total internal reflections in an isotropic medium is well known to be an essentially achromatic device for introducing a 90° phase difference in a beam of polarized light; however its inconveniences have led to repeated attempts to find combinations of birefringent crystal plates having this desirable property, for example by Perucca,[2] Longchambon,[3] Gaudefroy,[4] and Ehringhaus.[5] Such combinations apparently have come into very little actual use.

It is known too that sheets and films of practically all rubber-elastic and thermoplastic organic high polymers are readily put into a birefringent state by stretching. While a number of studies have been published on the birefringence of thermoplastic materials, previous work on the spectral dispersion thereof is in effect limited to cellulose nitrate sheets.[6] In particular the measurements of Savur[6c] and of Seth and Harris[6e] show that their stretched Celluloid sheets (cellulose nitrate containing 24 percent camphor) had a birefringence that approached achromatism quite closely.

In the present brief survey we find that with suitable apparatus and samples it is quite as easy to measure dispersion of birefringence throughout the visible spectrum as it is to measure birefringence at a single wave-length.

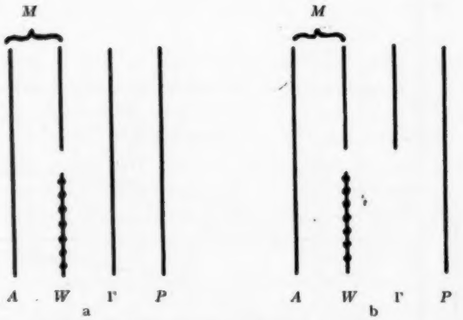

Fig. 1. Optical system for measurement of phase differences.

---

[1] A. Ehringhaus, Neues Jahrb. Mineral. Geol. Beilage B. 43, 557–618 (1920).

[2] E. Perucca, Atti Accad. Sci. Torino, 54, 1013–34 (1918).

[3] L. Longchambon, Bull. Soc. Franç. Phys. No. 195, 158 (1924).

[4] C. Gaudefroy, Comptes Rendus 189 1289–91 (1929); Bull. Soc. Franç. Min. 52, 147–60 (1929).

[5] A. Ehringhaus, U. S. Patent 1,926,716 (1933); Zeits. f. Krist. 75, 179–95 (1930).

[6] (a) M. Wachtler, Kolloidchem. Beihefte 20, 157 (1924); Zeits. f. tech. Physik 5, 418 (1924). (b) Ramspeck, Ann. d. Physik 74, 722 (1924). (c) Savur, Proc. Roy. Soc. (London) A109, 338 (1925). (d) Derksen, Katz, Hess, Trogus, Zeits. f. Physik. Chemie 149, 371 (1930). (e) Harris and Seth, Proc. Phys. Soc. (London) 48, 477 (1936).

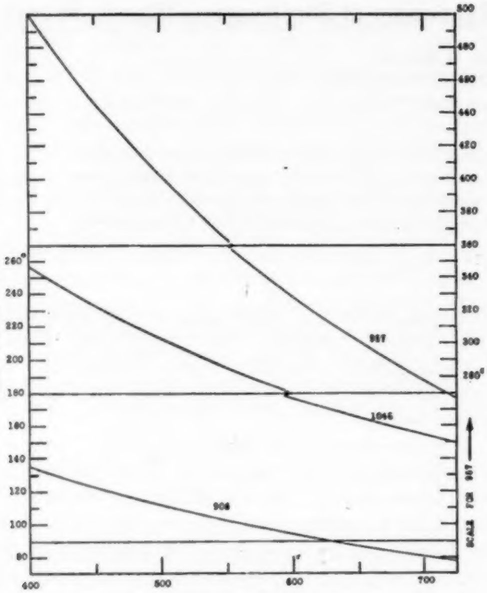

FIG. 2a. Curves of normal dispersion of phase difference.

MEASUREMENT OF PHASE DIFFERENCE

Since previous methods of measurement[1, 6e, 7] proved to be too laborious, after some consideration a simple optical system using a Gaertner polarizing spectrophotometer was found to be satisfactory. This system includes a Martens photometer, which is the preferred instrument for the measurement of dichroism as of sheet polarizers and the like.[8] The measurement of retardation Γ, phase difference δ, or ellipticity $\tan\vartheta = b/a$, where a high order of precision is not required, is illustrated in Fig. 1. In Fig. 1, W is the Wollaston prism with upper and lower windows W_u and W_e, A the analyzer of a Martens photometer. A is on a divided circle which reads zero when A is crossed with W_u, 90° when crossed with W_e, and 45° when the fields are balanced. P is a polarizer, for example a Polaroid polarizer, set exactly perpendicular to W_e, and therefore exactly parallel to W_u of the Wollaston. Γ is the retardation sheet covering W_u and W_e (Fig. 1a) and turned exactly 45° from its extinction position between P and W. These settings of P and Γ can be made very accurately. With the system thus adjusted, the light emerging from Γ is elliptic-polarized with the major axis of the ellipse parallel to the vibration direction of one of the Wollaston windows, for example W_u, and therefore perpendicular to W_e. If the ellipse axes are denoted by a and b, as is customary, then the intensities emerging from W_u and W_e are respectively a^2 and b^2. Now when the analyzer is turned to the azimuth α which balances the fields $J_u = J_e$, the intensity ratio is given by $\tan^2\alpha = J_e/J_u$, and in this way we arrive at the simple expressions $\tan^2\alpha = b^2/a^2$, $\tan\alpha = \tan\vartheta = b/a$, $2\vartheta = \delta$, etc. Or in words, the azimuth angle of the analyzer at balance is equal to the ellipticity angle of the vibration, or to one-half of the phase difference.

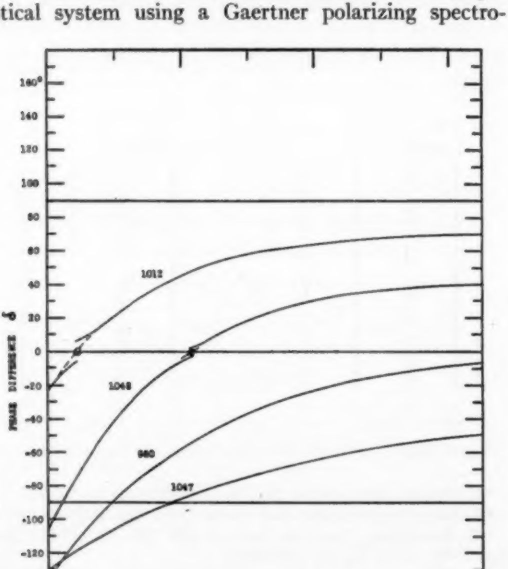

FIG. 2b. Abnormal dispersions.

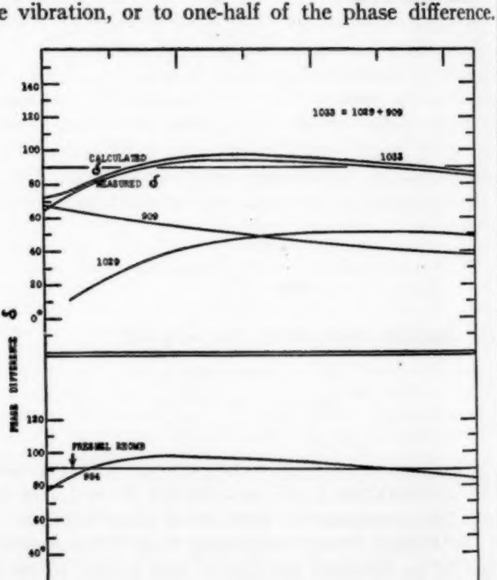

FIG. 2c. Achromatic dispersions.

---

[7] G. Szivessy, *Handbuch der Physik* (1928), Vol. 19, Chapter 28.

[8] M. Grabau, J. Opt. Soc. Am. **27**, 420–24 (1937).

This method does not distinguish between right and left ellipses.

By this method a good reproducibility of settings is found. For the purposes of this paper the results are plotted as dispersion curves of δ against λ from 400 to 760 mμ. The addition and subtraction of phase differences or retardations is readily demonstrated by this method (See Fig. 2). In Fig. 2 the sign of the ordinate is chosen to agree with the sign of birefringence, which in accordance with convention is taken as positive for $n_{\parallel} > n_{\perp}$, negative for $n_{\parallel} < n_{\perp}$, where $n_{\parallel}$ is the refractive index for light vibrating parallel to the direction of stretch.

In the regions where the dispersion curves cross the levels $\delta = 0°$, 180°, 360°—there is an inaccuracy in the settings, as illustrated in Figs. 2a, b. This inaccuracy is due to the failure of the light intensity through W_u or E_e, as the case may be, to fall to zero, as it should under ideal conditions; rather the intensity passes through a minimum whose wave-length is readily found. This departure from ideal conditions is due in part to imperfect collimation, and in part to inter-reflexion; it prevents this method from being directly applicable to the accurate measurement of very small ellipticities, but does not materially affect the measurement of larger ellipticities.

It is seen that if the sample contains an isotropic light-absorbing material, the measurements by this method will not be affected by its presence. The advantage of the present system over previous ones for measuring ellipticities and phase differences is that it does not require a birefringent crystal plate whose constants have first to be determined. It would not be difficult to adapt this method for settings outside the visual spectrum by means of a suitable photoelectric cell circuit.

A less convenient and no more accurate system for making measurements of this kind is illustrated in Fig. 1b, where the retardation sheet covers only one window W_u, of the Wollaston, and is free of absorption. In this system the relation at balance is $\tan^2\alpha = b^2/(a^2+b^2)$, from which the corresponding value of $\tan\vartheta = b/a$ could be derived.

RESULTS

The results of this study are presented as dispersion curves (see Fig. 2, Tables I and II), for each curve the value of Ehringhaus' function N has been computed. In appraising these curves, it should be recalled that a small increase in thickness, or in stretch, of a given sheet has the effect of increasing δ by a small factor.

These results suggest that while many common films have normal dispersion of birefringence, others are abnormal and offer the possibility of preparing retardation plates of a wide range of N values, including those having a fair approximation to achromatism. An approach to achromatism may be found either in a single sheet of suitable composition, for example cellulose nitrate (984), or by combining two or more sheets with vibration directions parallel, such as cellulose acetate with cellulose nitrate or acetatebutyrate (909 parallel to 1029). Although it is easy to make substantial improvements in this way over normal materials such as mica, admittedly it is not easy to achieve the high degree of achromatism of the Fresnel rhomb.

In calculating achromatic combinations of such sheets, one could follow the analytical method of Gaudefroy,[2] but in practice it is simpler to employ the formula of Ehringhaus[3] for the N of a combination of two birefringent sections characterized by N values N_1 and N_2 respectively and by retardations for the D line of Γ_1 and Γ_2 respectively:

$$N = \frac{N_1 N_2(\Gamma_1 \pm \Gamma_2)}{N_2\Gamma_1 \pm N_1\Gamma_2} = -3.46$$

for achromatism, where the + sign is used for the addition position, the − sign for subtraction. For example Gaudefroy calculated by his method that a 0.745-mm section of quartz crossed with a 0.038-mm section of calcite (both cut parallel to the axis, the thickness ratio being 1:0.0510) would give an achromatic phase difference of 180° through the visible spectrum. Employing Ehringhaus' N values of 33.67 and 23.68 respectively for quartz and calcite, and the respective birefringences for D light of 0.00911 and 0.17197, it is readily found by Ehringhaus' formula that

TABLE I. Description of Samples

Number	Sample	N	Γ_C	Γ_D	Γ_F
906	Stretched cellulose acetate	−45.0	158.5	157.0	155.0
1046	Mica	−42.6	299.0	298.0	292.0
957	Stretched polyvinyl alcohol	26.1	539.0	548.0	560.0
1048	Stretched cellulose nitrate (1) (36-mm film base)	−0.50	66.8	42.1	−17.6
1012	Stretched cellulose acetate butyrate	−1.48	122.5	102.4	53.4
980	Stretched cellulose nitrate (2) (Kodaloid)	0.67	−24.4	−42.6	−88.6
1047	Stretched cellulose triacetate	5.15	−103.7	−109.7	−125.0
909	Stretched cellulose acetate	−48.4	78.2	77.5	76.6
1029	Stretched cellulose nitrate (3) (unplasticized)	−1.96	92.3	81.4	50.8
1033	909 plus 1029	−3.73	164.6	152.4	123.7
984	Stretched cellulose nitrate (4)	−4.87	163.3	155.0	131.4
*	Fresnel rhomb (glass of $n_D = 1.517$, $\nu = 64.5$)	−3.50	164.0	147.2	122.0
*	Ideal	−3.46	164.0	147.2	121.5

* Calculated values.

TABLE II. Variation of N value with composition.

Number	Material	N values
—	Ramie*	26.0 at 20°. 24.4 at 50°.
978,976	Commercial Cellophane	122, 107
1053*a*, *b*	Cellulose acetate *E*-656 53.1% HOAc	−24, −41
1054*a*, *b*	Cellulose acetate *E*-309 56.3% HOAc	−8.1, −7.4
1047*a*, *b*	Cellulose triacetate 62.5% HOAc	5.2, 3.9

* Data of A. Frey-Wyssling, Helv. Chim. Acta **22**, 981–8 (1939).

0.05097 mm of calcite is required to achromatize 1-mm of quartz. The equality of the thickness ratios shows the concordance of the two methods.

It may be pointed out that Ehringhaus, after setting up correct and useful equations, by a peculiar confusion of phase difference with path difference failed to appreciate that a N value of -3.46 is the criterion of achromatism (phase difference constant as wave-length varies); instead he only calculated several combinations of constant *path difference*, characterized by $N=\pm\infty$, which are of little practical or theoretical importance.

A comparison of curves 957 and 1048 shows that they will have similar interference colors between crossed polarizers in white light, and that accordingly, since 957 is sensitive to the addition or subtraction of a small retardation, 1048 will be similarly sensitive; it seems appropriate to call it a *zero-order sensitive tint*. Curve 1048 is in fact approximately the reflexion of curve 957 across the line $\delta=180°$. It is a matter of observation that a zero-order sensitive tint plate of type 1048 differs in two respects from a *normal first-order sensitive tint* of type 957: first, it is easier to prepare, once a suitable material has been found, in particular the interference color is relatively insensitive to thickness changes; and second, the interference color is very insensitive to the angle of incidence. Zero-order sensitive tints could also be calculated for a combination of two sheets having suitably different N values.

It will furthermore be apparent that the addition of a zero-order sensitive tint plate to a first-order one of which it is the reflexion, will give a combination with an achromatic retardation of one wave-length ($\delta=360°$) through the visible spectrum.

An abnormal first-order sensitive tint could be made from a sheet (or combination of sheets) whose $\delta(\lambda)$-curve is the reflexion of the normal first-order sensitive tint curve across the level $\delta=360°$. This can be called a *reversed first-order sensitive tint*, and would be exemplified by a suitable thickness of the material of curve 1029.

If we take as characteristic values for an ideal normal first-order sensitive tint $N=\pm\infty$, $\Gamma=\lambda^*=560$ mμ (a constant), then it is easy to show that the corresponding ideal zero-order sensitive tint has $\Gamma'=\lambda^*-\lambda$ (a variable with wave-length) and $N'=-0.17$; and similarly the corresponding ideal reversed first-order sensitive tint has $\Gamma''=2\lambda-\lambda^*$ (also variable with wave-length) and $N''=-1.82$.

The foregoing discussion could also be applied to the curves resulting when the ordinates are changed from phase difference δ to path difference Γ, and the abcissas remain wave-lengths. The level lines $\delta=0°, 180°, 360° \ldots$ parallel to the λ-axis become slanting lines $\Gamma=0, \lambda/2, \lambda, \ldots$ passing through the origin.

The purpose of Table II is to illustrate by measurements on duplicate samples how the N value varies as the composition changes from cellulose through acetone-soluble cellulose acetates to cellulose triacetate. These acetates are commercial preparations supplied by Eastman Kodak Company, Rochester, New York.

Note:—To the foregoing report, substantially as it was written in June 1944, there is little new to add. We have not worked out a good way to handle the false discontinuities on the $\delta(\lambda)$-curves where they cross the levels δ equal to an integral multiple of π. These probably result from various stray lights in the system plus depolarization effects arising in some samples.

Destriau and Prouteau,[9] have described an ingenious new way to realize a quasi-achromatic quarter-wave combination by superposing a quarter-wave with a half-wave layer of the same non-achromatic material, such as mica, at a suitable fixed oblique angle. A complete bibliography is included in this paper.

Some of the foregoing material is presented in the specification of the author's U. S. Patent 2,441,049 of May 1948, "Composite Achromatic Wave Plates."

---

[9] Destrian and Prouteau, J. de phys. et rad. **10**, 53–55 (1949).

Letters to the Editor

The Optical Transmission of Additively Colored Alkali Halide Crystals in the Visible and Near Infra-Red

H. Friedman and C. P. Glover
U. S. Naval Research Laboratory, Washington, D. C.

THE crystals of the pure alkali halides exhibit sharp absorption bands in the far ultraviolet below about 2000 angstroms, but are almost perfectly transparent throughout the visible spectrum and the near infra-red. When these crystals acquire a stoichiometric excess of alkali metal they develop a deep visible coloration. The alkali metal may be introduced in a variety of ways: (1) photo-chemically, by the action of ultraviolet light, x-rays, or gamma-rays; (2) additively, by exposing the heated crystal to the vapor of an alkali metal, and (3) electrolytically, by allowing electrons to enter the heated crystal from a pointed cathode. The excess alkali metal supplies electrons which become trapped at halogen ion vacancies to form *F*-centers.[1] The characteristic absorption spectra of the *F*-centers are shown in Fig. 1 for the potassium halides. These absorption bands have a bell shape; the density of *F*-centers is related to the maximum absorption coefficient in the band and its width at half-maximum absorption coefficient. It is the purpose of this note to point out that additively colored alkali halide crystals can be filled with sufficiently high concentrations of *F*-centers, that they become virtually opaque throughout the visible spectrum, yet still transmit almost perfectly in the infra-red. Crystals which are colored additively retain the coloration permanently unless heated to temperatures near the melting point. Such additively colored crystals may find useful applications as infra-red transmitting filters.

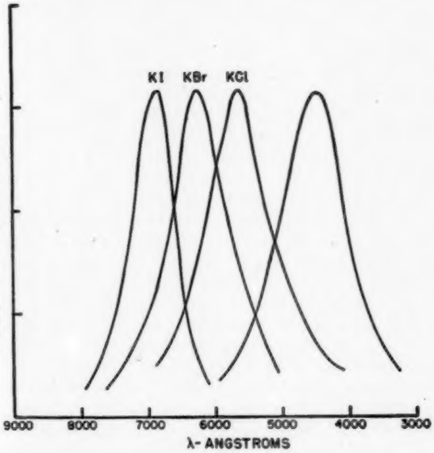

FIG. 1. *F* band absorption in potassium halides.

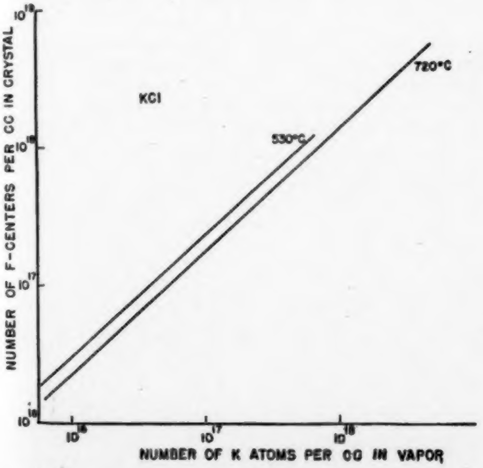

FIG. 2. Relation between *F*-center concentration in KCl and density of K atoms in vapor. (After Rogener, reference 2.)

The crystals whose characteristics are described here were prepared by enclosing them in a Pyrex glass envelope, which was first evacuated, then filled with a sufficient amount of alkali metal and sealed off. After heating to a temperature of 1000°F, near the melting point of the crystal, the envelope was quenched as rapidly as possible to room temperature by use of an air blast. The relationship between the density of *F*-centers produced in this manner and the temperature,[2] is shown in Fig. 2. When thick crystals are used, sufficient time must be allowed for equilibrium to be reached. With increasing density of *F*-centers, the absorption

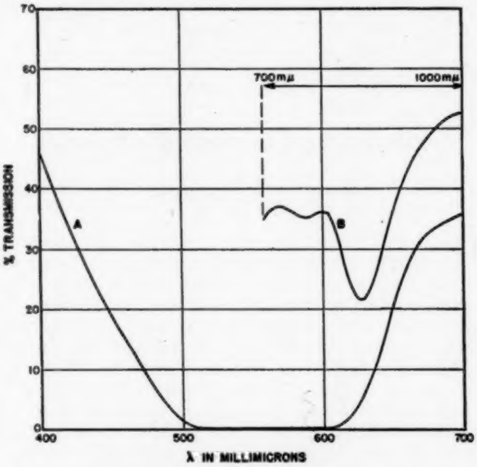

FIG. 3. Transmission of additively colored KCl (about 10^{18} color centers per cc; thickness, 6 mm).

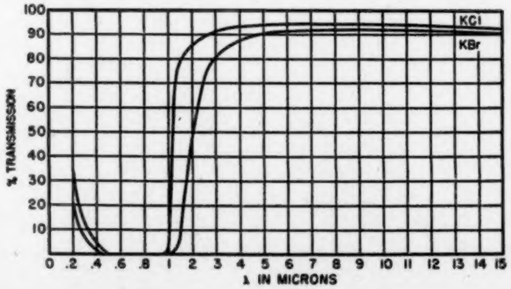

FIG. 4. Transmission of KCl and KBr crystals, one centimeter thick, containing about 5×10^{17} color centers per cc.

coefficients in the F band become great enough so that the transmission curve is essentially flat at zero transmission over a broad band and rises steeply on both sides as shown in Fig. 3. Additional subsidiary absorption bands appear which are too weak to be observed in less densely colored crystals. In Fig. 4 is shown the transmission characteristics of colored KCl and KBr crystals, one cm thick, containing about 5×10^{17} F-centers per cc. These crystals were virtually opaque throughout the visible spectrum, but the transmission rose abruptly above one micron to values characteristic of the original untreated crystals.

Since it has been established that F-center concentrations of 10^{19} per cc are obtainable in KCl and KBr, it is obvious that the transmission limit can be moved appreciably further out toward the infra-red than was accomplished with the crystals described here. Furthermore, the transmission curve for additively colored KI should be displaced as much toward the red with respect to KBr, as is the case for KBr relative to KCl. Attempts were made to color some samples of KI crystals, but, unfortunately, the specimens were not suitable for precise measurements of spectral transmission.

The authors are indebted to Miss D. V. Estes of this Laboratory for measuring the transmission curves shown in Fig. 4.

[1] R. W. Pohl, Physik. Zeits. **39**, 36 (1938).
[2] H. Rogener, Ann. d. Physik **29**, 386 (1937).

X-Ray Images by Refractive Focusing

Paul Kirkpatrick*
Bowdoin College, Brunswick, Maine

July 11, 1949

THE phenomenon of x-ray image formation by concave reflectors[1] is fully established. In spite of a long-standing impression to the contrary, *refractive* x-ray focusing is also a possibility. Many workers have photographed prismatic x-ray spectra, using prisms, usually of glass, with plane faces. Since deviations are always small the position of minimum deviation is avoided and the radiation is caused to pass through one of the prism faces as obliquely as is practicable. It is sometimes stated that when this is the face of emergence the outgoing rays are convergent, but this is incorrect. To produce convergence and a focused spectrum, using x-radiation from a point or slit source, it suffices to give the emergence face of the prism a concave curvature. As in the Fery spectrograph, one optical element performs the functions of dispersion and focusing. The writer has photographed the K line spectra of molybdenum with such converging prisms.

It may be shown by an elementary but tedious geometrical analysis that the focusing is governed by the approximate equation

$$1/p+c^2/q=(1-c)/Ri,$$

where, as shown in Fig. 1, R is the radius of curvature of the refracting surface, i is the angle between the surface and the external ray, c is the ratio of internal to external grazing angle at the point of incidence, and p and q are the object and image distances, p being associated with the external and q with the internal ray, regardless of the actual direction of ray propagation. The significant ray deviation is all in the plane of the figure, the focusing being practically that of a cylindrical lens, even though the actual surface curvature may be spherical. The circular aberration has been calculated and found to be about as serious as that of reflective focusing. The magnification is q/pc.

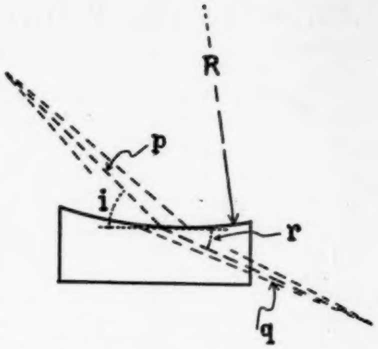

FIG. 1. Ray system of a focusing prism. Angles i and r are greatly exaggerated. With x-rays no appreciable deviation occurs at the right face of the prism.

Since all refracting materials are absorbent in the x-ray region only the portion of the prism within a few microns of the refracting angle will pass appreciable radiation. The prism aperture is thus so narrow that diffraction plays a detectible part in determining the width of a slit image. The diffraction width is less when radiation leaves prism at the refracting face than when it enters there.

An achromatic prism, that is, one producing deviation without dispersion is an untried theoretical possibility. The ratio of dispersion to deviation is a function of the electron density of the prism material, so two properly designed dissimilar components should form a combination producing equal deviation for two wave-lengths.

An x-ray lens capable of producing a point image of a point object (with radiation of one wave-length) would consist of two focusing prisms mounted close together with their refracting edges normal to each other. Radiation would pass through them in succession, being focused in, say, a horizontal plane by one prism and in a vertical plane by the other. Such achievement of point focusing by two strongly astigmatic optical elements would be in complete analogy with the demonstrated focusing of x-rays by two mirrors. Although the x-ray lens is thus possible it has the disadvantages of high absorption and strong chromatic aberration, and so would probably be generally inferior to mirror systems.

* On leave from Stanford University, California.
[1] W. Ehrenberg, Nature **160**, 330 (1947). P. Kirkpatrick and A. V. Baez, J. Opt. Soc. Am. **38**, 766 (1948).